OPTIMIZATION TECHNIQUES APPLIED TO PASSIVE MEASURES FOR IN-ORBIT SPACECRAFT SURVIVABILITY:

CONTRACT NAS8-37378

FINAL REPORT

JUNE 1992

PREPARED FOR:

GEORGE C. MARSHALL SPACE FLIGHT CENTER

MARSHALL SPACE FLIGHT CENTER, AL 35812

PREPARED BY:

ROBERT A. MOG

MICHAEL J. HELBA

JANEIL B. HILL

Science Applications International Corporation
6725 Odyssey Drive, Huntsville, AL 35806-3301 • (205) 971-6400

OPTIMIZATION TECHNIQUES APPLIED TO PASSIVE MEASURES FOR IN-ORBIT SPACECRAFT SURVIVABILITY: CONTRACT NAS8-37378 FINAL REPORT

JUNE 1992

PREPARED FOR:

GEORGE C. MARSHALL SPACE FLIGHT CENTER

MARSHALL SPACE FLIGHT CENTER, AL 35812

PREPARED BY:

ROBERT A. MOG

MICHAEL J. HELBA

JANEIL B. HILL

SAIC®
Science Applications
International Corporation
An Employee-Owned Company

ACKNOWLEDGMENTS

We would like to thank Jennifer Robinson, Joel Williamsen, Sherman Avans, and Ben Hayashida of the Marshall Space Flight Center and Marv Price of SAIC for their direction and contributions to these developments under NASA Contract NAS8-37378. In particular, we thank Jennifer Robinson for recommending the approach and numerous trades for the advanced shielding concepts, Joel Williamsen for suggesting many of the features and development approaches for the Monte Carlo simulation tool, Sherman Avans for recommending many of the initial features of IMPACT10V and PSDOC, Ben Hayashida for suggesting various improvements to PSDOC, and Marv Price for providing the key initial technology and various suggestions along the way.

LIST OF SYMBOLS

a_i = estimated parameters for regression

a_{ij} = exponent for objective function term i and variable j

a_{ijl} = exponent for term i, variable j, in constraint l

A = spacecraft space debris area

A_l = acceleration factor of primal penalty function for constraint l

B = spacecraft orientation factor

c_i = coefficient for objective function term i

c_{il} = coefficient for term i in constraint l

c_{is} = coefficient for posyseparable term i

C = bumper material speed of sound

d,D = projectile diameter

DOD = geometric programming degree of difficulty

f = non-normalized impact velocity distribution

f_n = normalized impact velocity distribution

F = space debris flux

F_h = fraction of hyperspace for random search

g_l = constraint l

h = spacecraft altitude

i = spacecraft inclination

k = number of independent variables

K_l = right hand side of primal constraint l

L_2 = wall material constant

m = projectile mass

m_h = number of random search points

m_l = number of terms in constraint l

n = number of terms in objective function or number of plates (bumpers and wall)

n_j = positive integer value corresponding to variable j

N = cumulative space debris flux or number of "walls" penetrated (including witness plates)

N_1 = number of walls penetrated (normal impact)

N_t = total meteoroid flux

p = number of constraints

P = space debris growth rate

P_h = required confidence for random search

P_0 = spacecraft probability of no penetration

q = number of discrete variables

r_j = discrete availability factor for variable j

s = solar flux

S, S_i = bumper/wall separation

t_1, t_i = bumper thickness

t_2, t_n = wall thickness

T = mission duration

V = projectile impact velocity

V_{max} = maximum space debris impact velocity

W = structure mass per unit area or weight

α_l = acceleration factor of primal penalty function for discrete constraint l

δ_i = dual variable corresponding to objective function term i

δ'_{jl} = dual variable corresponding to term j in constraint l

δ_l = binary factor of primal penalty function for constraint l

δ_{1j} = first dual variable for discrete constraint of variable j

δ_{2j} = second dual variable for discrete constraint of variable j

Δ_l = binary factor of primal penalty function for discrete constraint l

ε = convergence parameter for penalty function

ε_1 = initial exploratory step size for Hooke and Jeeves

ε_2 = final exploratory step size for Hooke and Jeeves

θ = impact angle from surface normal

μ_l = dual objective function variable in constraint l

ν = dual objective function

ϕ = primal penalty function

ρ_1, ρ_i = bumper density

ρ_2, ρ_n = wall density

ρ_p = projectile mass density

ψ = spacecraft inclination factor

$[\ ]_{n.i.}$ = nearest integer of quantity in brackets

A 0 subscript denotes optimal value for a primal variable.

A * superscript denotes optimal value for a dual variable.

Table of Contents

1 INTRODUCTION

1.1 Problem Statement

Spacecraft designers have been concerned since the 1960's about the effects of meteoroid impacts on mission safety. Recent concerns have extended to the space debris environment, which typically displays more massive particles than the meteoroid environment for the same risk level. Additionally, the higher exposure area-time product of future space missions (e.g., Space Station) poses a more critical design problem than current short term missions. Finally, the inherent uncertainties in projectile mass, velocity, density, shape, and impact angle make the traditional deterministic design approach impractical.

The engineering solution to this design problem has generally been to erect a bumper or shield placed outboard from the spacecraft wall to disrupt/deflect the incoming projectiles. This passive measure has resulted in significant structural weight savings relative to a single wall concept with the same protective capability. The problem, then, is how to efficiently design these protective structures so that the bumper disrupts the projectile without posing a lethality problem to the wall protecting the crew and equipment.

Spacecraft designers have a number of tools at their disposal to aid in the design process. These include hypervelocity impact testing, analytic impact predictors, and hydrodynamic codes. Perhaps the most widely accepted of these tools is impact testing, which has the advantage of providing actual spacecraft design verification. On the other hand, maximum test velocities are currently limited (8 km/sec) relative to maximum space debris (about 15 km/sec) and meteoroid (about 72 km/sec) velocities. Also, extensive testing is required to develop statistically significant trends for the large number of parameters associated with hypervelocity

impact. Hydrodynamic code analysis can overcome the velocity limitation problem. However, this method is very computer (and time) intensive, and there is a fair amount of controversy involved in the selection of appropriate codes and code-specific parameters.

Analytic impact predictors generally provide the best quick-look estimate of design tradeoffs. Their use is constrained by the limitations of the testing from which they are experimentally derived, the assumptions used in their theoretical derivation, or the regression analysis used in their statistical formation. However, analytic predictors may provide information that is clearer than that obtained from the examination of experimental results.

The most complete way to determine the characteristics of an analytic impact predictor is through (nonlinear) optimization of the protective structures design problem formulated with the predictor of interest. Optimization techniques provide analytic or numerical solutions depending on the nature of the predictor, the problem formulation, and the technique used.

1.2 Contract Purpose

The purpose of this contract is to provide Space Station *FREEDOM* protective structures design insight through the coupling of design/material requirements, hypervelocity impact phenomenology, meteoroid and space debris environment sensitivities, optimization techniques and operations research strategies, and mission scenarios. Major findings from contract inception to the beginning of this study are detailed in References 100-105 and are shown below:

	PROTECTIVE STRUCTURES DESIGN
1	The Nysmith Predictor Has a Systemic Inequality Constraint.
2	All Predictors Investigated Show a Large Relative Incentive for Increasing Bumper/Wall Separation from 10 to 15 cm. (Shift to Knee)
3	All Predictors Investigated Show a Large Relative Disincentive for Increasing System Probability of No Penetration. (Already at Knee)
4	All predictors reflect increasing design sensitivity to projectile diameter and decreasing design sensitivity to bumper/wall seperation.
5	Optimal Design Ratios Vary With Mission, Requirements, Environment, and Materials Parameters. Variations in Bumper/Wall Materials Show Large Design/Weight Differentials. (Even Among Aluminum Alloys only)
6	Optimal Bumper Thickness is Most Heavily Influenced by Projectile Melt/Vaporization Region While Optimal Wall Thickness is Most Heavily Influenced by Projectile Shatter Region.
7	Posynomial Programming May Be Useful in Predicting Design Trends as Functions of Estimated Regression Parameters Before Testing.
	ENVIRONMENT SENSITIVITY
8	Debris Dominates Meteoroids From a Design Standpoint, But Optimal Ratios are Considerably Different.
9	Debris Growth Rate, Mission Altitude, Schedule, Safety, and Duration All Have Significant Effects on Optimal Design Values and Ratios.
	OPTIMIZATION APPROACHES
10	Global Protective Structures Design Optimization Is Achievable Using Many Hypervelocity Impact Predictors (e.g. Nysmith, Burch, Wilkinson, Madden, Maiden, 42 Test Sub-database).
11	Global analytic nonlinear design optimization can be performed for the projectile melt/vaporization region (Wilkinson), for normal impacts in the projectile shatter region (Burch), and for the Nysmith predictor using Geometric Programming.
12	Differences Between Global and Local Design Optimization May Result in Large Weight Differentials.
13	The Power of the Geometric Programming Optimization Method Increases With Increasing Design Complexity (More Bumpers, Materials, etc.).
14	Material Properties Optimization Can Be Achieved Using a Hooke and Jeeves Pattern Search Approach.
15	Discrete Protective Structures Design Optimization Can Be Efficiently Performed Using Dual and Primal Methods.
16	Global (and sometimes analytic) optimization of discrete posynomial programs can be performed using dual approaches coupled with partial invariance techniques.
17	Primal methods require less "pencil and paper" effort than dual methods and are more easily applied to most problems.
18	Primal methods do not generally obtain global solutions for the discrete posynomial program.
19	The dual method may be advantageous in cases where the objective function may be sufficiently separable, since posyseparable programs do not require solutions of coupled nonlinear equations in the dual-to-primal variable transformation.
	STATISTICAL ANALYSES
20	Posynomial Regression Can Be Performed To a Statistically Significant Level for Hypervelocity Impact Test Databases.

1.3 Study Goals

The goals of this study are to:

1. Develop a Monte Carlo simulation tool which will provide top level insight for Space Station protective structures designers.
2. Develop advanced shielding concepts relevant to Space Station *Freedom* using unique multiple bumper approaches.
3. Investigate projectile shape effects on protective structures design.

The period of performance for this effort is 7-1-91 through 6-30-92.

1.4 Study Results

1. Goal 1 was completed and is discussed in Section 2. A source listing is provided in Appendix A.
2. Goal 2 was completed and is discussed in Section 3.
3. Goal 3 was completed and is discussed in Section 4.

1.5 Major Findings of This Study

1. The Monte Carlo simulation tool is feasible from a development standpoint and appears to have advantages over current expected value models.
2. A numerical approximation to a nonstationary Poisson arrival process for impact events appears to be sufficient.
3. Both the Wilkinson and ballistic PEN4 predictors may be extended to multiple bumper models.
4. The multiple bumper Wilkinson predictor optimization problem is a 0 degree of difficulty posynomial programming formulation.
5. Intrinsically Linear Posynomial Regression Can Be Performed to Statistically Significant Levels for Multiple Bumpers.
6. Residual Plot vs. Number of Bumpers Draws Suspicion to That Parameter.
7. Other Residual Plots Seem Appropriate.
8. Resulting Geometric Program has 0 Degree of Difficulty.
9. Optimal Areal Densities are Equal for Bumper(s).
10. Optimal Bumper(s) and Wall Areal Densities are Generally Not Equal.
11. Bumper Areal Density Dominates Wall Areal Density for Single Bumper Case.
12. Wall Areal Density Dominates Bumper Areal Densities for Multiple Bumpers.
13. Optimal Individual Separations are Equal.
14. Optimal Number of Bumpers Increases with Increasing Particle Diameter. (Note Transition Region Between d=1 cm and d=1.25 cm. particle sizes.)
15. Penalty for Selecting Wrong Number of Bumpers is Not Symmetric about Optimal Solution.
16. Protective Structures Design Sensitivity to Velocity is Flat with Constant Optimal Number of Bumpers = 1.
17. Transition from Single to Double Bumper System is Found for Total Standoffs Between 15 and 20 cm.
18. Impact Angle Sensitivity is Monotonically Decreasing with Constant Optimal Number of Bumpers = 1.
19. Transition from Single to Double Bumper System is Found for Particle Densities Between 4.5 and 5 gm/cm^3.
20. Minimum System Mass Per Unit Area is Sensitive to Wall Penetration Factor. (Transition From 2 Bumpers to 1 is Found Between 0.5 and 0.6.)
21. Minimum System Mass Per Unit Area is Sensitive to the Number of Bumpers.
22. Three Year Schedule Slippage Results in 33% Increase in Design.
23. Optimal Protective Structures Design is Very Sensitive to Mission Duration.
24. Transition Region From 1 to 2 Bumpers is Between 10 and 15 Year Durations.
25. Optimal Protective Structures Design is Very Sensitive to Average Mission Altitude Above 400 km.
26. Transition Region From 1 to 2 Bumpers is Between 400 and 500 km Altitudes.
27. Optimal Protective Structures Design is Very Sensitive to Mission PNP Above 0.96.
28. Knee of the PNP Curve is Compatible With Baseline Requirement of 0.9733.
29. Transition Region From 1 to 2 Bumpers is Between 0.9733 and 0.98 PNP. (0.9955 and 0.9966/Element).
30. Optimal Protective Structures Design is Very Sensitive to Total Debris Area.
31. Transition Region From 1 to 2 Bumpers is Between 700 and 800 m^2.
32. Optimal Protective Structures Design is Sensitive to Total Bumper/Wall Separation Between 5 and 20 cm.
33. Knee of the Separation Curve Appears to Be Between 10 and 15 cm.
34. Shift to 15 cm Separation Results in About 33% Reduction in Protective Weight.

2 MONTE CARLO SIMULATION DEVELOPMENT TASK

2.1 Monte Carlo Simulation Purpose

The purpose of this simulation is to provide a statistical tool to address and quantify protective structures design risks, uncertainties, and options, and to address system-level issues relevant to designer decision-making and possible implications. The system of initial interest is the structural configuration of WP01, including the Core Module Configuration. "Grow-to" systems include module internal configurations and external structures (trusses, solar arrays, etc.) as specified in the redesign.

Initial investigations of interest include statistical analyses of primary impacts, penetrations, and vulnerable areas. "Grow-to" investigations include interior effects, secondary ricochet effects, and SSF element interrelations.

Risk considerations include environment particle velocity, impact angle, and component probability of impact. Uncertainty considerations include SSF IOC/FOC, particle diameter, mass-density, shape, and uncertainties in particle velocity and impact angle distributions.

2.2 Monte Carlo Simulation Development Approach

The tool development approach is to define the current SSF mission parameters and design configuration, and interpret the geometry mathematically using FASTGEN. The mission parameters drive requirements specification, including environment definitions. These considerations, combined with appropriate random number modules and the FASTGEN results, produce the necessary shotline time histories and intersecting body calculations. Survivability assessments follow and employ deterministic models for hypervelocity penetration prediction. Statistical assessments follow to supply answers to the questions of interest.

2.3 Particle Time-Arrival Process for Monte Carlo Simulation Development

Several algorithms have been developed for the particle time-arrival process. The standard assumption in this area is that arrival times are Poisson distributed. This means that the inter-arrival times are exponentially distributed, and sorting of arrival times is not required. Mean data is derived from the environment flux and appropriate spacecraft areas. This algorithm leads to a terminating simulation defined by the mission profile.

Realistically, however, the meteoroid and debris environments are both nonstationary Poisson processes, at best, since the mean arrival rates vary in time over the mission profile. An approximation algorithm has been developed which alters the mean arrival rate to represent the time period under consideration. However, this algorithm is not exact, since a period of high arrival rates could be neglected using a low arrival rate corresponding to the previous period, or vice versa. Thus, a more exact (continuous) algorithm should be developed. The approximating algorithm for the space debris environment is given as:

1. *Input* $T_i, T_f, d_{max}, d_{min}, \Delta d$. *Set* $t = T_i$.

2. Using equations [1]-[7], develop a cumulative flux-diameter distribution:

$$P(x \le d) = \frac{\sum_{x=0}^{\left[\frac{d+1-d_{min}}{\Delta d}\right]_{Int}+1} F\left(d_{min} + \sum_{x=0}^{\left[\frac{d+1-d_{min}}{\Delta d}\right]_{Int}+1} \Delta dx, h, i, t, s\right)}{\sum_{x=0}^{\left[\frac{d_{max}+1-d_{min}}{\Delta d}\right]_{Int}+1} F\left(d_{min} + \sum_{x=0}^{\left[\frac{d_{max}+1-d_{min}}{\Delta d}\right]_{Int}+1} \Delta dx, h, i, t, s\right)}$$

$$\forall d = d_{min} + \Delta dx, x \in \left[0, \frac{d_{max} - d_{min}}{\Delta d}\right]$$

3. Draw $U_1 \sim U[0,1]$.

4. Find $F \ni P(x \le d) = U_1$.

5. Set $\beta = 1/F$.

6. Draw $U_2 \sim U[0,1]$.

7. Set $\Delta t = -\beta \ln(U_2)$.

8. Update simulation time: $t = t + \Delta t$.

9. Is $t \ge T_f$?

No, then go to 2 to create next event.

Yes, then quit and gather statistics.

In step 1, the mission start date and end date are input as reals, followed by the maximum and minimum particle diameters of interest and the associated particle step size. The maximum particle of interest is generally that particle size above which protective structures designers reasonably assume no liability in their considerations. For instance, there is a small but nonzero

probability that the Space Station will be impacted by a truck-size particle. However, designers could not be reasonably expected to defeat that particle size given weight constraints. Under current environment expectations, the choice of maximum particle diameter could reasonably be in the 10-1000 cm range. The choice of maximum particle diameter affects result accuracy and run time. The minimum particle diameter of interest is generally considered to be that size below which impacts are highly unlikely to lead to perforations, contamination, or any other measure of effectiveness which is of interest to the protective structures designer. This value is very much a function of the ballistic limit curves of interest. Reasonable values for current design scenarios might be found below 0.1 or 0.2 cm. The designer may wish to vary this value to investigate the sensitivity of designer measure of performance to this input. A sufficiently low value for this parameter would be one below which no appreciable difference resulted in design measure of effectiveness. It should be noted that the minimum diameter should be carefully selected due to its strong effect on run time and result accuracy. The diameter step size is also a critical factor in these two areas. This value determines the fidelity of the resulting flux-diameter distributions. The smaller this value is, the more accurate will be the distribution in a continuous sense. However, the run time increases with decreasing step size, since the flux distributions are being evaluated at each event time. (The requirement for re-evaluation of flux distributions at each event is due to the nonstationary Poisson characteristic of the space debris process. Generally, the diameter step size is chosen to be some fraction, say 10-20%, of the minimum particle diameter. The maximum, minimum, and step size values for the particle diameter are tuning parameters whose optimal values will vary depending on mission, configuration, and design measure of effectiveness. Thus, it is highly recommended that these values be adjusted before final results are displayed for each individual analysis.

In step 2, the flux-diameter distribution is developed at the given mission time as a function of the tuning parameters. This distribution is then transformed to a cumulative flux-diameter distribution, which is normalized to achieve a valid probability distribution from which random numbers may be drawn. The file size of this distribution is completely determined by the tuning parameters. A switch in the program input file allows the user to print out these distributions throughout the mission. This option should be carefully used for long missions or large distribution sizes due to the potentially large files that would be created.

In step 3, a uniform random variate is drawn. This variate is compared in step 4 with the normalized cumulative flux-diameter (probability) distribution to determine the particle diameter at the next event. The (absolute) value of the flux is then inverted in step 5 to determine the exponential (interarrival) parameter. A second uniform random variate is drawn in step 6 for determining the interarrival time for the particle diameter determined from step 4. Step 7 uses the exponential distribution and the results of steps 5 and 6 to determine the particle interarrival time. In step 8, the mission clock is updated and compared with the final mission time in step 9. If the clock is past the end of the mission, the mission is terminated and statistics are gathered. Otherwise, the process reverts to step 2 for creation of new distributions and events.

If independent mean and variance data for arrival rates are available, a uniform arrival process may be used as an alternative to Poisson arrivals. To compare this approach with the Poisson process, the variance may be set equal to the square of the mean. An algorithm has been developed for independent mean and variance data.

Augmentation/repair times may be modelled using a number of distributions, if this modelling is of interest. If mean data only for time to repair is available, an exponential service model may be used. If independent mean and variance data are available, the gamma, weibull, lognormal, or beta distributions may be appropriate.

2.4 Simulation Status

To date, the following items have been completed:

A. Enveloping Geometries Established For:
   1. Sphere: Enter Radius
   2. Cylinder: Enter Radius, Length
   3. Box: Enter length, Width, Height
B. Nonstationary Poisson Arrival Process Algorithm For Space Debris
   1. First Random Variate Establishes Point On Cumulative Flux-Diameter Curve At Current Mission Time
   2. Absolute Flux Is Inverted To Give Mean Interarrival Time
   3. Second Random Variate Establishes Time Between Arrivals Using Exponential Distribution
   4. Cumulative Flux-Diameter Curve Is Updated For New Mission Time
C. Impact Characteristics For Space Debris
   1. Impact Velocity
   2. Impact Angle
   3. Particle Density/Mass
D. Look-Up Tables
   1. Solar Flux (Monthly)
   2. Inclination Factor
   3. Flux-Diameter Curves
E. Impact History Data Including Event Time, Diameter, Density, Mass, Velocity, Angle
F. Fixed Time Data Including Absolute Flux, Normalized Flux, Cumulative Normalized Flux Distributions As Functions of Diameter
G. Geometry/Shotline Integration to Include Impact Location
H. Stationary Poisson Arrival Process Algorithm For Meteoroids

2.5 Selected Results

A great many sensitivities may be generated using this simulation. **Figures 2.5-1 through 2.5-21** provide examples of a few possible results. The following tables provide the input values for these example cases. (Results are for the enveloping geometry only.) **Figures 2.5-22 through 2.5-25** show results for the current baseline configuration, shield design and mission.

* Mission
  1. 1995-2004
  2. 460 km Altitude
  3. 28.5 degree Inclination
* Configuration
  1. Spherical Enveloping Geometry
  2. Radius = 72.5 m
* Recorded Particles
  1. 0.02 - 5.0 cm
  2. Spherical
  3. 5% Debris Growth Rate
* Flux Distribution Fidelity: 0.01 cm
* NASA TM-100471 (Debris)
* NASA SP-8013 (Meteoroids)

SINGLE RUN STATISTICS

* 2125 Debris Impacts
  1. Average Diameter = 0.0474 cm
  2. Average Velocity = 10.26 km/sec
  3. Average Interarrival Time = 1.971 Days

* 9453 Meteoroid Impacts
  1. Average Diameter = 0.0259 cm
  2. Average Velocity = 21.06 km/sec
  3. Average Interarrival Time = 0.372 Days

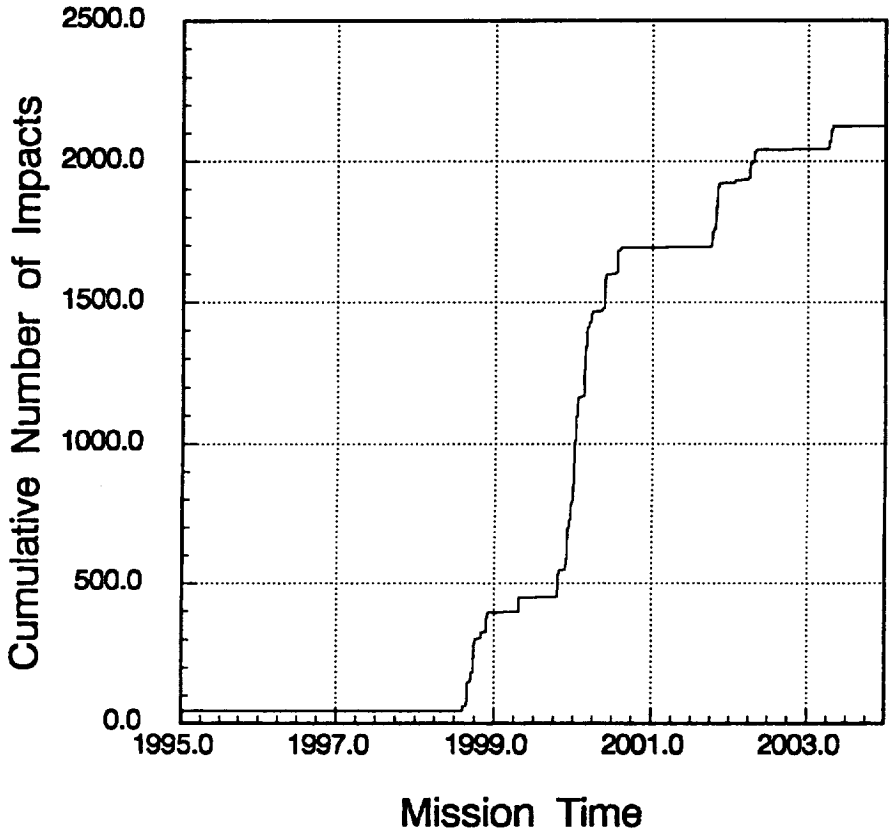

Figure 2.5-1. Cumulative Debris Impacts vs. Mission Time

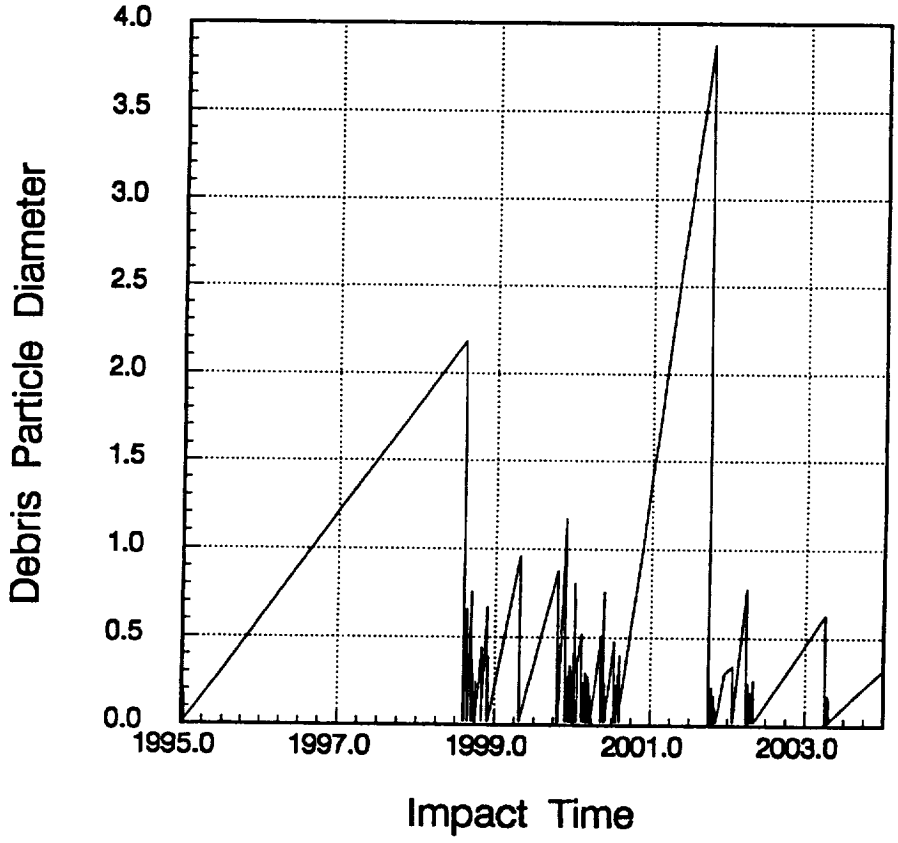

Figure 2.5-2. Debris Particle Diameter vs. Impact Time

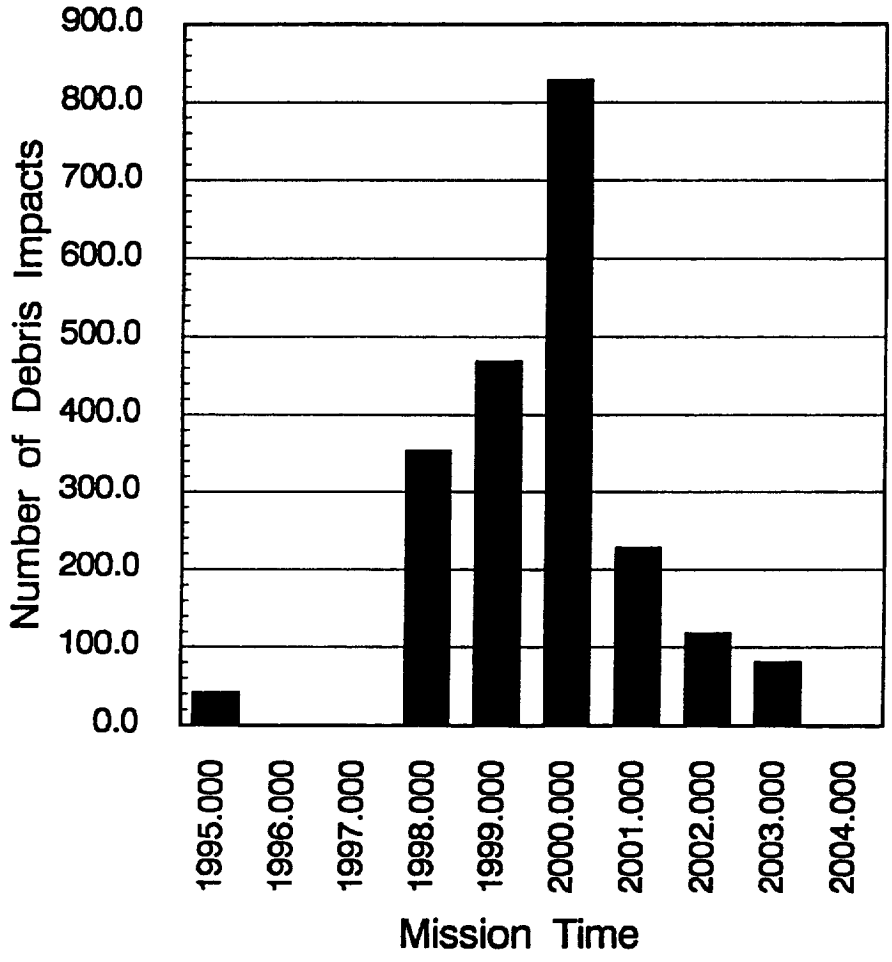

Figure 2.5-3. Debris Impacts vs. Mission Time

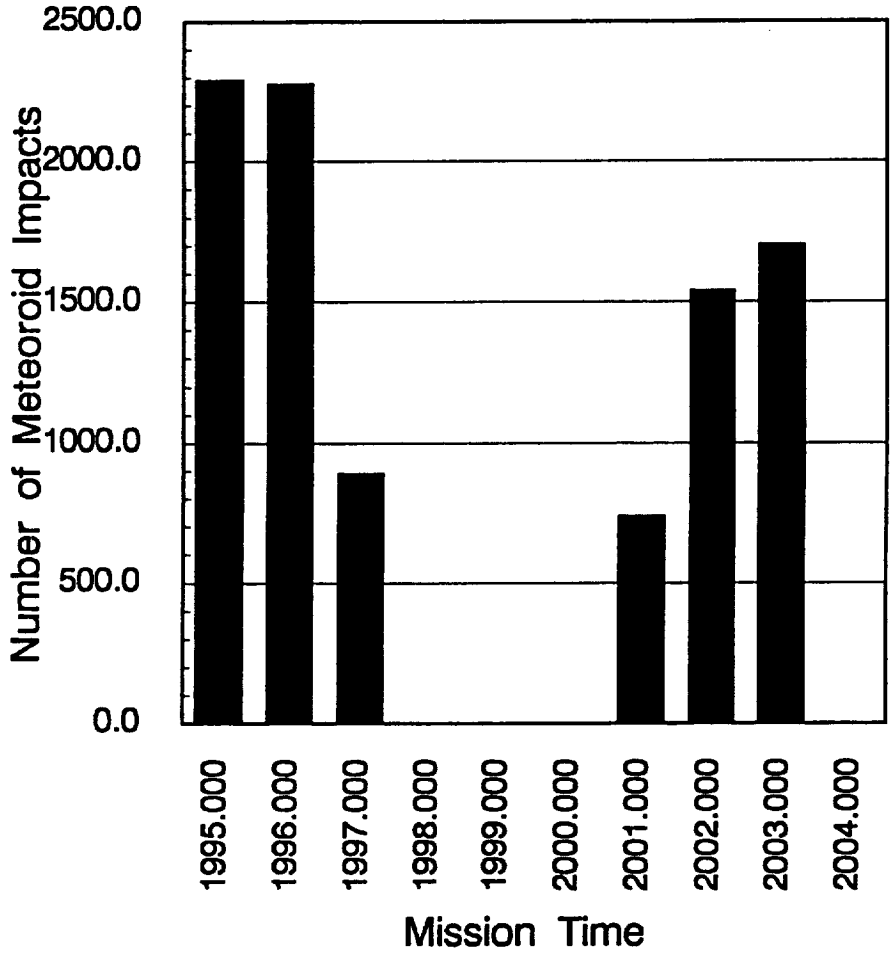

Figure 2.5-4. Meteoroid Impacts vs. Mission Time

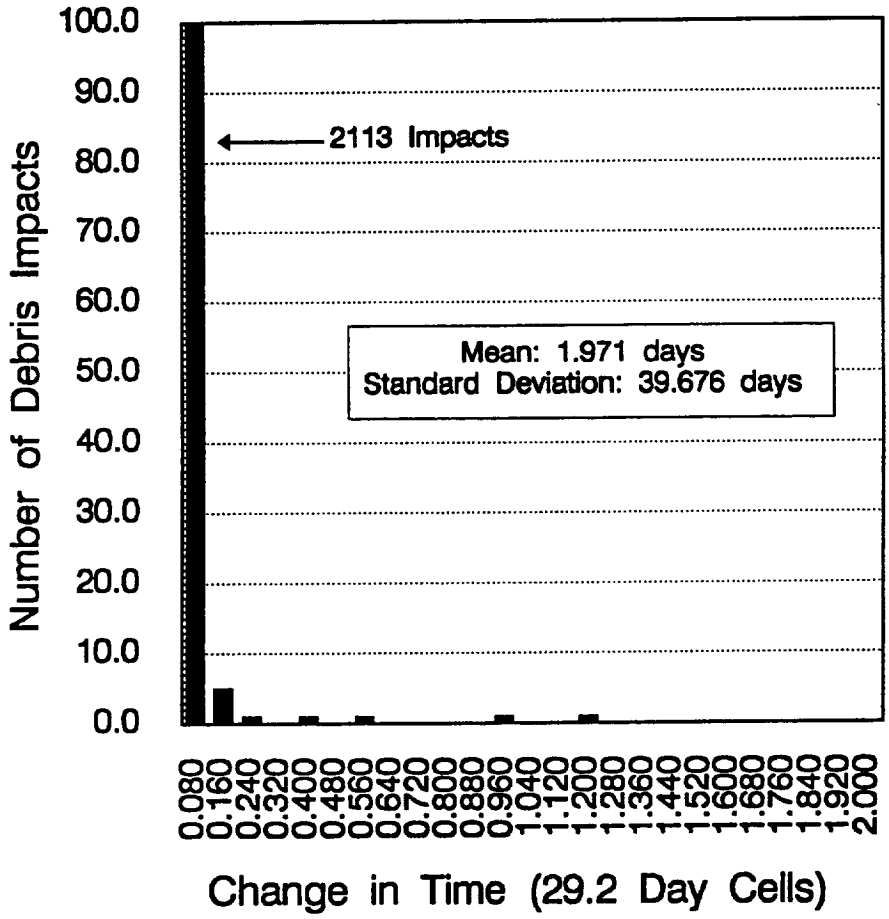

Figure 2.5-5. Debris Impacts vs. Change in Time

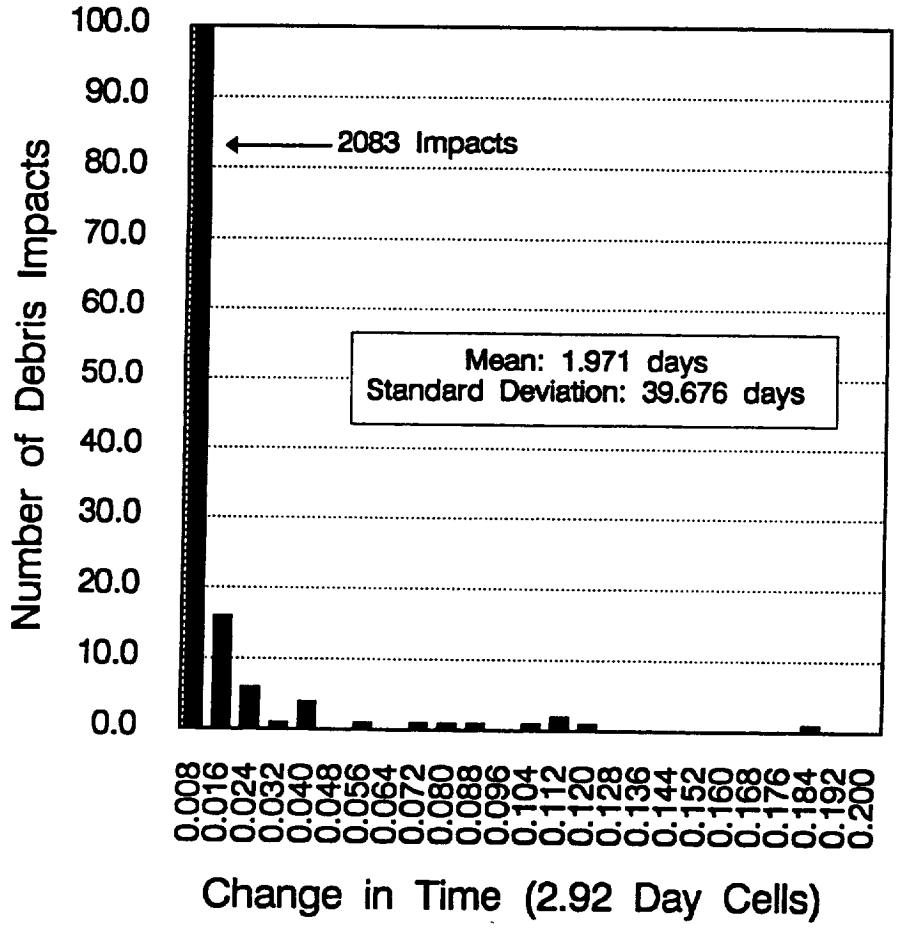

Figure 2.5-6. Debris Impacts vs. Change in Time

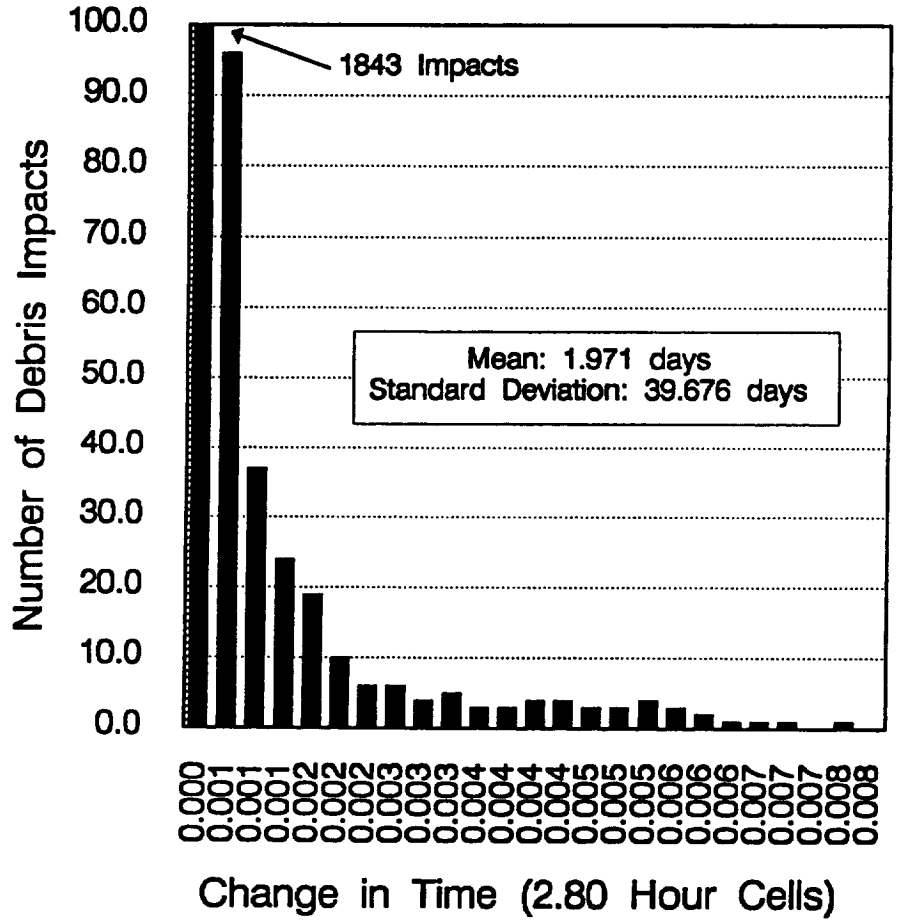

Figure 2.5-7. Debris Impacts vs. Change in Time

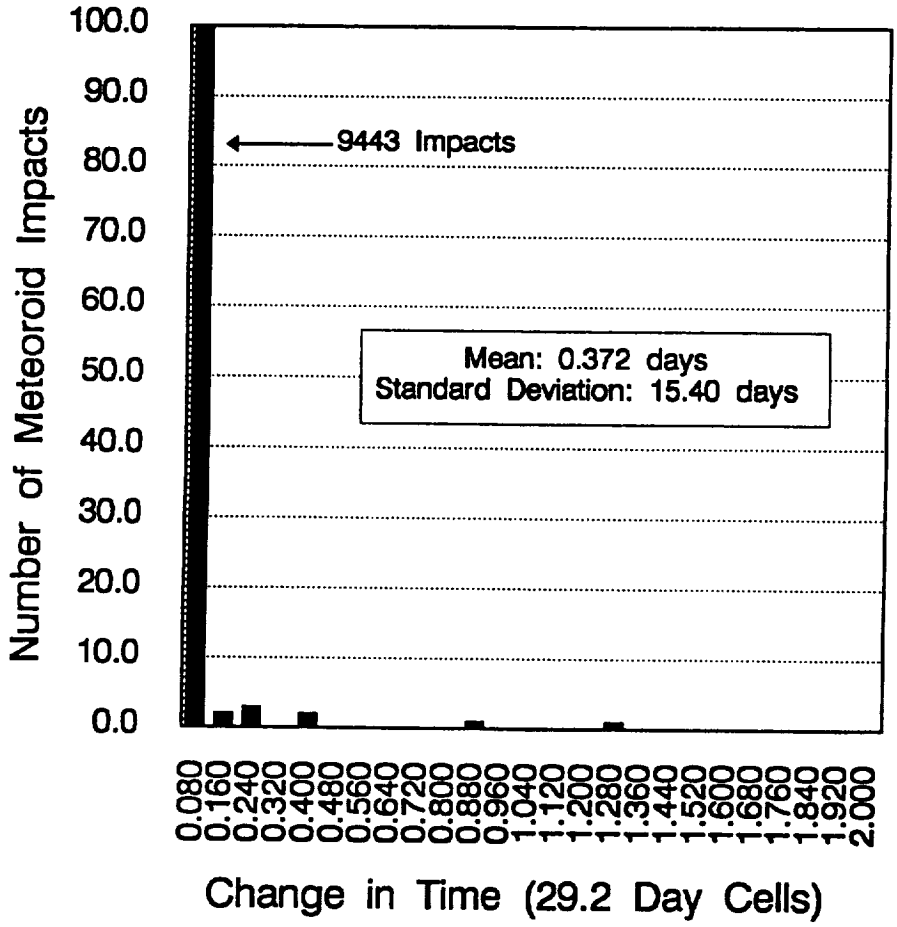

Figure 2.5-8. Meteoroid Impacts vs. Change in Time

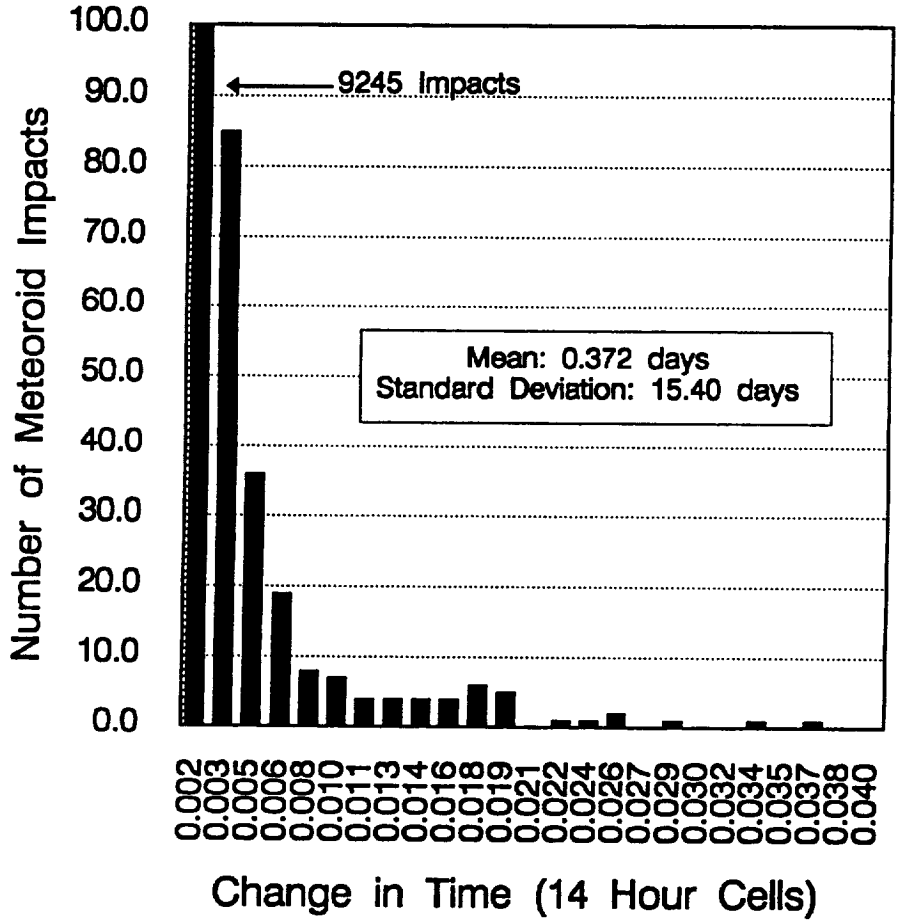

Figure 2.5-9. Meteoroid Impacts vs. Change in Time

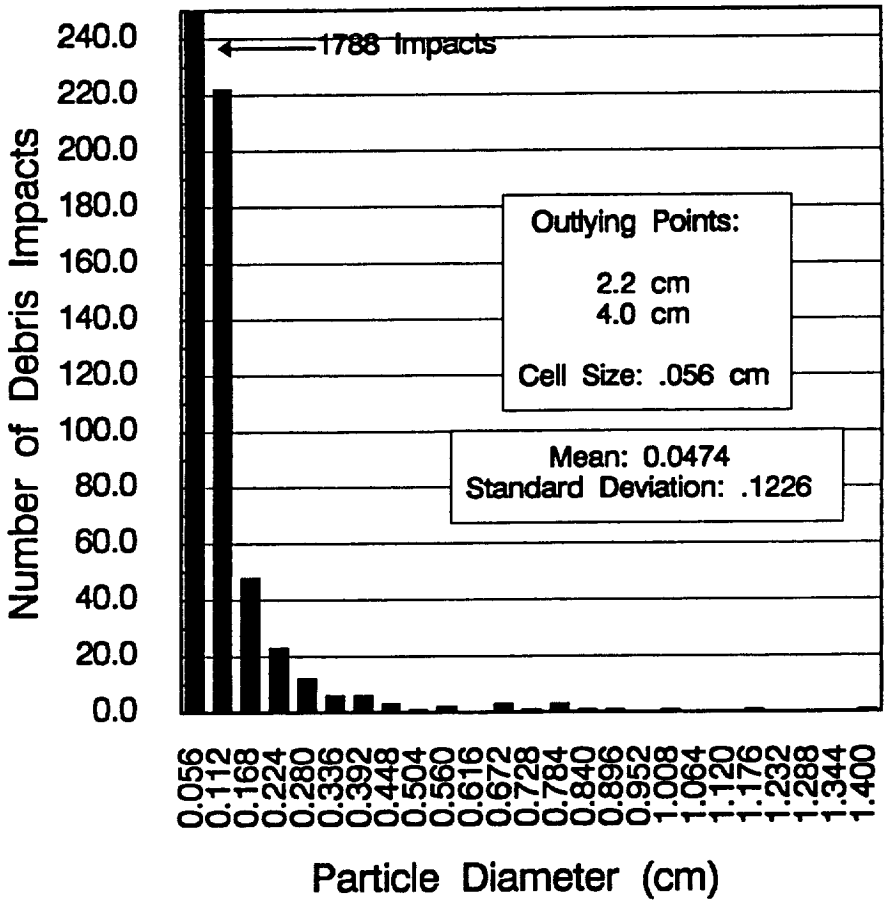

Figure 2.5-10. Debris Impacts vs. Particle Diameter

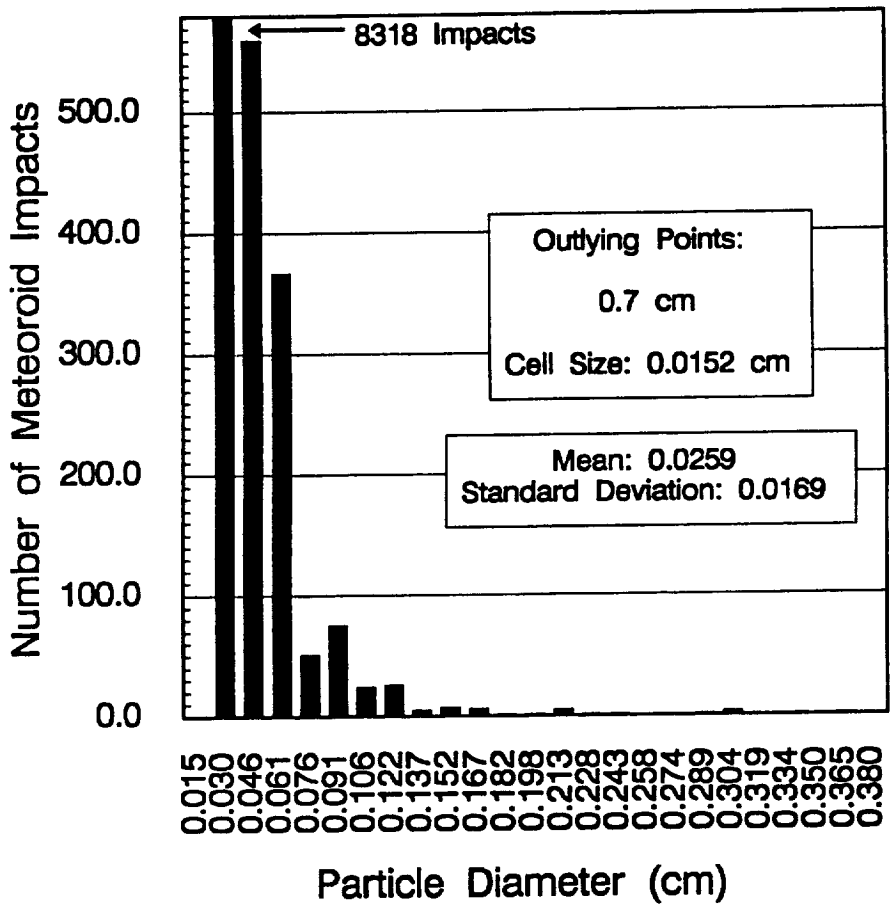

Figure 2.5-11. Meteoroid Impacts vs. Particle Diameter

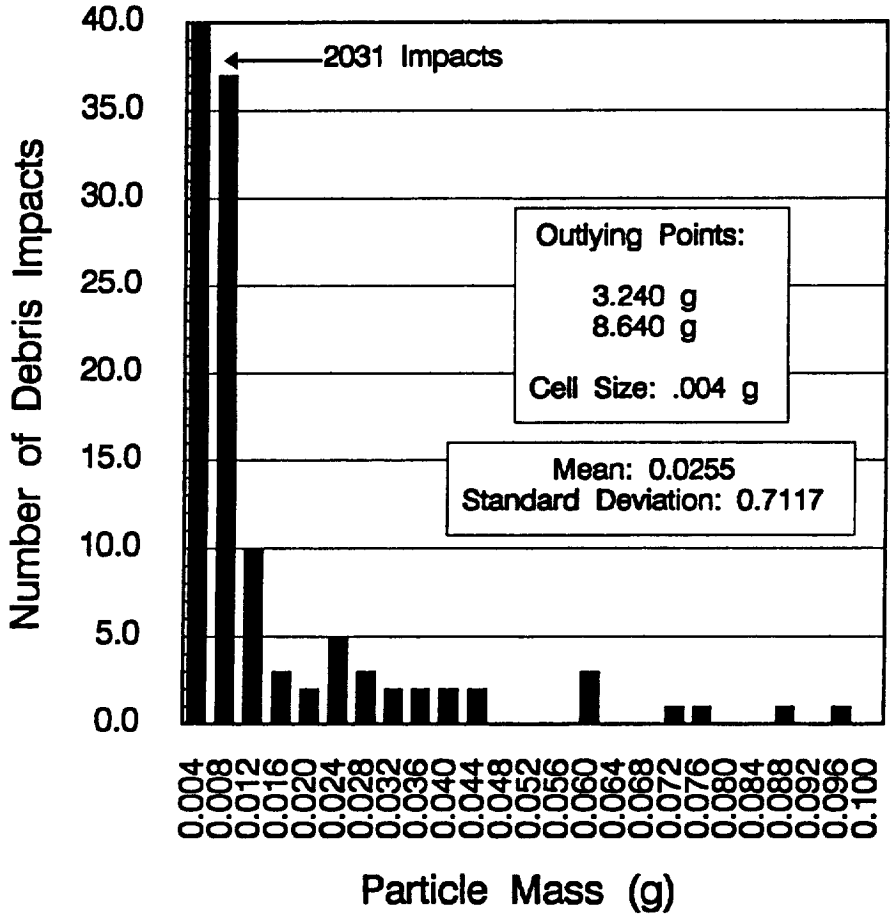

Figure 2.5-12. Debris Impacts vs. Particle Mass

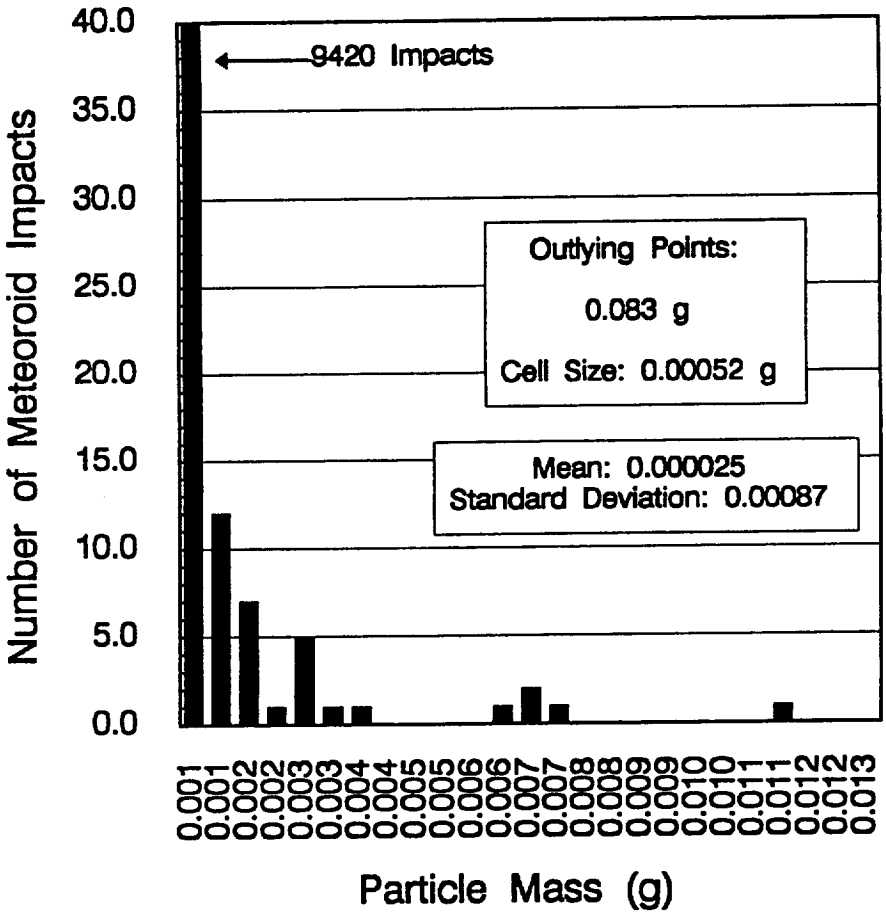

Figure 2.5-13. Meteoroid Impacts vs. Particle Mass

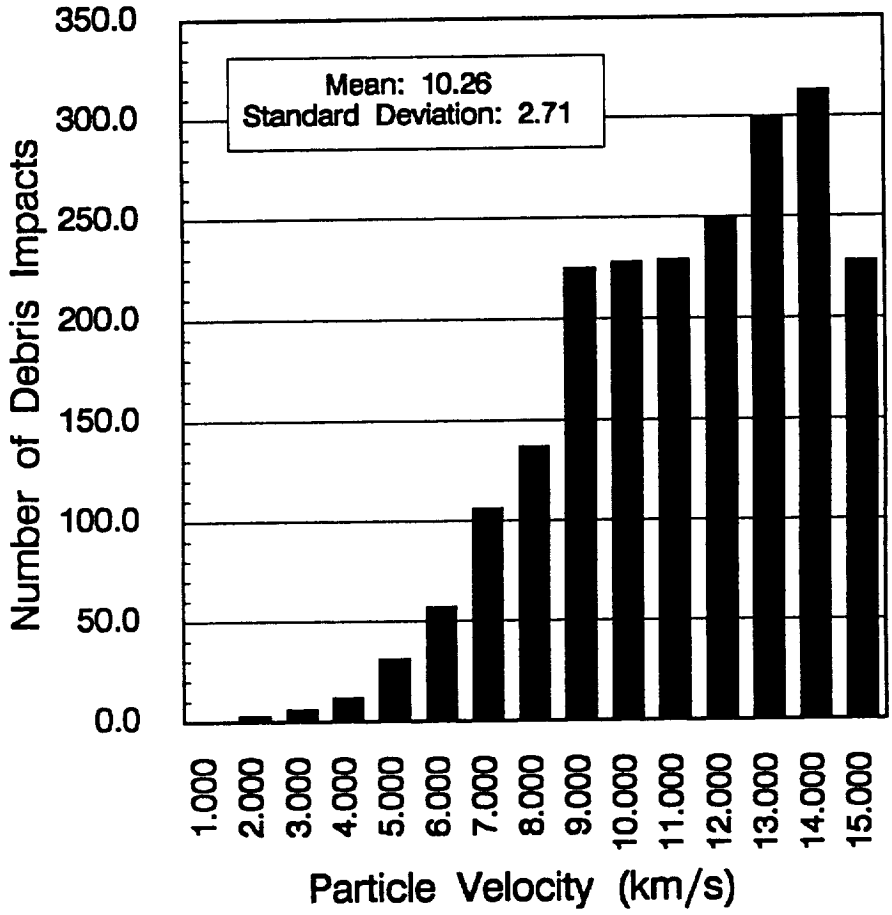

Figure 2.5-14. Debris Impacts vs. Particle Velocity

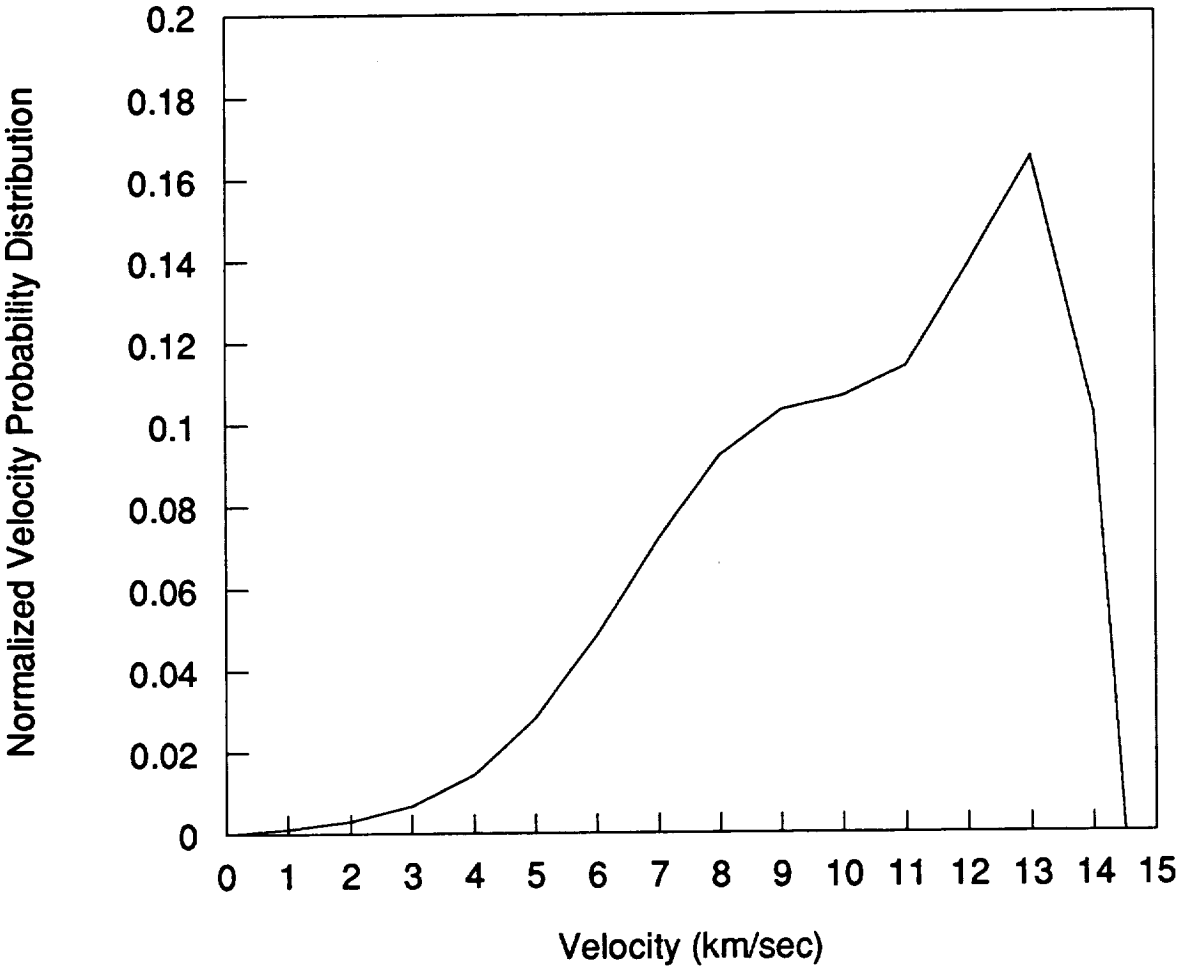

Figure 2.5-15. Velocity Probability Distribution for 28.5 Degrees Inclination

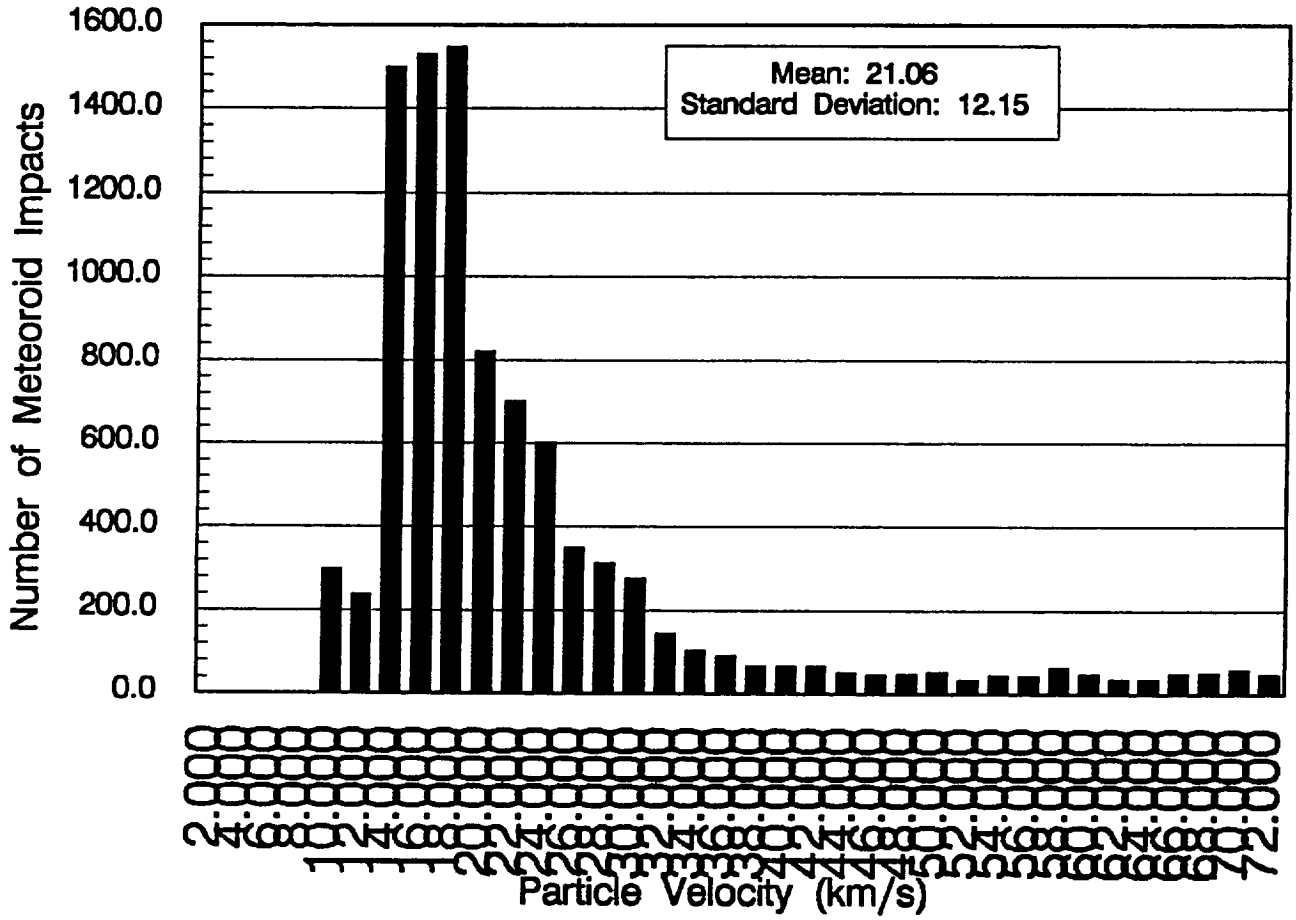

Figure 2.5-16. Meteoroid Impacts vs. Particle Velocity

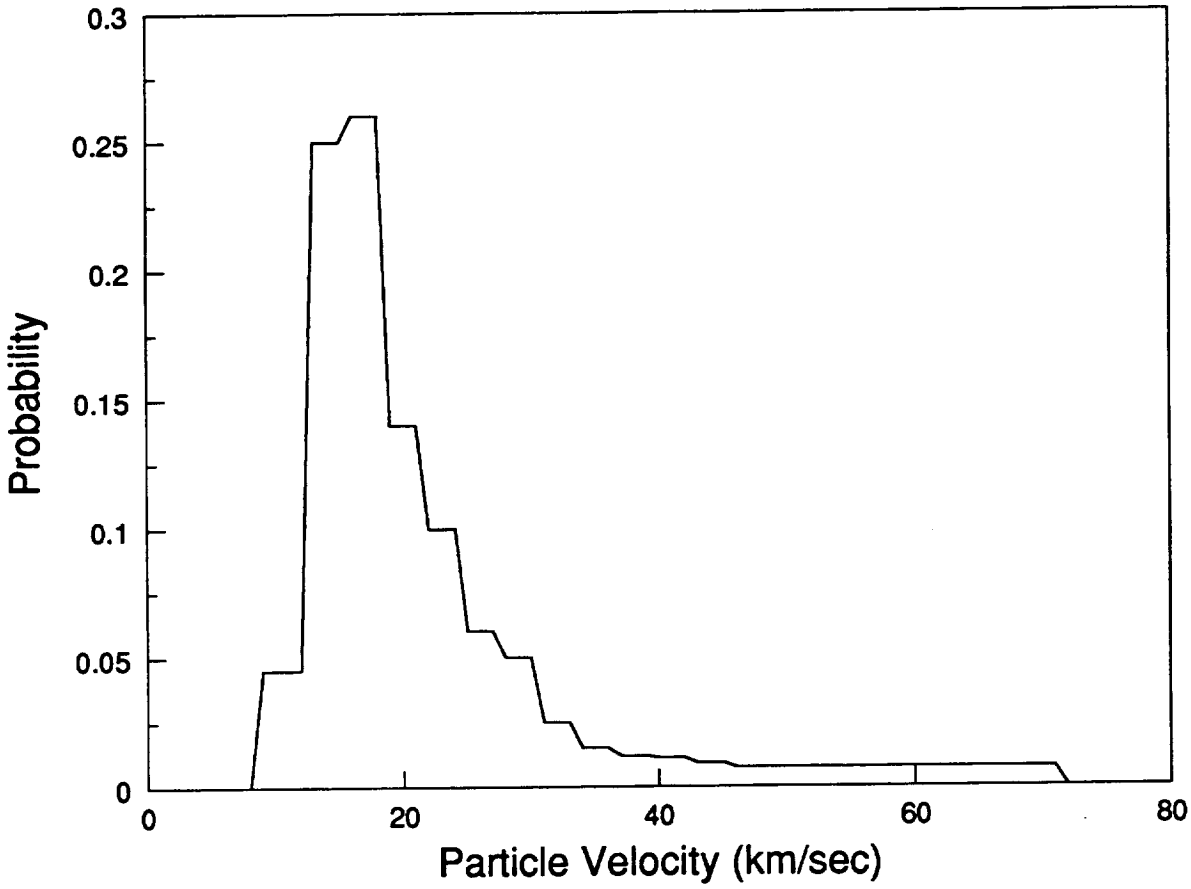

Figure 2.5-17. Meteoroid Velocity Probability Distribution

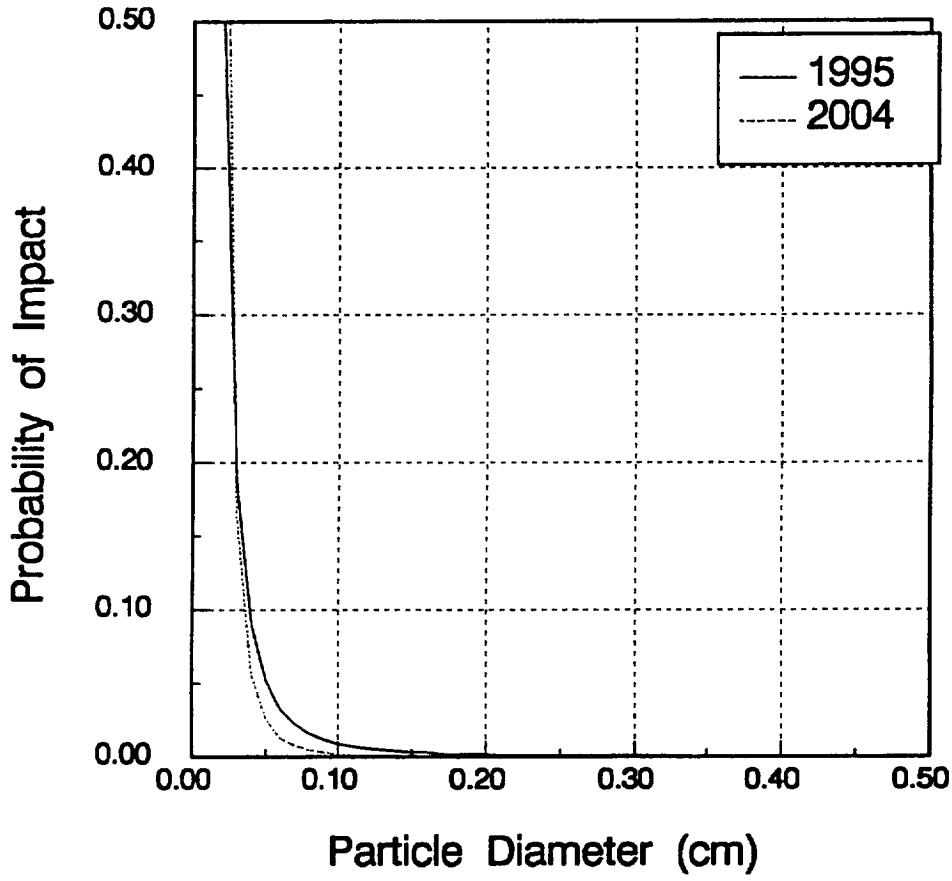

Figure 2.5-18. Debris Flux at Beginning and End of Mission

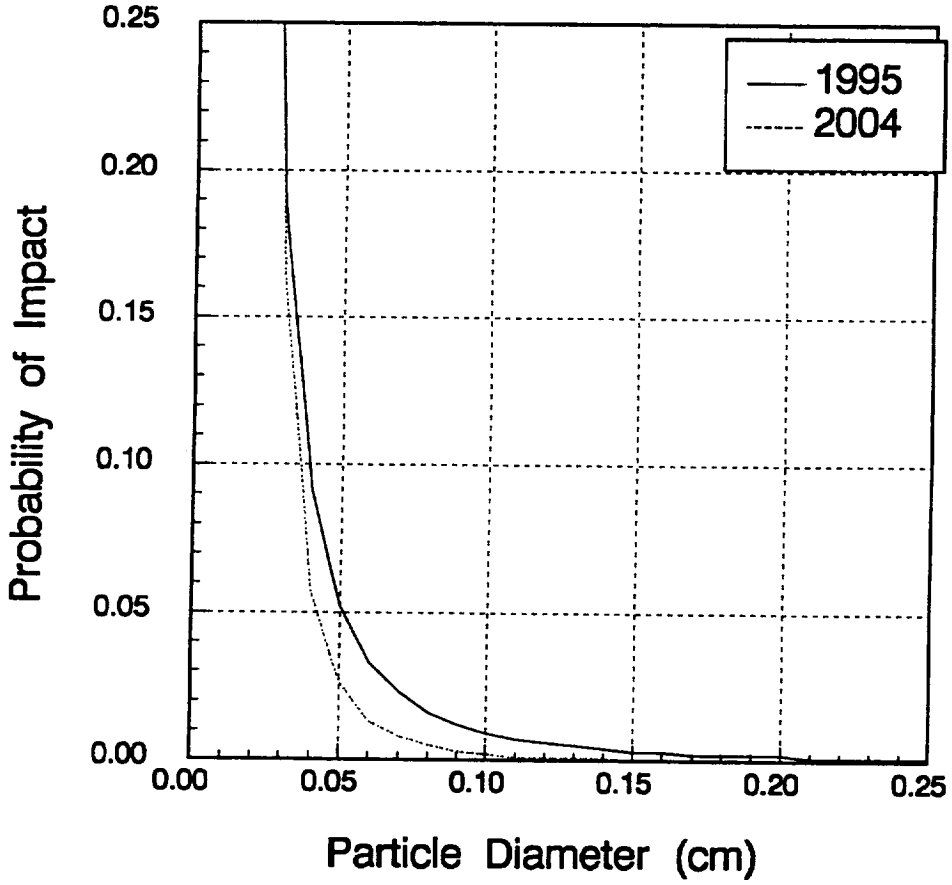

Figure 2.5-19. Debris Flux at Beginning and End of Mission

MULTIPLE RUN STATISTICS

Average CPU Time = 278.61 secs (Fidelity = 0.01 cm)

Average CPU Time = 319.13 secs (Fidelity = 0.02 cm)

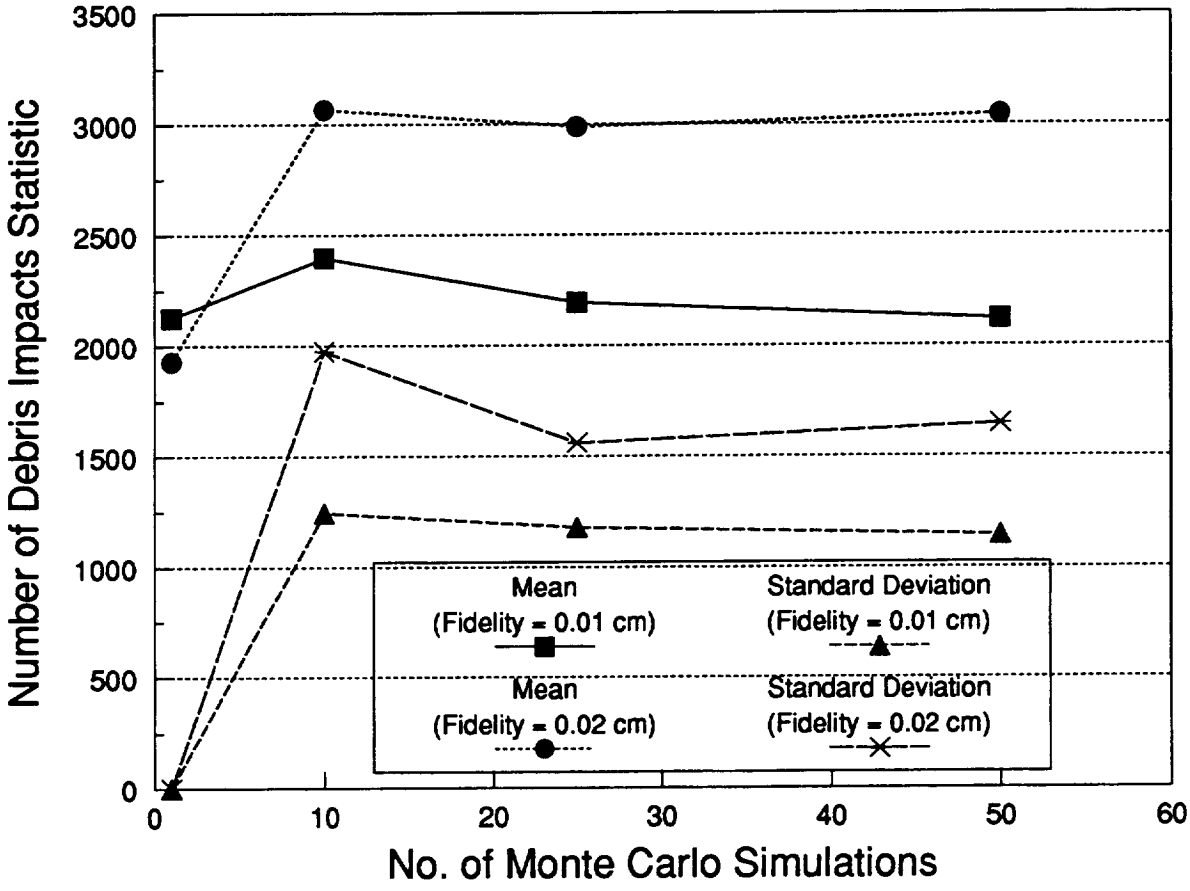

Figure 2.5-20. Multiple Run Statistics (Debris)

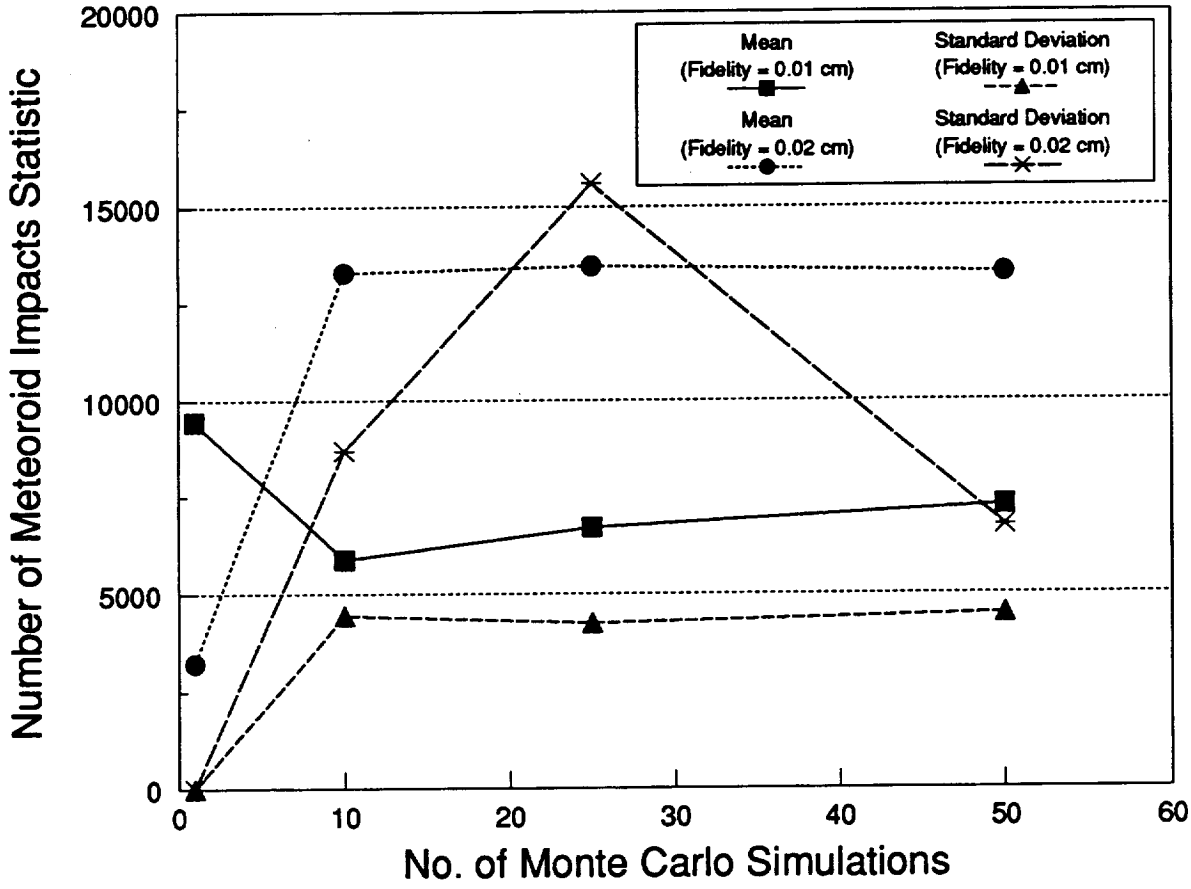

Figure 2.5-21. Multiple Run Statistics (Meteoroids)

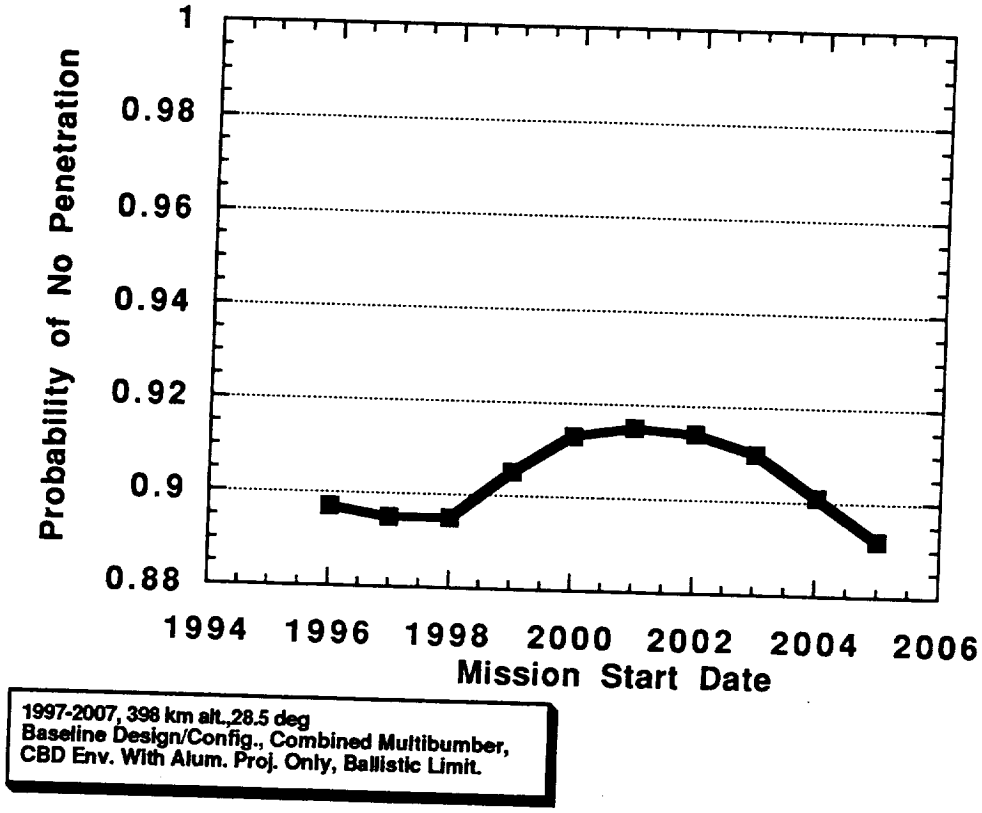

Figure 2.5-22. PNP VS. Mission Start Date

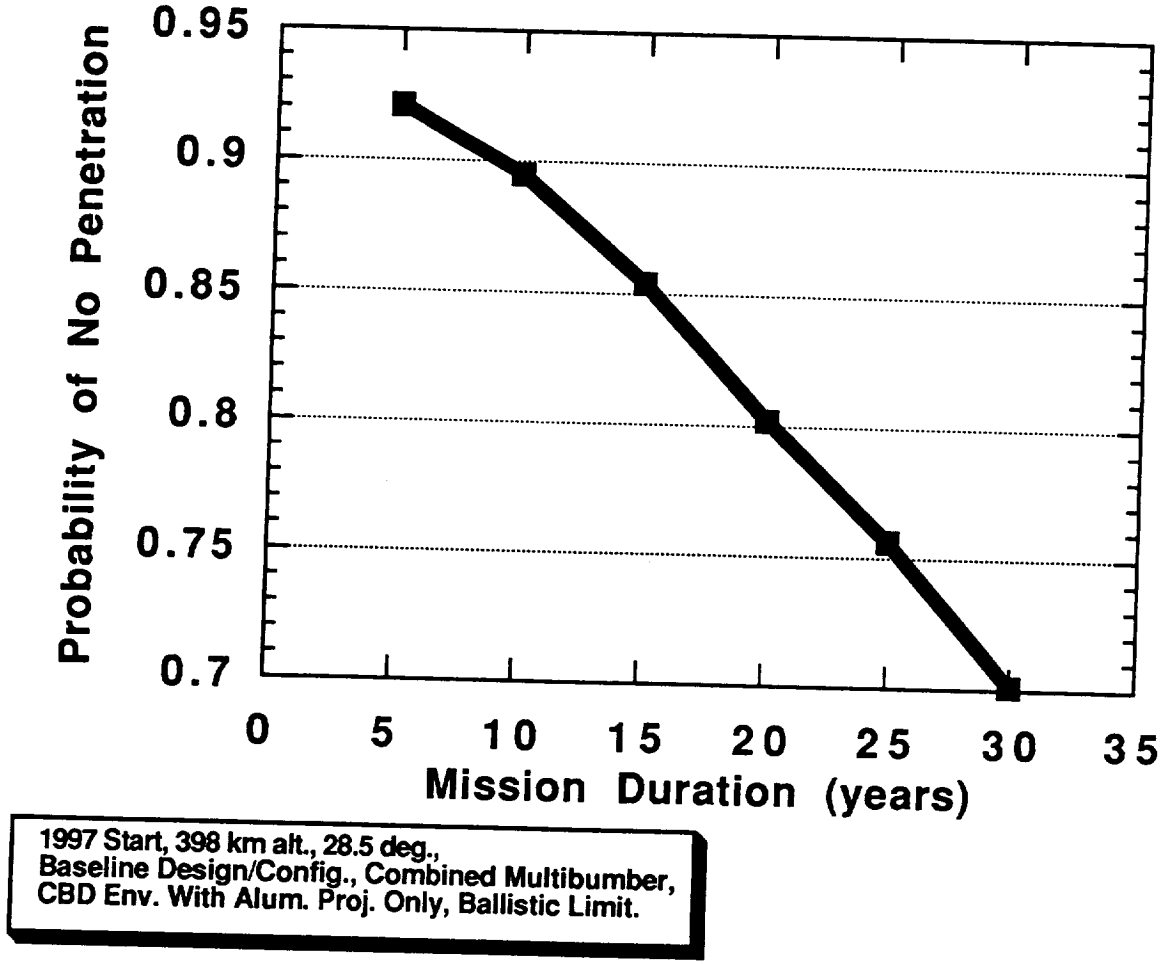

Figure 2.5-23. PNP VS. Mission Duration

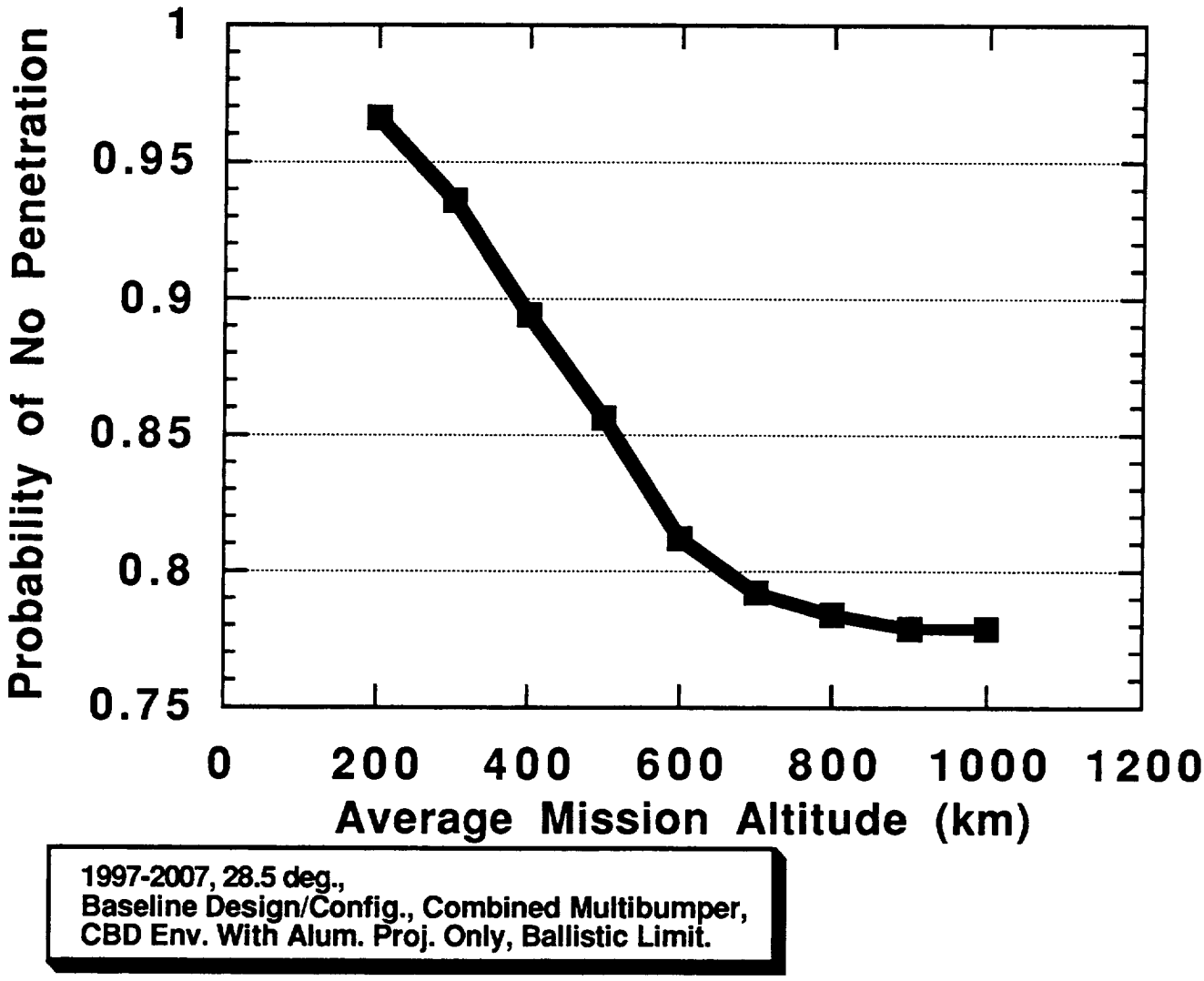

Figure 2.5-24. PNP VS. Average Mission Altitude

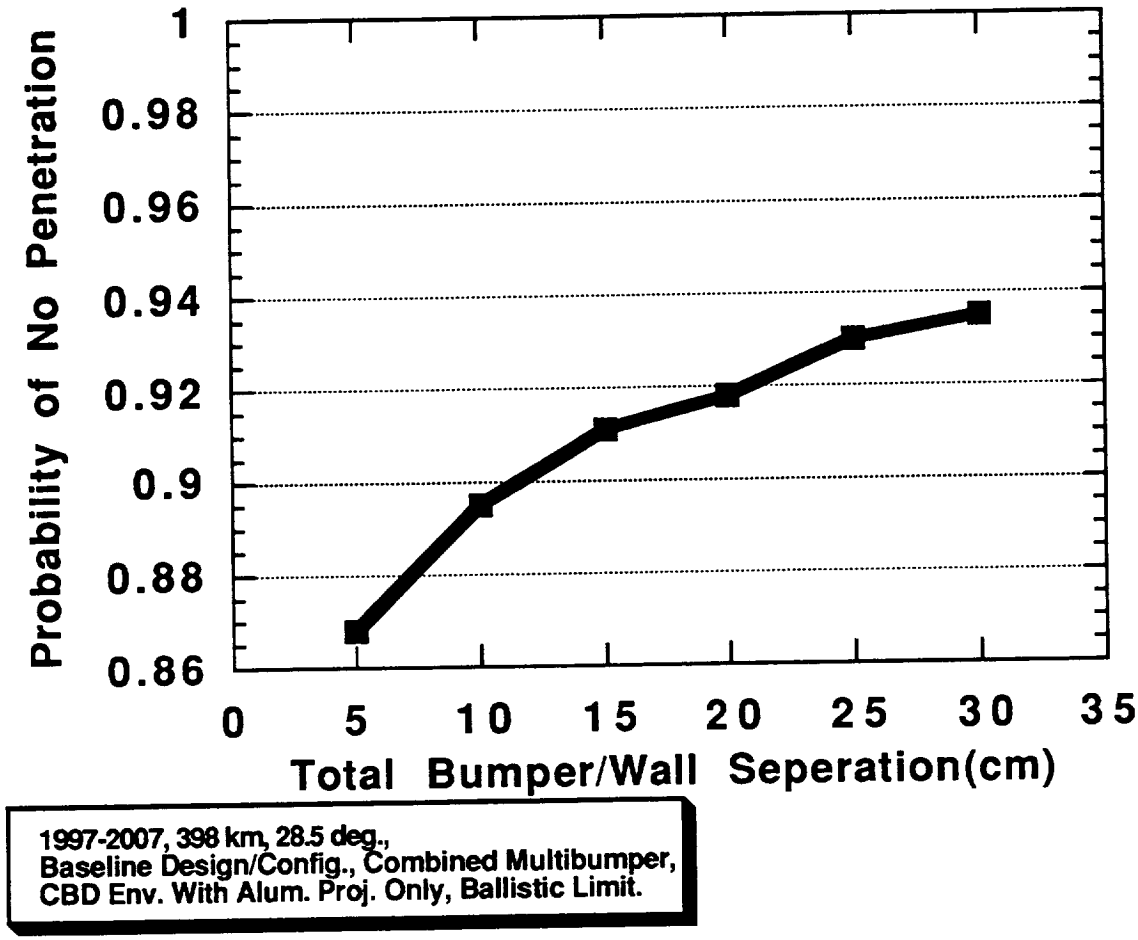

Figure 2.5-25. PNP VS. Total Bumper/Wall Separation

3 ADVANCED SHIELDING CONCEPTS TASK

3.1 Introduction

The development of advanced shielding concepts presented in this section includes a preliminary theoretical modification of the Wilkinson and ballistic PEN4 predictors to multiple bumper situations and nonlinear regression of multibumper test data from the MSFC Hypervelocity Impact Test Database.

3.2 Extension to Multiple Bumpers for Wilkinson Predictor

A number of different approaches have been attempted to modify the Wilkinson predictor theoretically for multiple bumper systems. The one successful approach (physically) found from these approaches is given as follows:

Modify the Wilkinson form in a product sense as:

$$t_n = \frac{0.364 D^3 \rho_p V \cos(\theta)}{L_n \left(\prod_{i=1}^{n-1} S_i^2 \right) \rho_n} \quad \text{for} \quad \frac{D \rho_p}{\prod_{i=1}^{n-1} \rho_i t_i} \le 1, \qquad [3.2-1]$$

$$t_n = \frac{0.364 D^4 \rho_p^2 V \cos(\theta)}{L_n \left(\prod_{i=1}^{n-1} S_i^2 \right) \left(\prod_{i=1}^{n-1} \rho_i t_i \right) \rho_n} \quad \text{for} \quad \frac{D \rho_p}{\prod_{i=1}^{n-1} \rho_i t_i} > 1. \qquad [3.2-2]$$

If our goal is to minimize system mass per unit area subject to the total separation between first bumper and last wall equal to some desired value, we may write this as

$$\min W = \sum_{i=1}^{n-1} m_i + \frac{0.364 D^4 \rho_p^2 V \cos\theta}{L_n \left(\prod_{i=1}^{n-1} S_i^2 \right) \left(\prod_{i=1}^{n-1} m_i \right)} \qquad [3.2-3]$$

$$s.t. \sum_{i=1}^{n-1} S_i = S_{ToT} \qquad [3.2-4]$$

$$where \quad m_i = \rho_i t_i \qquad [3.2-5]$$

S_{ToT} is the total separation between the first bumper and the wall, and n-1 is the total number of bumpers (n is the total number of plates).

Under condition [3.2-2], the dual Geometric Programming objective function is given by

$$\max v(\delta) = \prod_{i=1}^{n-1} (1/\delta_i)^{\delta_i} (K/\delta_n)^{\delta_n} \mu_1^{\mu_1} \prod_{j=1}^{n-1} \left(\frac{1}{S_{ToT}\delta_j'} \right)^{\delta_j'} \qquad [3.2-6]$$

$$K = \frac{0.364 D^4 \rho_p^2 V \cos(\theta)}{L_n} \qquad [3.2-7]$$

$$\sum_{i=1}^{n} \delta_i = 1 \qquad [3.2-8]$$

$$\delta_i - \delta_n = 0, \qquad i = 1,2,\ldots,n-1 \qquad [3.2-9]$$

$$-2\delta_n + \delta_j' = 0, \qquad j = 1,2,\ldots,n-1 \qquad [3.2-10]$$

$$\mu_1 = \sum_{j=1}^{n-1} \delta_j' \qquad [3.2-11]$$

Note that the degree of difficulty is 0, with 2n-2 independent variables corresponding to the n-1 bumper areal densities and the n-1 separations.

Equations [3.2-9] and [3.2-10] together imply

$$\delta_i = \delta_n = 1/n, \qquad i = 1,2,\ldots,n-1 \qquad [3.2-12]$$

$$\delta_j' = 2\delta_n = 2/n, \qquad j = 1,2,\ldots,n-1 \qquad [3.2-13]$$

The minimum weight and globally areal densities are given by

$$W_0 = n \left[\frac{0.364 D^4 \rho_p^2 V \cos(\theta)}{L_n} \right]^{1/n} \left(\frac{n-1}{S_{ToT}} \right)^{\frac{2n-2}{n}} \qquad [3.2-14]$$

$$m_{i_0} = \left[\frac{0.364 D^4 \rho_p^2 V \cos(\theta)}{L_n} \right]^{1/n} \left(\frac{n-1}{S_{ToT}} \right)^{\frac{2n-2}{n}}, \qquad i = 1,2,\ldots,n \qquad [3.2-15]$$

The optimal individual separations are given by

$$S_{j_0} = \frac{S_{ToT}}{n-1}, \qquad j = 1,2,\ldots,n-1 \qquad [3.2-16]$$

The optimal separations are equal and uniformly distributed over the total available separation. Thus, the globally optimal algorithm for the multi-bumper Wilkinson Predictor is

1. Determine $\prod_{i=1}^{n-1} m_{i_0}$ from equation [3.2-15].

2. Compute $\dfrac{D\rho_p}{\prod_{i=1}^{n-1} m_{i_0}}$.

3. If $\dfrac{D\rho_p}{\prod_{i=1}^{n-1} m_{i_0}} > 1$, then quit.

4. If $\dfrac{D\rho_p}{\prod_{i=1}^{n-1} m_{i_0}} \le 1$, the optimal design is $\left(m_{1_0}, m_{2_0}, \ldots, m_{n_0} / \left(\dfrac{D\rho_p}{\prod_{i=1}^{n-1} m_{i_0}}\right)\right)$.

3.3 Results

Several results using the development of Section 3.2 are given in this section. The baseline assumptions are a particle density of 2.8 gm/cm^3, velocity of 9 km/sec, diameter of 1 cm, impacting normally into a configuration with a total bumper/wall separation of 10 cm.

Figures 3.3-1 and 3.3-2 show how the optimal protective structures design configuration varies with number of bumpers for projectile diameters of 1 and 3 cm, respectively. Note that

for a 1 cm particle diameter, the optimal number of bumpers is 2, while for 3 cm, it is 3 bumpers. Also, note the significant penalty for choosing the wrong number of bumpers in these cases, as well as the lack of symmetry of these penalties about the optimal number of bumpers.

Figure 3.3-3 shows the optimal protective structures design configuration including optimal number of bumpers as a function of particle diameter. Increasing particle diameter results in an increasing optimal number of bumpers to defeat the particle. Note the optimal transition regions between 1 and 2 bumpers (corresponding to particle diameters between 0.75 and 1 cm) and 2 and 3 bumpers (corresponding to particle diameters between 2.25 and 2.5 cm). Also, note the very linear minimum system areal density, showing the stabilizing effect of increasing the number of bumpers in the configuration.

Figure 3.3-4 shows the optimal protective structures design configuration including optimal number of bumpers as a function of particle velocity. The most striking feature of this trade is the relative insensitivity to velocity for a dual bumper system.

Figure 3.3-5 shows the optimal protective structures design configuration as a function of total bumper/wall separation. As in previous studies, there is a large weight incentive for increasing the total separation. Furthermore, increased separation allows for more bumpers to disrupt the incoming particle.

Figure 3.3-6 is a replica of **Figure 3.3-5**, except that the optimal individual separations are included.

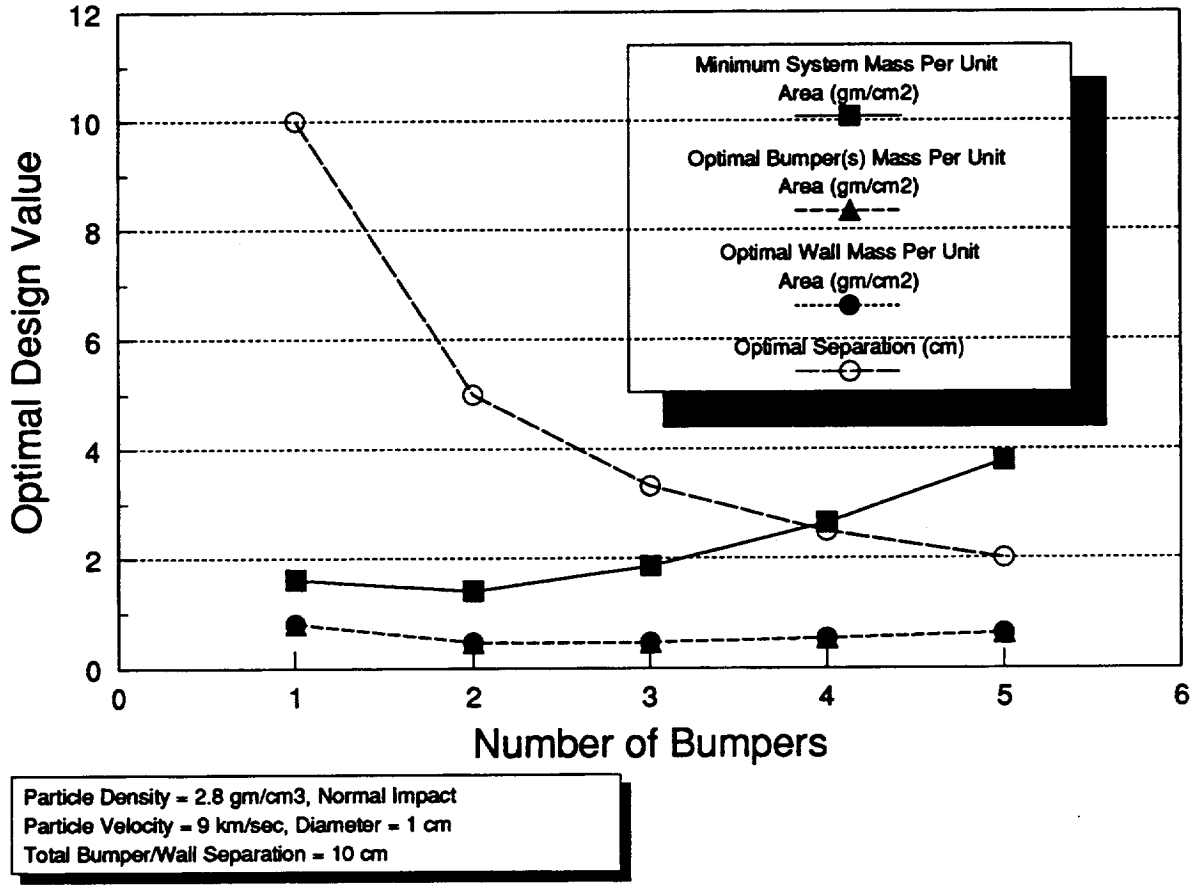

Figure 3.3-1. Determining Optimal Number of Bumpers for Multibumper Wilkinson

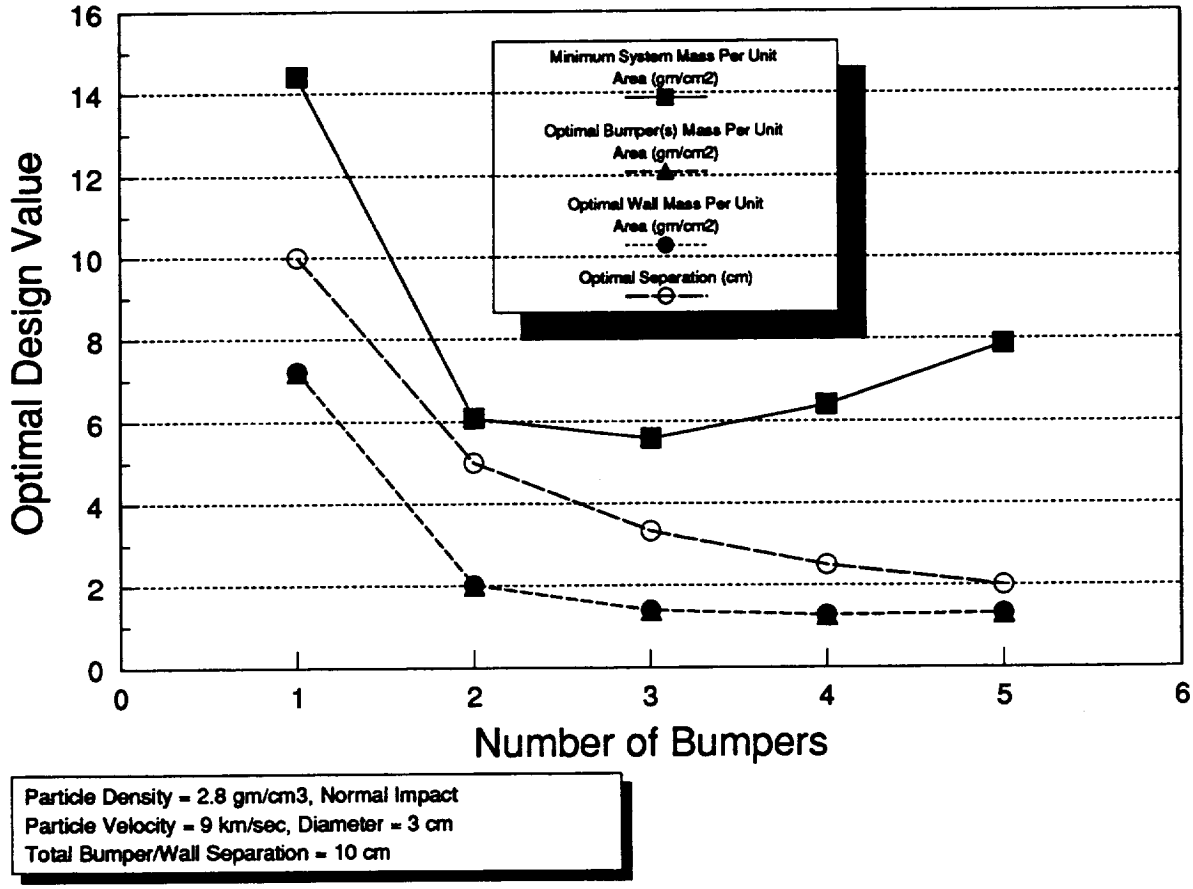

Figure 3.3-2. Determining Optimal Number of Bumpers for Multibumper Wilkinson

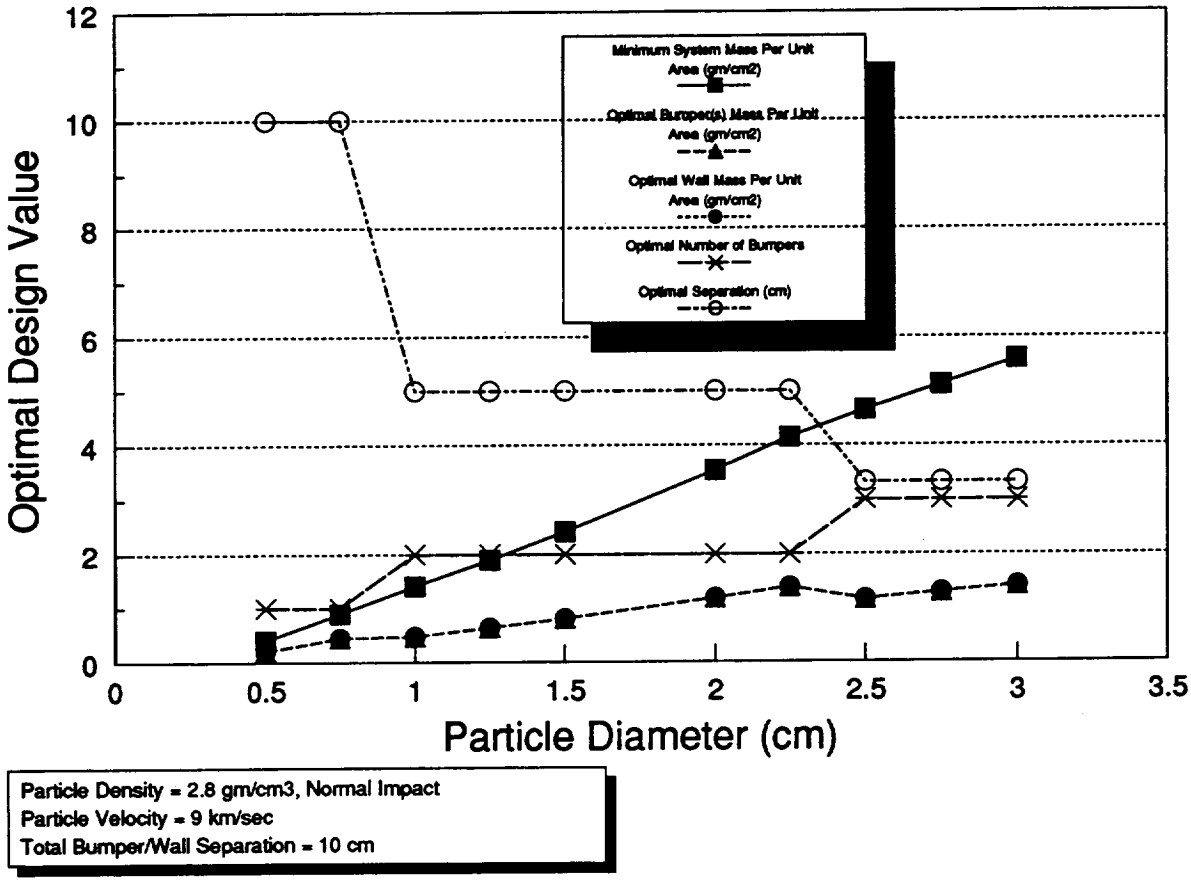

Figure 3.3-3. Optimal Protective Structures Design Values vs. Particle Diameter (Multibumper Wilkinson)

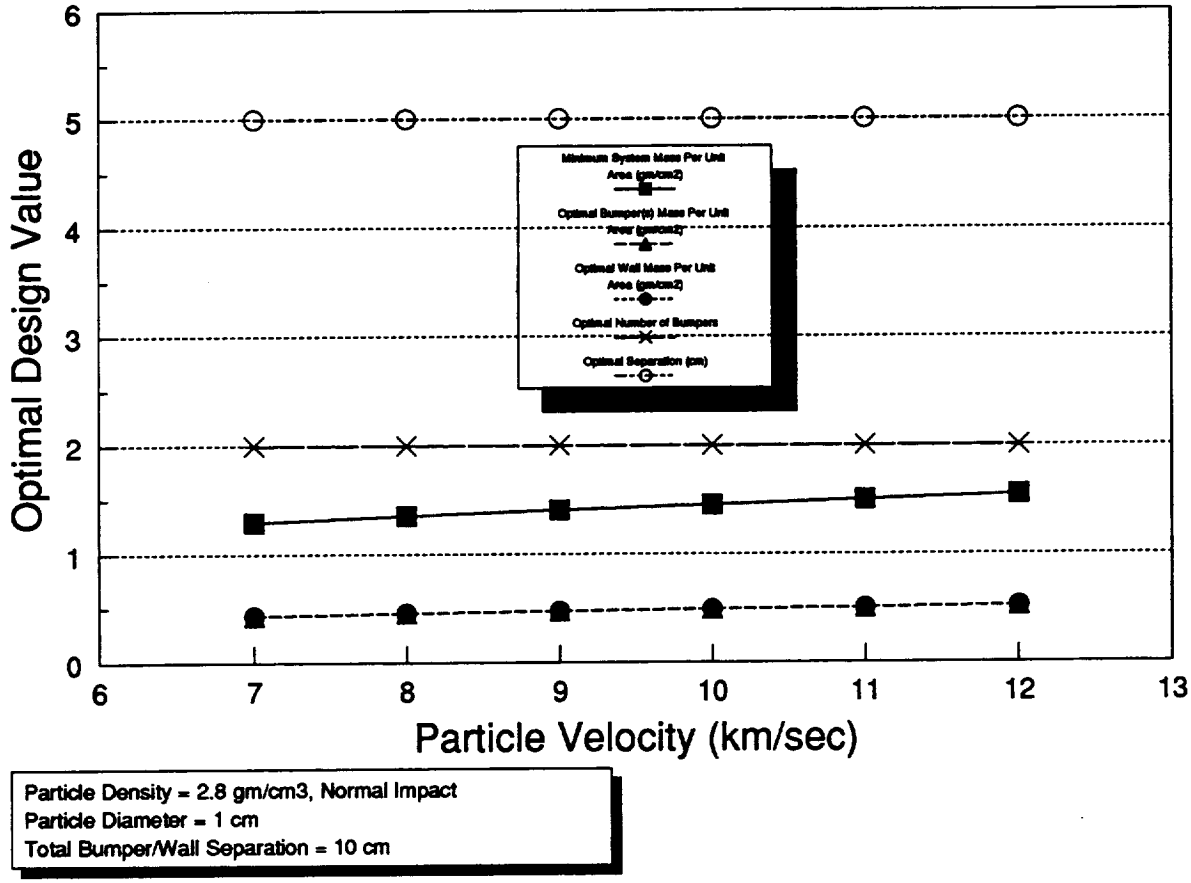

Figure 3.3-4. Optimal Protective Structures Design Values vs. Particle Velocity (Multibumper Wilkinson)

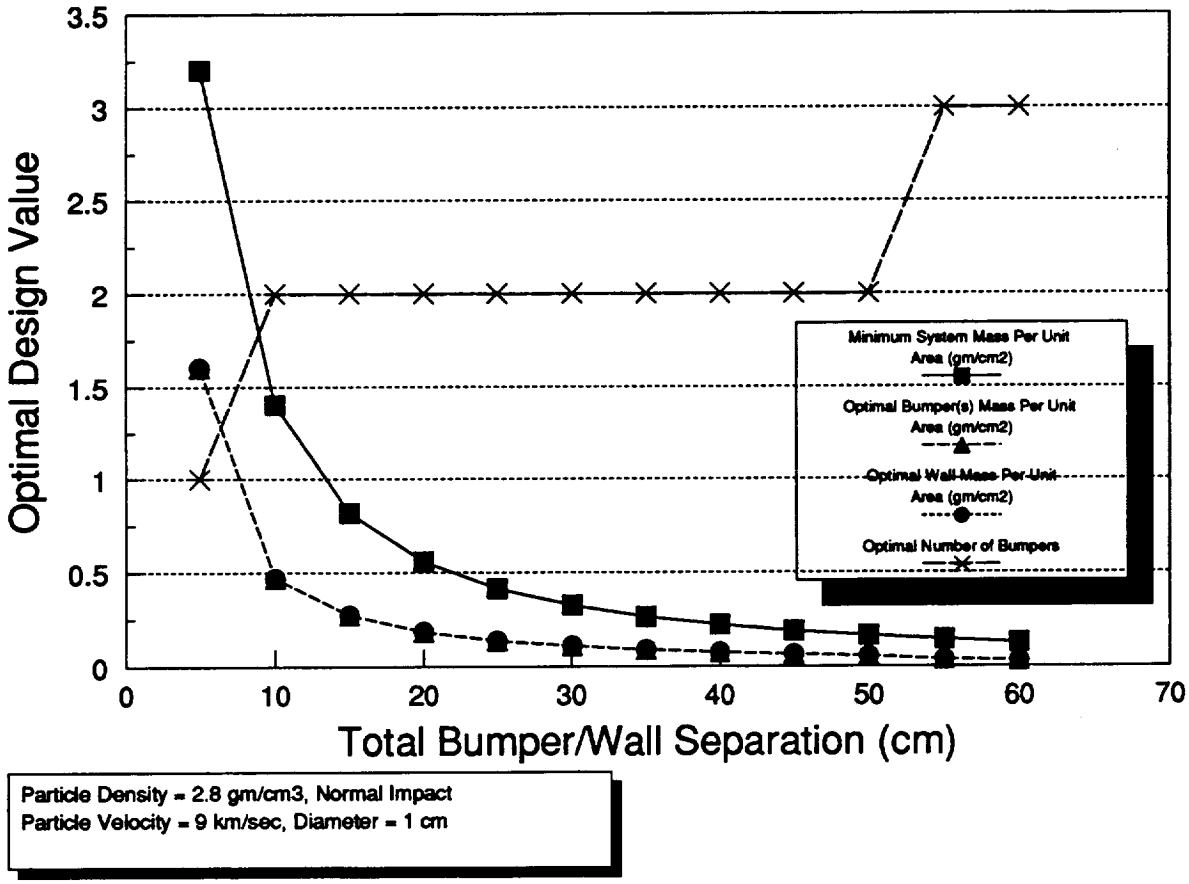

Figure 3.3-5. Optimal Protective Structures Design Values vs. Total Bumper/Wall Separation (Multibumper Wilkinson)

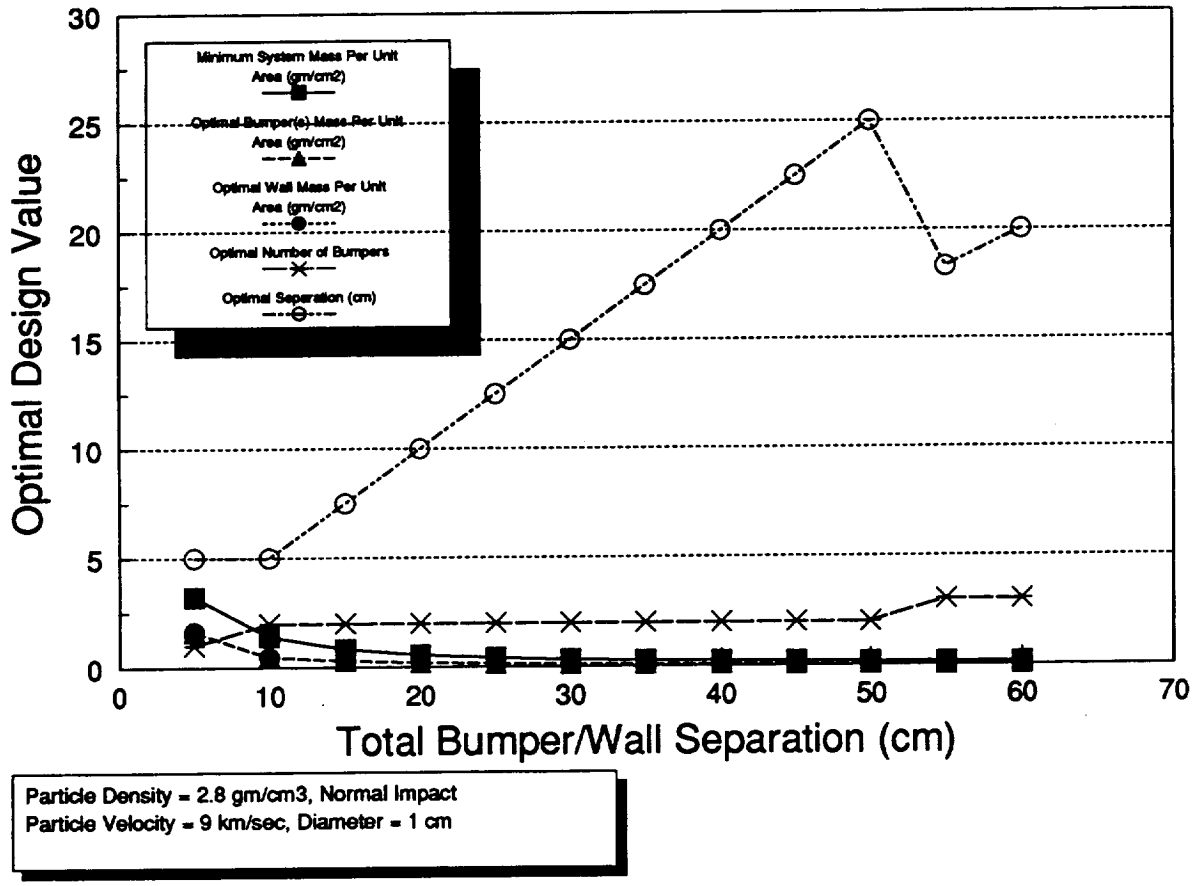

Figure 3.3-6. Optimal Protective Structures Design Values vs. Total Bumper/Wall Separation (Multibumper Wilkinson)

3.4 Extension to Multiple Bumpers for Ballistic PEN4 Predictor

The multiple bumper recursion equations are given by:

$$V_f = 4100, \quad \frac{T_1}{D} \le 0.4 \qquad [3.4-1]$$

$$V_f = 4986\left(\frac{T_1}{D}\right)^{0.21}, \quad \frac{T_1}{D} > 0.4 \qquad [3.4-2]$$

$$V_{50_j} = \left[\left(\frac{0.6T_j}{\left(\frac{0.281D\rho_p}{\rho_j}\right)^{1/3}\cos(\theta)}\right)^{1/0.31}\frac{2S_{y_j}}{\rho_p}\right]^{1/2} \qquad [3.4-3]$$

The first bumper is penetrated if

$$V > V_{50_{j-1}} \qquad [3.4-4]$$

The residual velocity (from the first bumper) is

$$V_{R_1} = \left[\frac{1.33V^2R_p^2\rho_p - \left(8S_{y_1}T_1e^{-0.0003125V}\right)/\cos(\theta)}{1.33R_p^2\rho_p + R_pT_1\rho_1/\cos(\theta)}\right]^{1/2} \qquad [3.4-5]$$

The second bumper is penetrated if

$$V_{R_1} > V_{50_{j-2}} \qquad [3.4-6]$$

The residual velocity (from the second bumper) is

$$V_{R_2} = \left[\frac{1.33V_{R_1}^2R_p^2\rho_p - \left(8S_{y_2}T_2e^{-0.0003125V_{R_1}}\right)/\cos(\theta)}{1.33R_p^2\rho_p + R_pT_2\rho_2/\cos(\theta)}\right]^{1/2} \qquad [3.4-7]$$

The third bumper is penetrated if

$$V_{R_2} > V_{50_{j=3}} \qquad [3.4-8]$$

.

.

.

The residual velocity (from the (n-1)st bumper) is

$$V_{R_{n-1}} = \left[\frac{1.33V_{R_{n-2}}^2 R_p^2 \rho_p - \left(8S_{y_{n-1}} T_{n-1} e^{-0.0003125V_{R_{n-2}}} \right) / \cos(\theta)}{1.33R_p^2 \rho_p + R_p T_{n-1} \rho_{n-1} / \cos(\theta)} \right]^{1/2} \qquad [3.4-9]$$

The nth bumper is penetrated if

$$V_{R_{n-1}} > V_{50_{j=n}} \qquad [3.4-10]$$

3.5 Advanced Shielding Task For Projectile Shatter (Multibumpers)

The database used for regression is the MSFC Hypervelocity Impact Test Database Developed by the Materials & Processes Lab. Database filtering was performed by Bill Jolly of Sverdrup Technology Inc. Data constraints include metallic configurations with velocities greater than 2.5 km/sec and no MLI present. The database filtering resulted in 234 single bumper tests, 72 double bumper tests, and 7 triple bumper tests. A preliminary investigation using various posynomial regression forms was performed. The fact that Space Station *Freedom* has sufficiently low curvature in primary areas needing protection allows for the assumption of minimizing system mass per unit area. The "best" intrinsically linear posynomial form resulting from this preliminary investigation is given by:

$$N+1 = Kd^{a_1} \rho_p^{a_2} V^{a_3} \left[\cos\left(\frac{\theta}{g(n-1)} \right) \right]^{a_4} \left(\prod_{i=1}^{n-1} S_i \right)^{\frac{a_5}{\lambda(n-1)}} \left(\prod_{i=1}^{n-1} \rho_i t_i \right)^{\frac{a_6}{\lambda(n-1)}} (\rho_n t_n)^{a_7} (n-1)^{a_8} \qquad [3.5-1]$$

A linear least squares analysis results in:

$$K = 3.8010, \quad a_1 = 1.0301, \quad a_2 = 0.3892, \quad a_3 = 0.2879,$$

$$a_4 = 0.3288, \quad a_5 = -0.4876, \quad a_6 = -0.3464, a_7 = -0.2929, \quad a_8 = -0.6137 \qquad [3.5-2]$$

with optimal bumper scaling functions (found through search) of

$$g(n-1) = n-1, \quad h(n-1) = (n-1)^{0.65} \qquad [3.5-3]$$

Table 3.5-1 shows the resulting analysis of variance.

Table 3.5-1. Analysis of Variance

Source	Degrees of Freedom	Sum of Squares	Mean Square	F Value
Total (uncorrected)	313	284.03	0.9074	-----
Mean	1	185.81	185.81	-----
Total (corrected)	312	98.22	0.3148	-----
Regression	8	29.56	3.695	16.363
Residual	304	68.66	0.2258	-----

The regression F value of 16.363 is greater than the table value corresponding to the 1% significance level with 8 numerator degrees of freedom and 312 denominator degrees of freedom. This table value is roughly 2.51. Therefore, we reject the null hypothesis that the slope vector of the regression plane is significantly close to 0, and we conclude that the assumption of a linear relationship between the natural log values is statistically significant.

The correlation coefficient is given by

$$R^2 = 0.301 \qquad [3.5-4]$$

$$R = 0.549 \qquad [3.5-5]$$

The table value for the correlation coefficient at the 1% significance level, 9 total estimated values, and 312 degrees of freedom is well below 0.5. Since R is greater than this table value, we reject the null hypothesis that there is low statistical correlation in this regression. Additionally, the student-t statistic of 13.85 is well above the table value of 2.576 corresponding to a significance of 0.5% and an infinite number of degrees of freedom. This allows us to reject the null hypothesis that the correlation is low.

The residual plots are shown in **Figures 3.5-1 through 3.5-9**. The only suspicious plot appears to be the one for residuals vs. number of bumpers. This correlation could be due to the fact that a single term posynomial does not sufficiently represent the hypervelocity impact phenomena over potentially complex differences between 1, 2, and 3 bumpers.

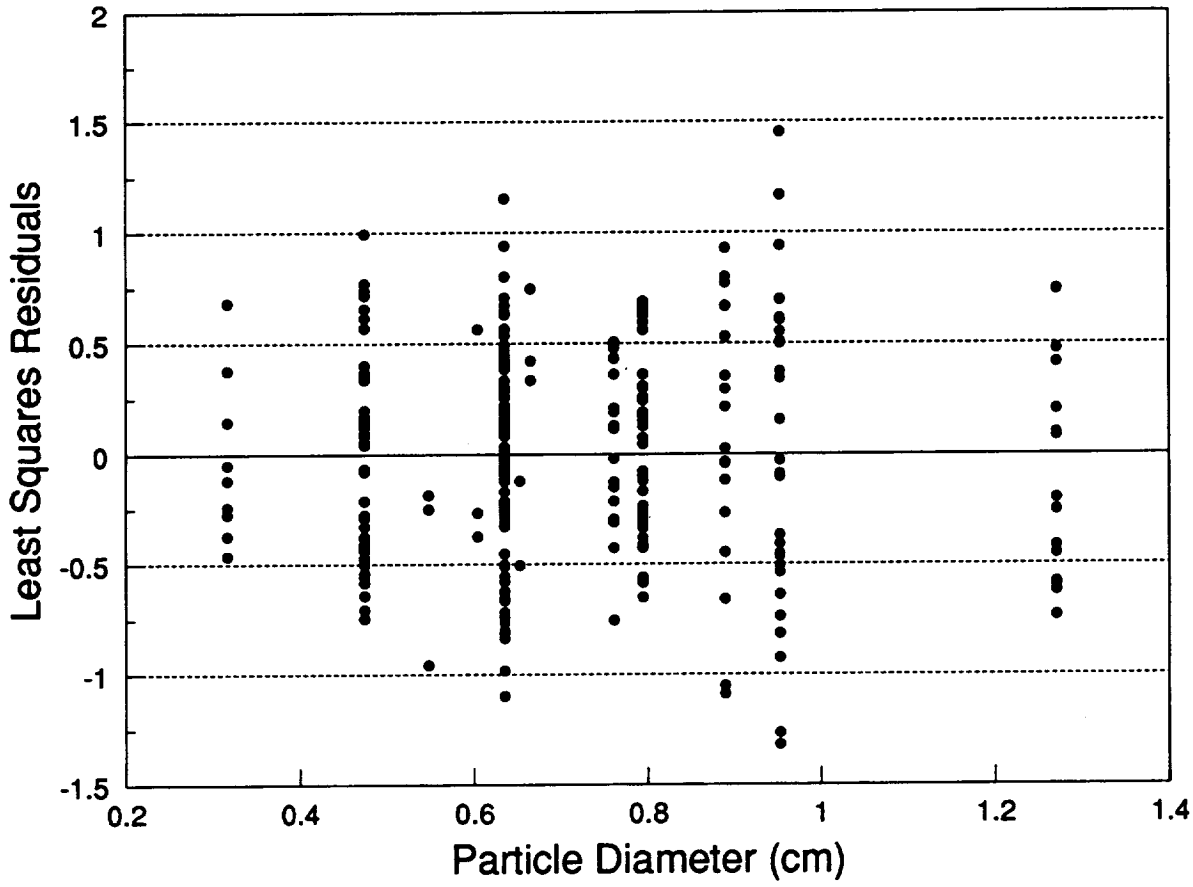

Figure 3.5-1. Residuals vs Particle Diameter for Shatter Region

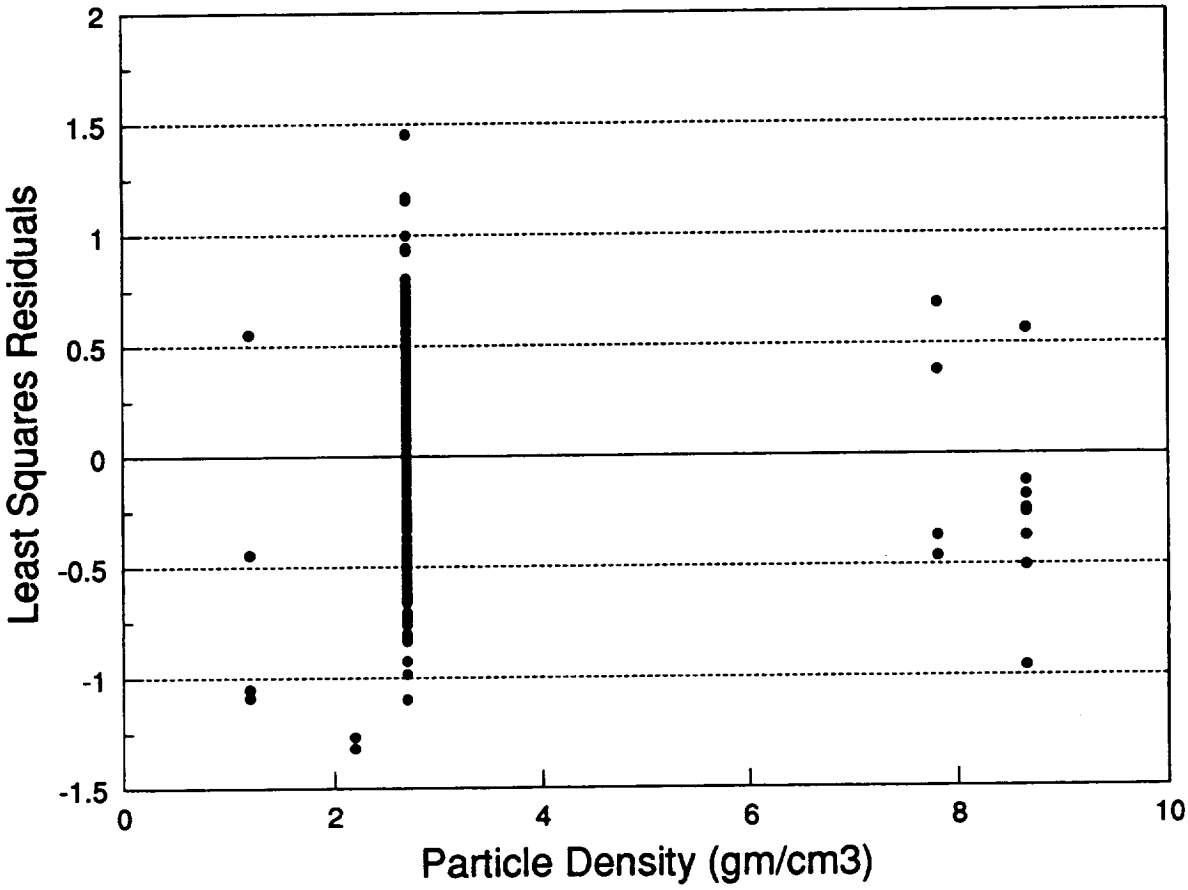

Figure 3.5-2. Residuals vs Particle Density for Shatter Region

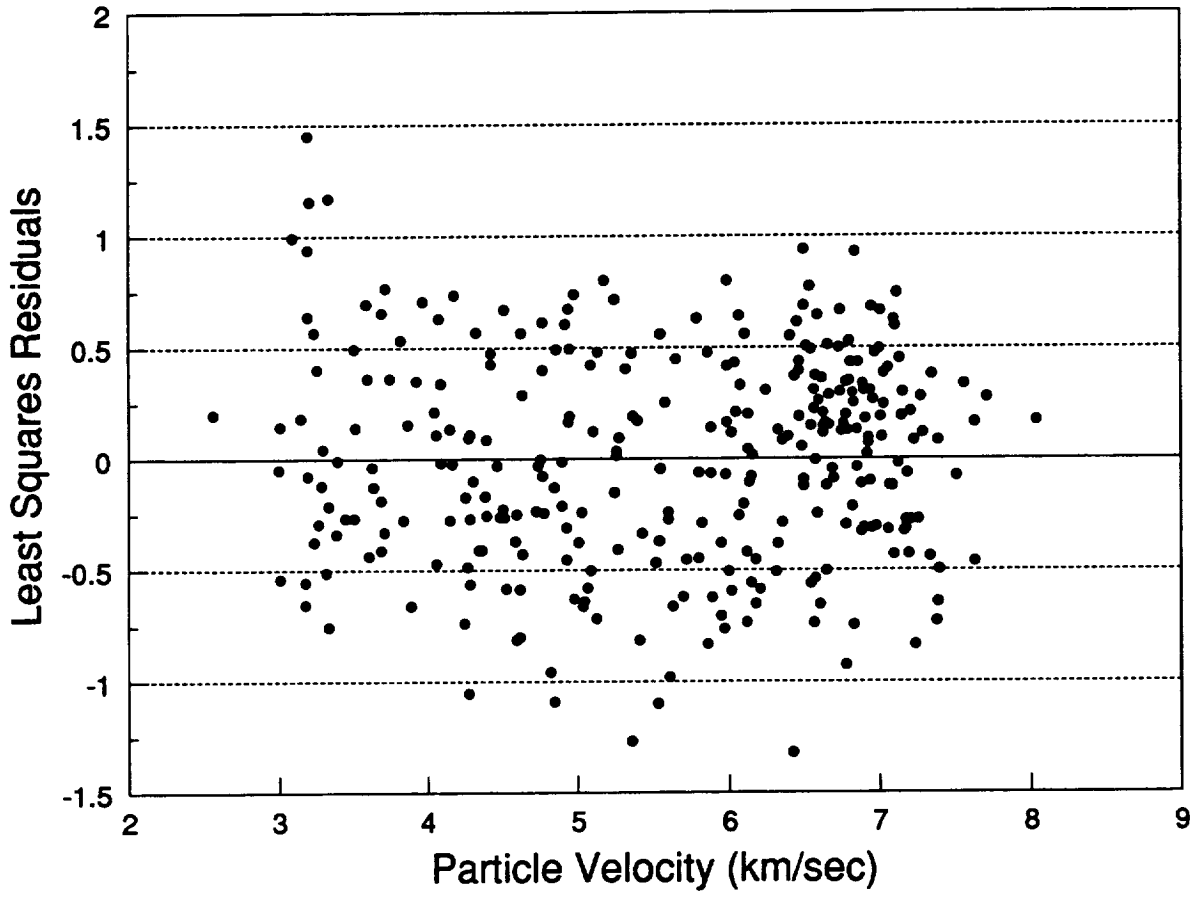

Figure 3.5-3. Residuals vs Particle Velocity for Shatter Region

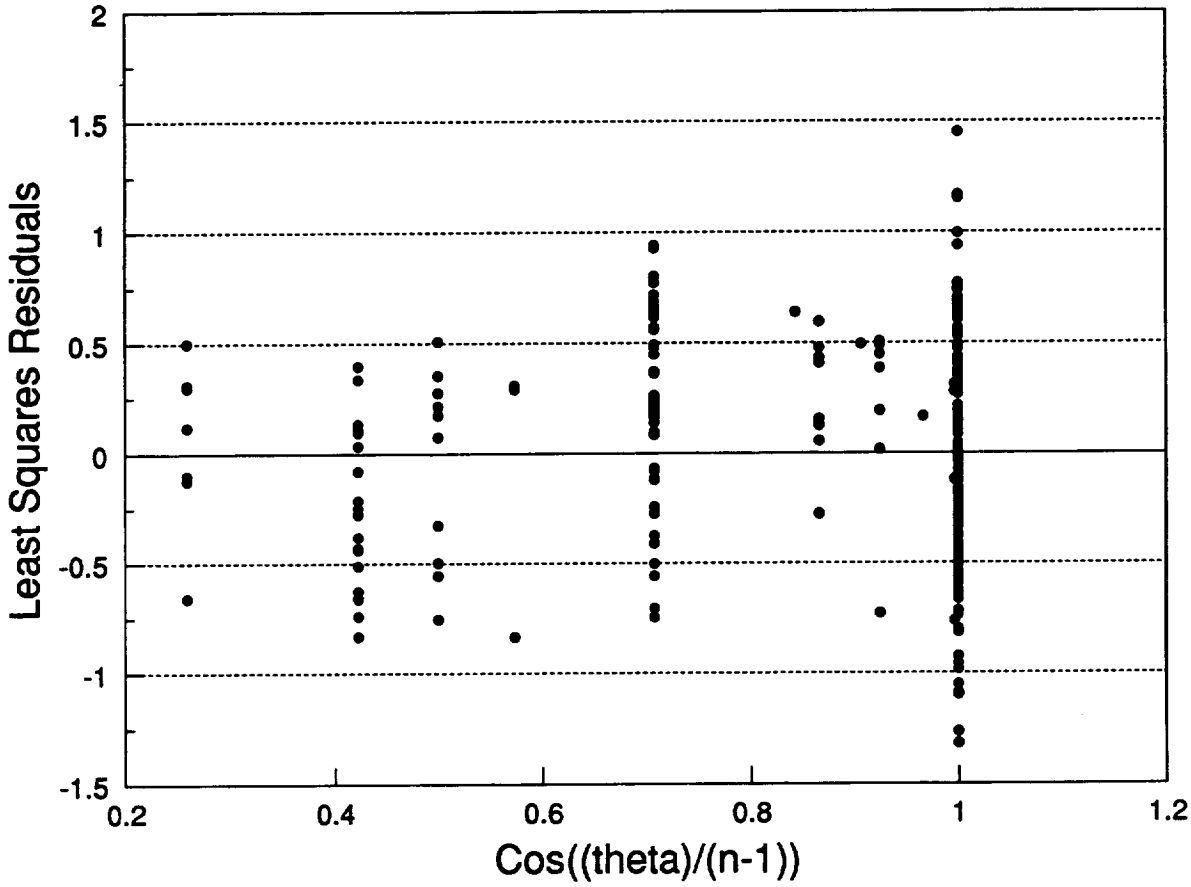

Figure 3.5-4. Residuals vs Particle Impact Angle from Normal Factor for Shatter Region

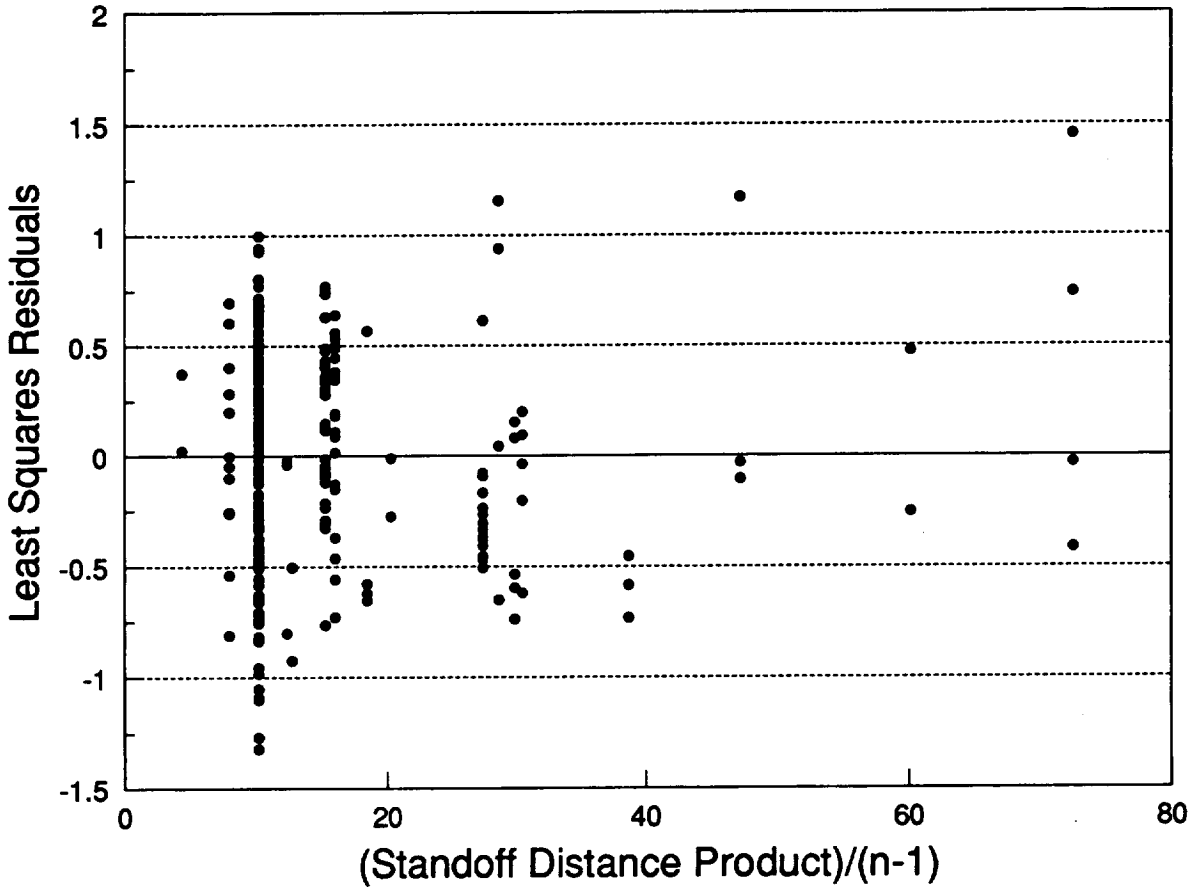

Figure 3.5-5. Residuals vs Standoff Distance Factor for Shatter Region

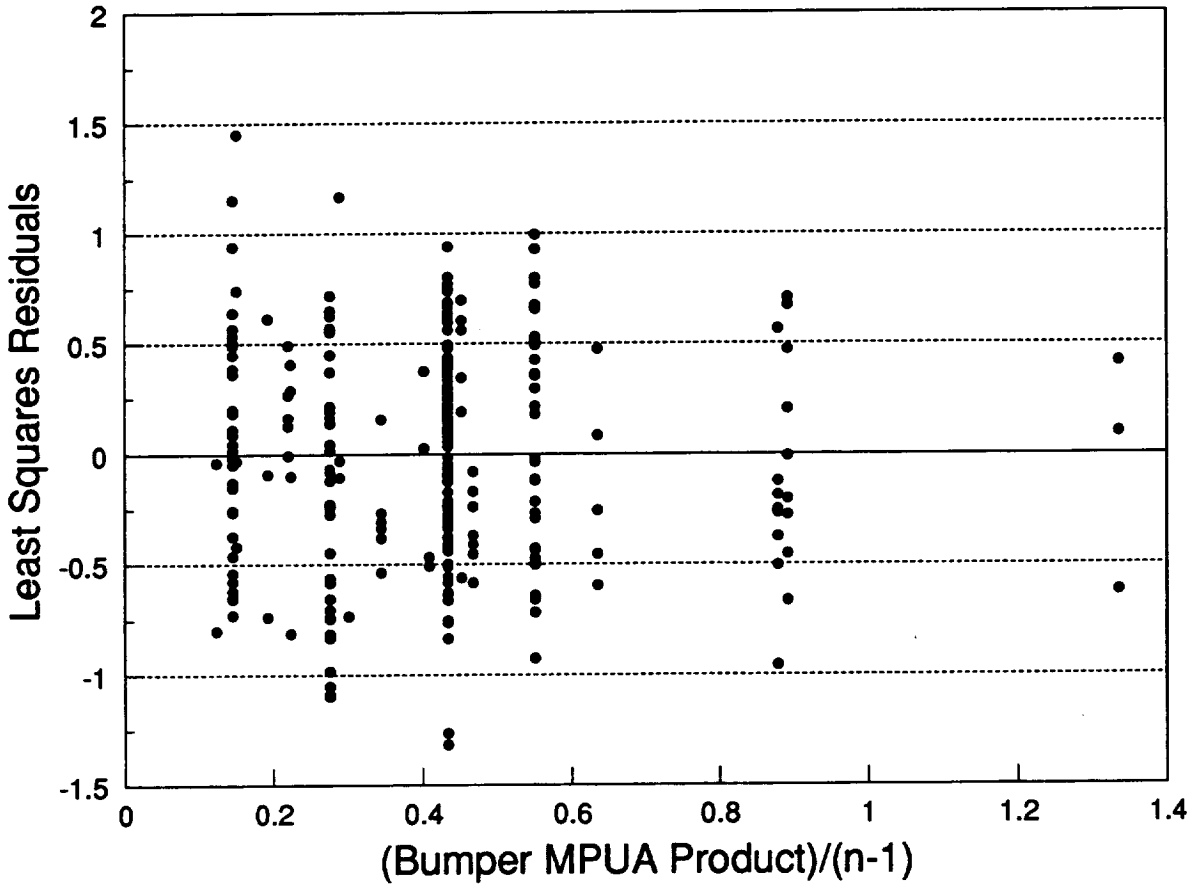

Figure 3.5-6. Residuals vs Bumper Mass Per Unit Area Factor for Shatter Region

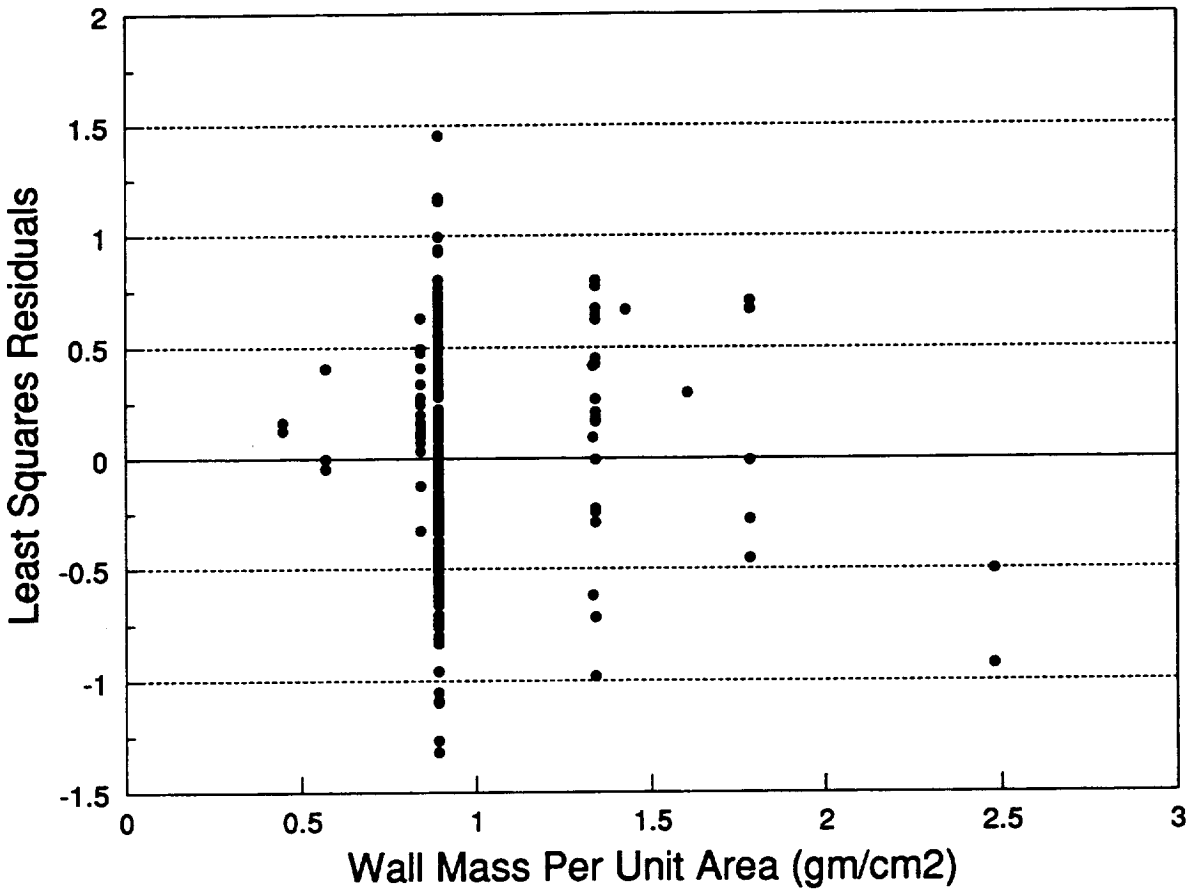

Figure 3.5-7. Residuals vs Wall Mass Per Unit Area for Shatter Region

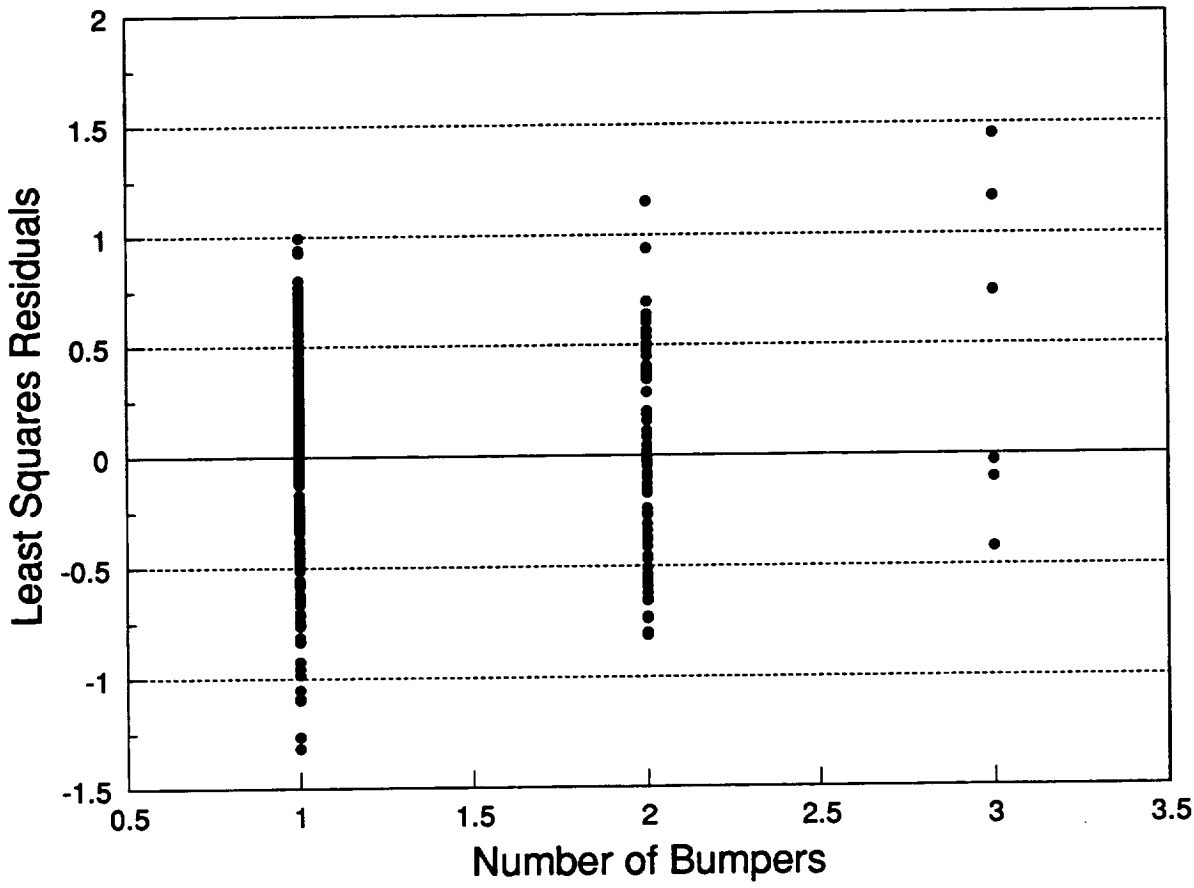

Figure 3.5-8. Residuals vs Number of Bumpers for Shatter Region

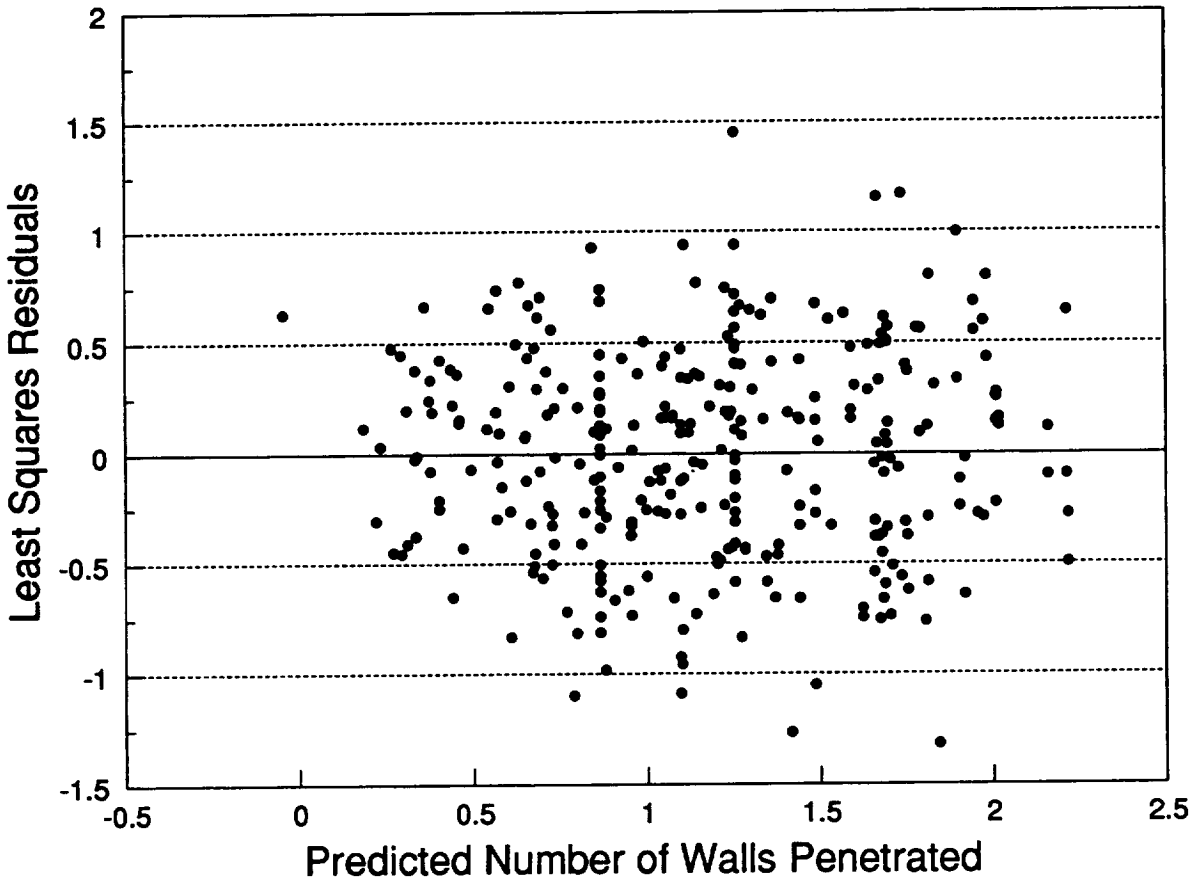

Figure 3.5-9. Residuals vs Predicted Values for Shatter Region

The designer problem statement is given by:

Minimize system mass per unit area:

$$\min W = \sum_{i=1}^{n-1} m_i + \frac{K}{\left(\prod_{i=1}^{n-1} S_i^{\frac{1.6647}{(n-1)^{0.65}}}\right)\left(\prod_{i=1}^{n-1} m_i^{\frac{1.1827}{(n-1)^{0.65}}}\right)} \qquad [3.5-6]$$

where

$$K = \frac{9.5466 d^{3.5169} \rho_p^{1.3288} V^{0.9829} \left[\cos\left(\frac{\theta}{n-1}\right)\right]^{1.1226}}{(N+1)^{3.4141}(n-1)^{2.0953}} \qquad [3.5-7]$$

subject to the following constraint: The total separation (first bumper to wall) is limited to a prespecified value

$$s.t. \sum_{i=1}^{n-1} S_i = S_{ToT}$$

$$where \quad m_i = \rho_i t_i \qquad [3.5-8]$$

We must determine the optimal values of the mass per unit area for the bumper(s) and wall, the optimal individual separations, and the minimum system mass per unit area. (S_{ToT} is the total separation between the first bumper and the wall, and n-1 is the total number of bumpers (n is the total number of plates).)

The problem solution is developed using Geometric Programming. The dual Geometric Programming objective function is given by

$$\max v(\delta) = \prod_{i=1}^{n-1} (1/\delta_i)^{\delta_i} (K/\delta_n)^{\delta_n} \mu_1^{\mu_1} \prod_{j=1}^{n-1} \left(\frac{1}{S_{ToT}\delta_j'}\right)^{\delta_j'} \qquad [3.5-10]$$

$$\sum_{i=1}^{n} \delta_i = 1 \qquad [3.5-11]$$

$$m_i: \qquad \delta_i - \frac{1.1827}{(n-1)^{0.65}}\delta_n = 0, \qquad i = 1,2,\ldots,n-1 \qquad [3.5-12]$$

$$S_i: \qquad \frac{-1.6647}{(n-1)^{0.65}}\delta_n + \delta_j' = 0, \qquad j = 1,2,\ldots,n-1 \qquad [3.5-13]$$

$$\mu_1 = \sum_{j=1}^{n-1} \delta_j' \qquad [3.5-14]$$

Note that the degree of difficulty is 0, with 2n-2 independent variables corresponding to the n-1 bumper areal densities and the n-1 separations.

These equations imply

$$\delta_i = \frac{1.1827}{(n-1)^{0.65}}\delta_n \qquad i = 1,2,\ldots,n-1 \qquad [3.5-15]$$

$$\Rightarrow \delta_n = \frac{1}{1.1827(n-1)^{0.35}+1} \qquad [3.5-16]$$

$$\Rightarrow \delta_i = \frac{1.1827}{1.1827(n-1)+(n-1)^{0.65}} \qquad i = 1,2,\ldots,n-1 \qquad [3.5-17]$$

$$\delta_j' = \frac{1.6647}{1.1827(n-1)+(n-1)^{0.65}} \qquad j = 1,2,\ldots,n-1 \qquad [3.5-18]$$

$$\mu_1 = \frac{1.6647(n-1)}{1.1827(n-1)+(n-1)^{0.65}} \qquad [3.5-19]$$

The minimum weight and globally optimal areal densities are given by

$$W_0 = \left(\frac{1.1827(n-1)+(n-1)^{0.65}}{1.1827}\right)^{\frac{1.1827(n-1)}{1.1827(n-1)+(n-1)^{0.65}}} [K(1.1827(n-1)^{0.35}+1)]^{\frac{1}{1.1827(n-1)^{0.35}+1}}$$

$$\cdot\left(\frac{1.6647(n-1)}{1.1827(n-1)+(n-1)^{0.65}}\right)^{\frac{1.6647(n-1)}{1.1827(n-1)+(n-1)^{0.65}}} \left(\frac{1.1827(n-1)+(n-1)^{0.65}}{1.6647 S_{ToT}}\right)^{\frac{1.6647(n-1)}{1.1827(n-1)+(n-1)^{0.65}}} \qquad [3.5-20]$$

$$m_{i_0} = \delta_i W_0 \qquad [3.5-21]$$

$$m_{n_0} = [1-(n-1)\delta_i]W_0 \qquad [3.5-22]$$

The optimal individual separations are given by

$$S_{j_0} = \frac{S_{ToT}}{n-1}, \qquad j = 1,2,\ldots,n-1 \qquad [3.5-23]$$

Baseline Parameters

The baseline parameters for an impact systemic parameter sensitivity study are given in **Table 3.5-1.**

Table 3.5-1. Baseline Systemic Impact Parameters

* Particle Diameter = 1 cm
* Particle Density = 2.8 gm/cm^3
* Particle Velocity = 5 km/sec
* Total Bumper/Wall Separation = 10 cm
* Normal Impact
* Ballistic Limit (N = 1)

Figure 3.5-10 shows the sensitivity of the optimal protective structures design mass per unit area to the number of bumpers in the configuration for a particle diameter of 1 cm and velocity of 5 km/sec. The optimal number of bumpers is one. **Figure 3.5-11** shows the same sensitivity except for a particle diameter of 2 cm. In this case, the optimal number of bumpers

is 2. Thus, the optimal number of bumpers is clearly a function of the systemic impact parameters.

Figure 3.5-12 shows the sensitivity of optimal protective structures design variables (including optimal number of bumpers) to particle diameter. A transition region is found between 1 and 1.25 cm. In this region, the optimal number of bumpers changes from 1 to 2 due to increases in diameter penetrability.

Figure 3.5-13 shows the sensitivity of optimal protective structures design variables (including optimal number of bumpers) to particle velocity. The significant conclusion here is the lack of sensitivity of the design over a fairly wide velocity range (3-7.5 km/sec).

Figure 3.5-14 shows the sensitivity of optimal protective structures design variables (including optimal number of bumpers) to total bumper/wall separation. A transition region is found between 15 and 20 cm total separation. In this region, the optimal number of bumpers changes from 1 to 2 due to increased spacing availability. Thus, as the allowable spacing from first bumper to pressure wall increases, the more incentive there is to add bumpers.

Figure 3.5-15 shows the sensitivity of optimal protective structures design variables (including optimal number of bumpers) to particle impact angle from surface normal. No transition region is found in this sensitivity. The optimal number of bumpers remains at 1.

Figure 3.5-16 shows the sensitivity of optimal protective structures design variables (including optimal number of bumpers) to particle density. A transition region is found between 4.5 and 5 gm/cm^3. In this region, the optimal number of bumpers changes from 1 to 2 due to increases in particle density penetrability.

Figure 3.5-17 shows the sensitivity of optimal protective structures design variables (including optimal number of bumpers) to wall penetration factor (1 being ballistic limit). A transition region is found between 50% and 60% penetration. In this region, the optimal number of bumpers decreases from 2 to 1 due to increased allowable particle penetration.

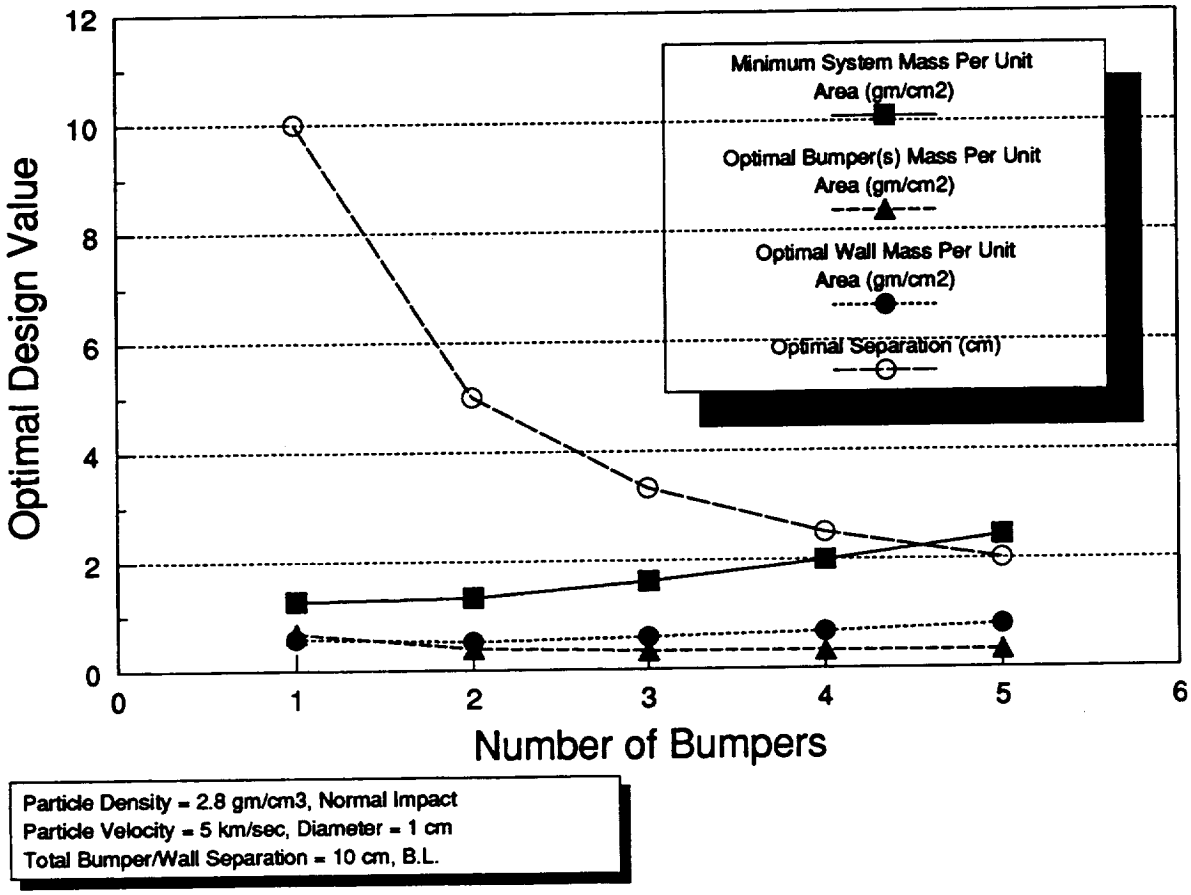

Figure 3.5-10. Determining Optimal Number of Bumpers for Shatter Region

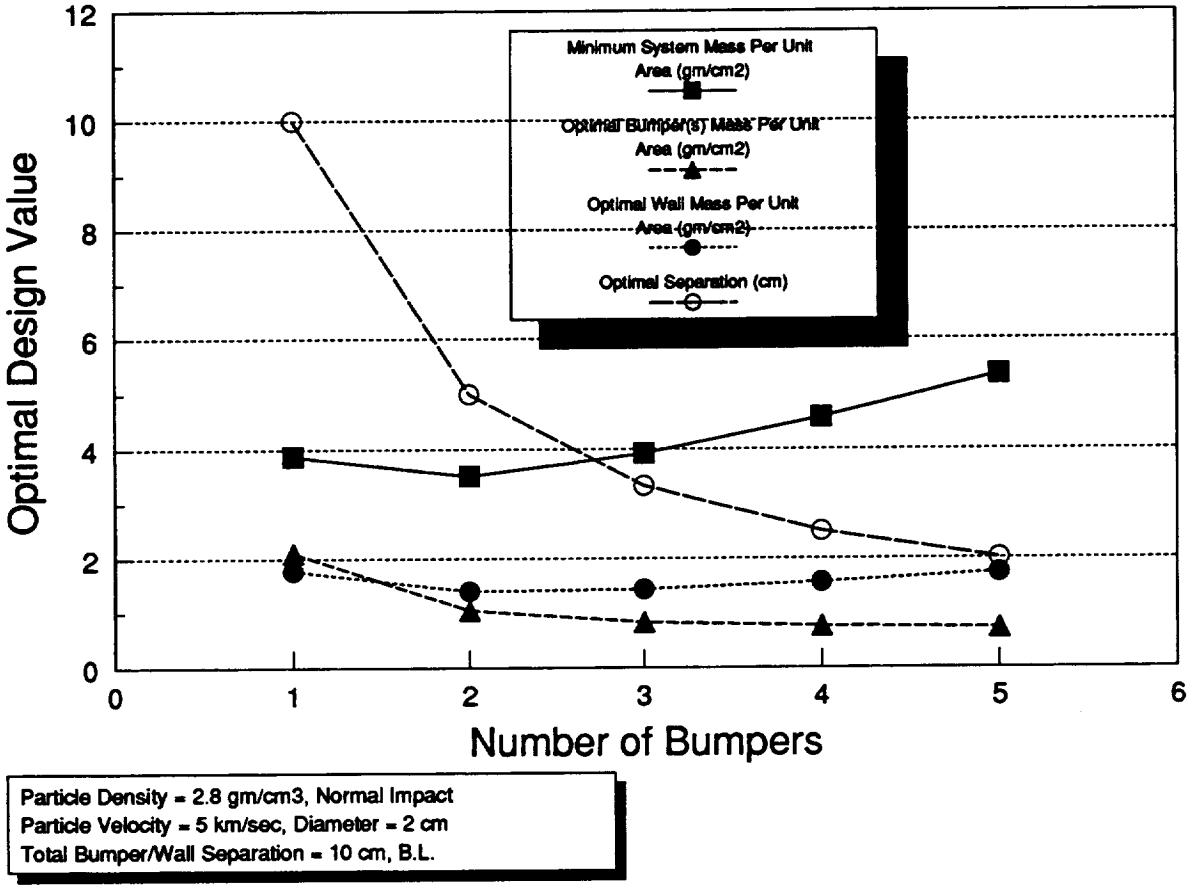

Figure 3.5-11. Determining Optimal Number of Bumpers for Shatter Region

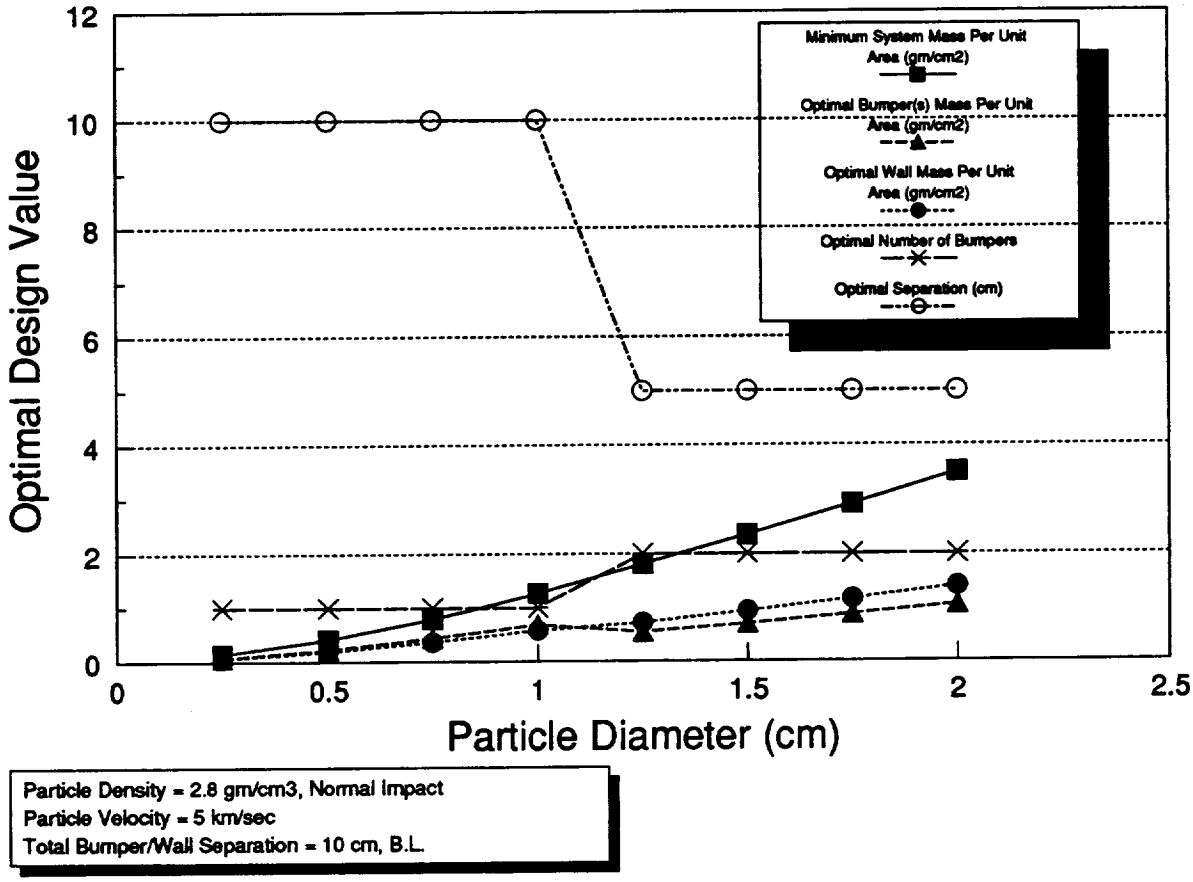

Figure 3.5-12. Optimal Protective Structures Design Values vs. Particle Diameter (Shatter Region)

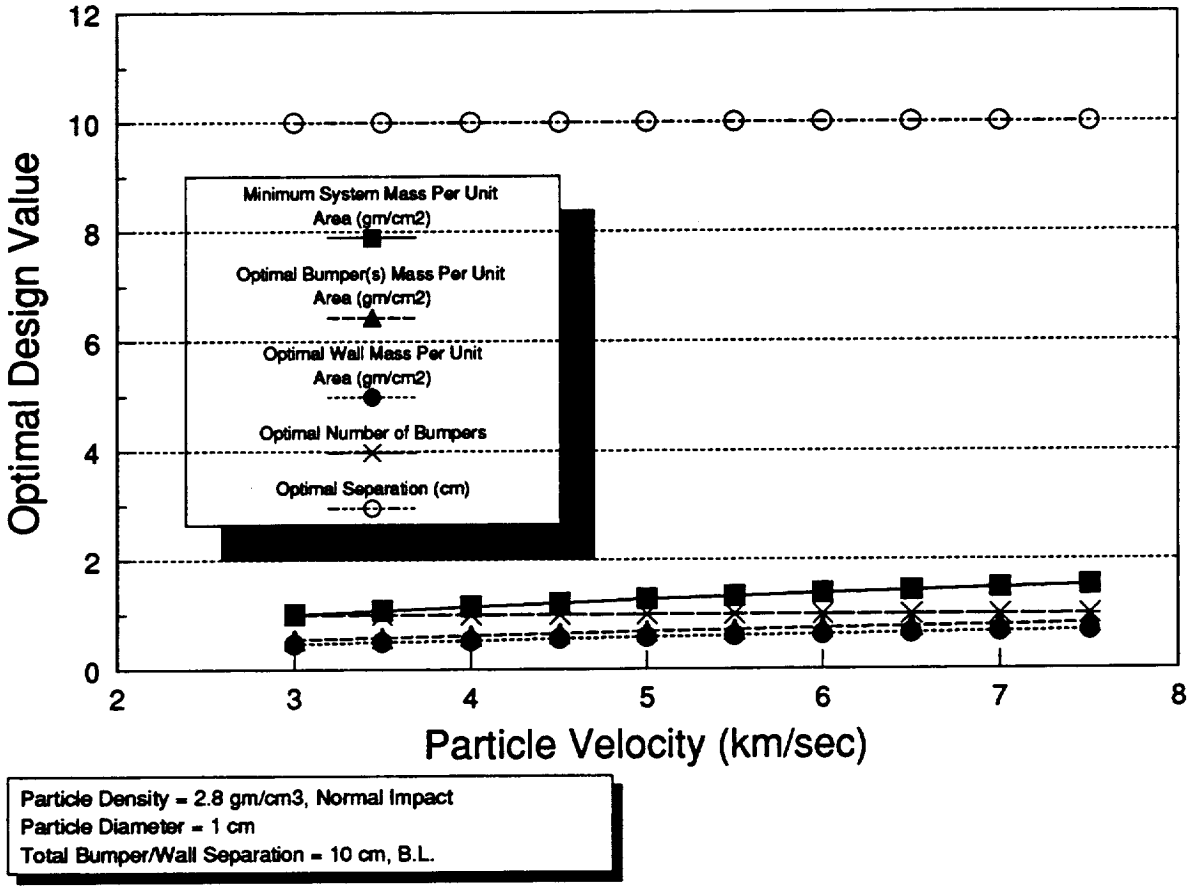

Figure 3.5-13. Optimal Protective Structures Design Values vs. Particle Velocity (Shatter Region)

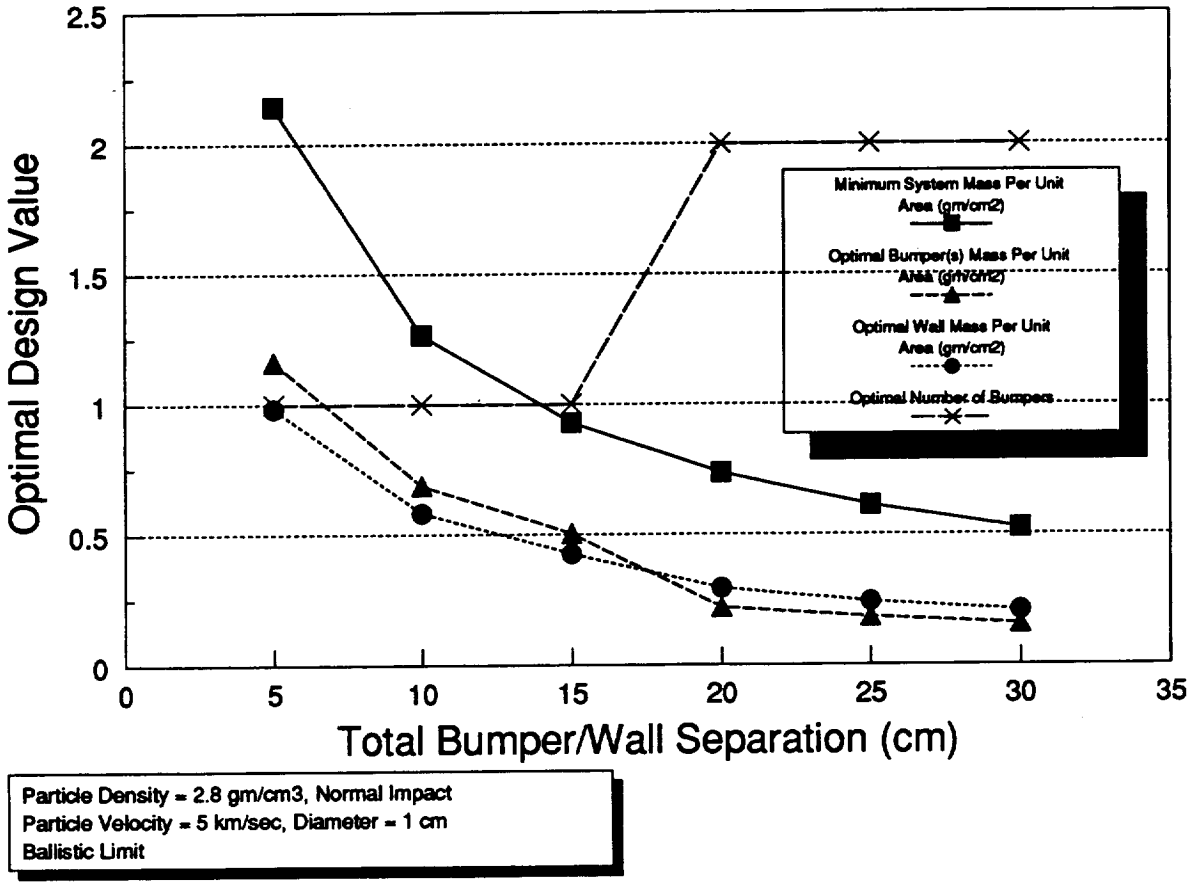

Figure 3.5-14. Optimal Protective Structures Design Values vs. Total Bumper/Wall Separation (Shatter Region)

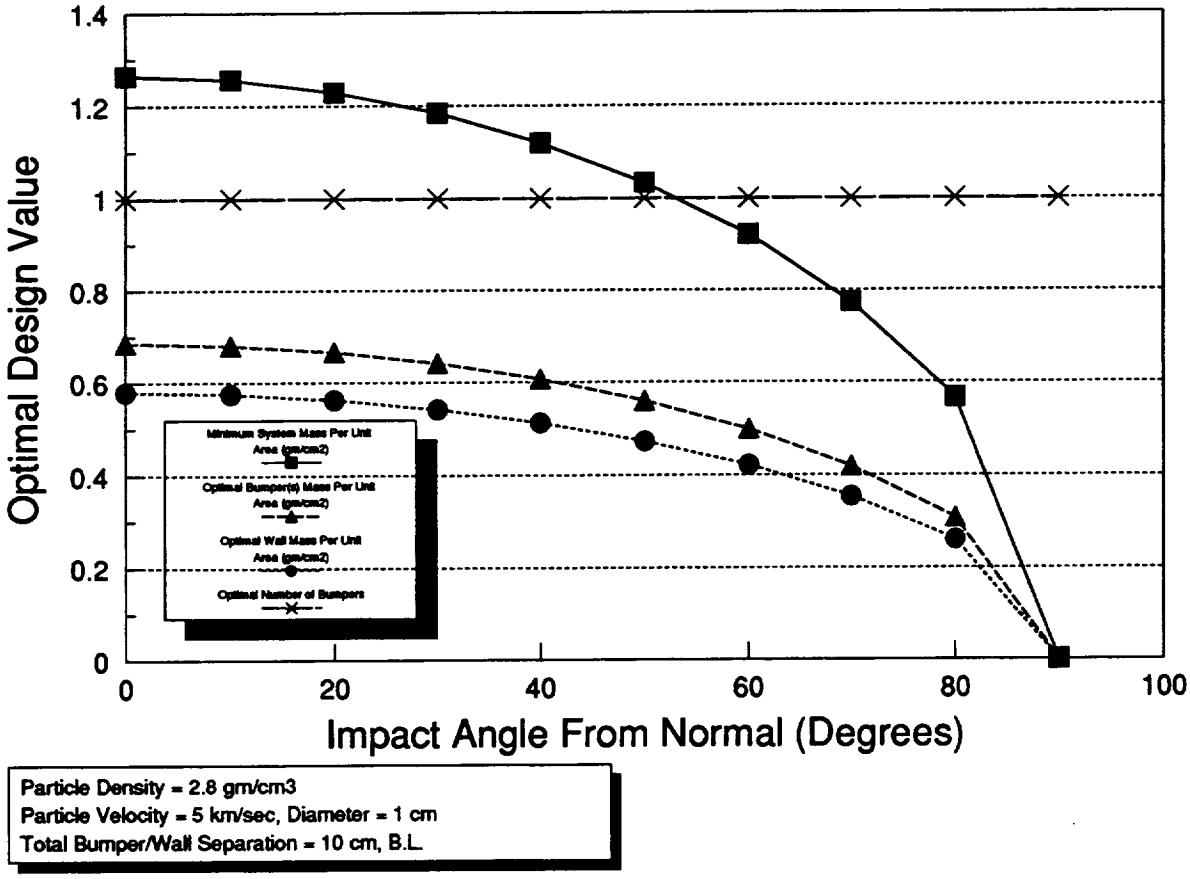

Figure 3.5-15. Optimal Protective Structures Design Values vs. Impact Angle (Shatter Region)

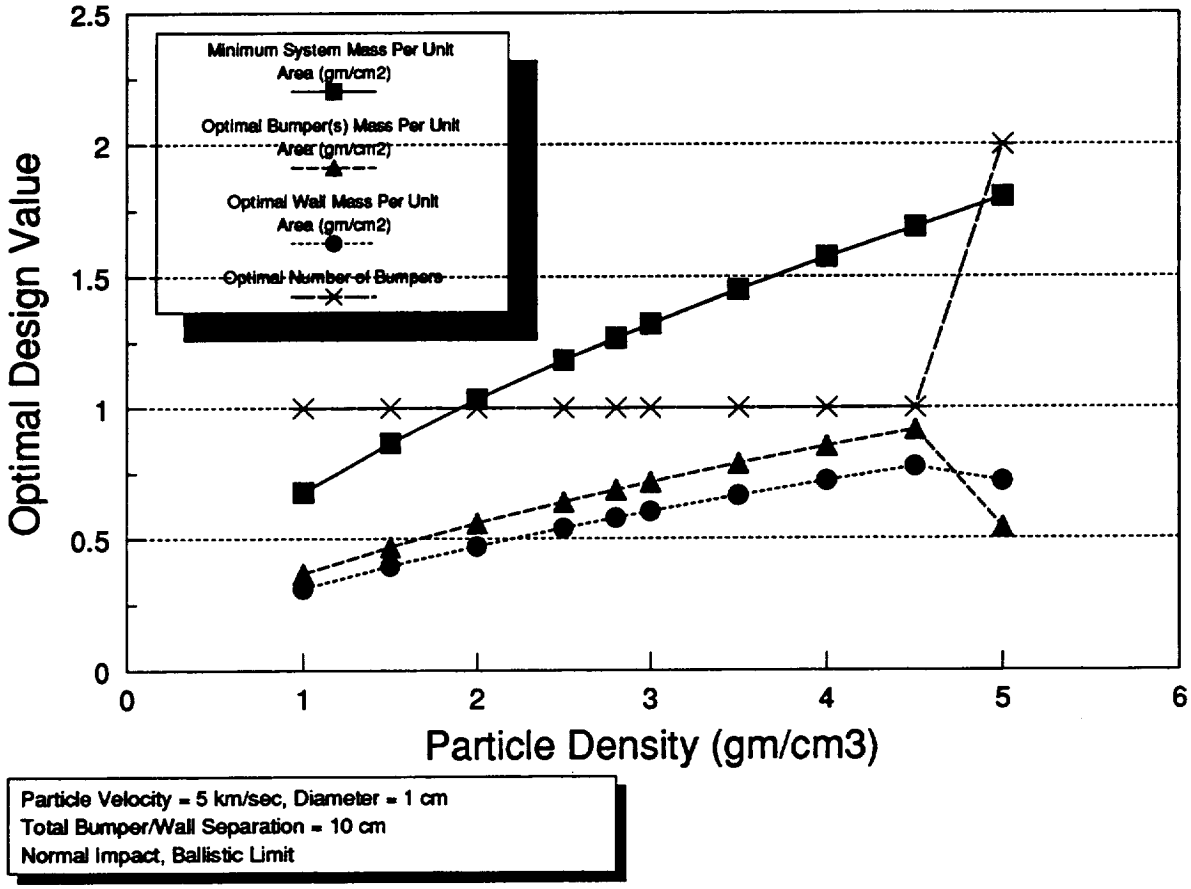

Figure 3.5-16. Optimal Protective Structures Design Values vs. Particle Density (Shatter Region)

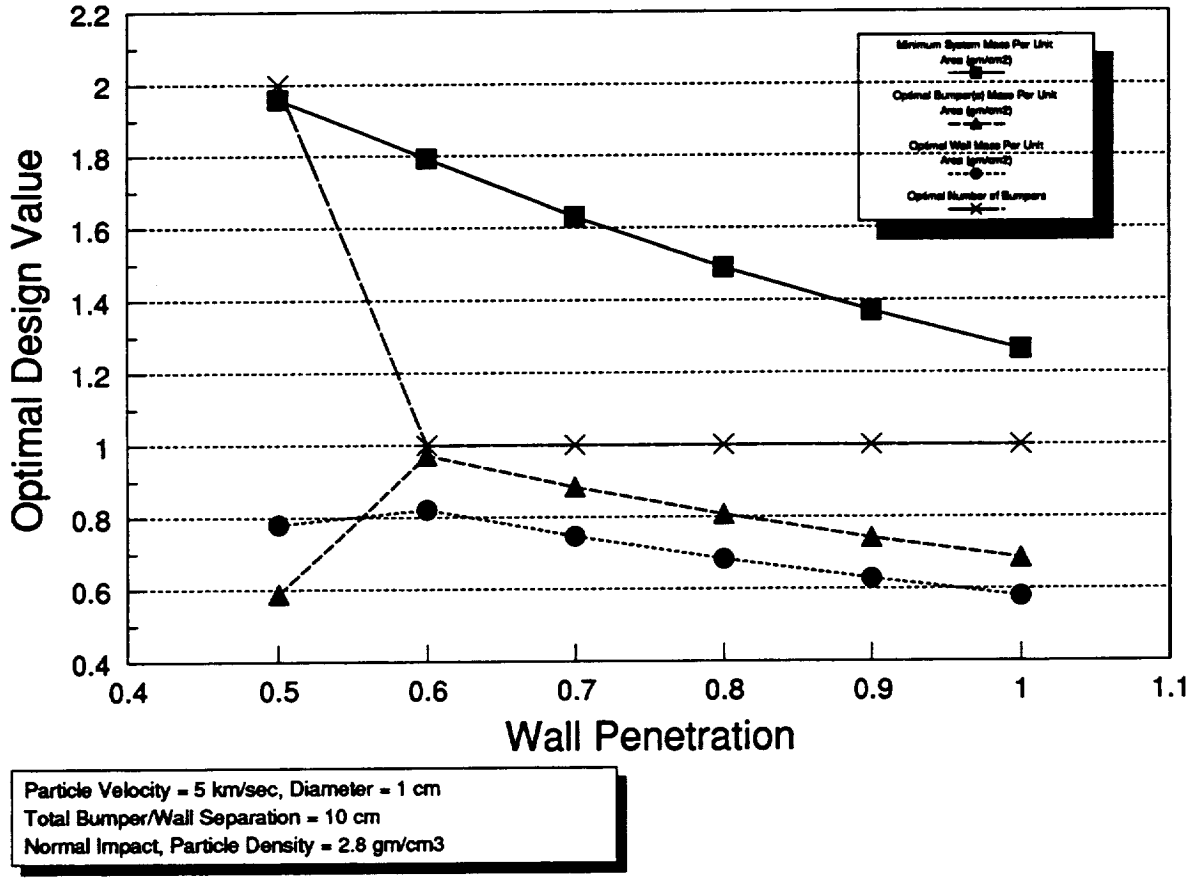

Figure 3.5-17. Optimal Protective Structures Design Values vs. Wall Penetration (Shatter Region)

3.6 Multibumper Protective Structures Design Trades

The baseline parameters and assumptions for an orbital debris analysis of multibumper systems is shown below. The parametric sensitivities investigated are also shown.

* Change Board Directive Debris Environment Except Particle Density = 2.8 gm/cm^3
* 1997-2007 Mission Timeline
* Altitude = 398 km
* Inclination = 28.5 deg.
* Total Mission PNP = 0.9733 (Lab.,Hab.,Node,Node with Cupola,2 LOX Cryo,2 N_2 Cryo,0.9955/element)
* Total Debris Area = 603 m^2
* "0.8" Multibumper Wilkinson/Shatter Regression (Integrated)
* Total Bumper/Wall Separation = 10 cm
* Ballistic Limit

* Mission Start Year: 1997-2005
* Mission Duration: 5-30 years
* Average Mission Altitude: 200-1000 km
* Total Mission PNP: 0.8-0.99
* Total Debris Area: 100-1000 m^2
* Total Bumper/Wall Separation: 5-30 cm

Figure 3.6-1 shows the sensitivity of the optimal protective structures design mass per unit area to the number of bumpers in the configuration for the baseline parameters. The optimal number of bumpers is one.

Figure 3.6-2 shows the sensitivity of optimal protective structures design variables (including optimal number of bumpers) to mission start date. A three year slip in the mission start date results in a 33% increase in protective structures design weight. The optimal number of bumpers remains constant at one for mission start dates through 2005.

Figure 3.6-3 shows the sensitivity of optimal protective structures design variables (including optimal number of bumpers) to mission duration. A transition region from one bumper to two is found in the 10-15 year duration range. The shape of this curve is partly reflective of the space debris growth rate model and partly reflective of the solar flux effect.

Figure 3.6-4 shows the sensitivity of optimal protective structures design variables (including optimal number of bumpers) to average mission altitude. A transition region is found between 400 and 500 km altitude. In this region, the optimal number of bumpers changes from 1 to 2 due to increased particle threat.

Figure 3.6-5 shows the sensitivity of optimal protective structures design variables (including optimal number of bumpers) to total mission probability of no penetration. A transition from 2 bumpers to one is found in the region between 0.9733 and 0.98 PNP. This corresponds to element PNP's between 0.9955 and 0.9966.

Figure 3.6-6 shows the sensitivity of optimal protective structures design variables (including optimal number of bumpers) to total mission debris area. A transition region is found between 700 and 800 m^2. In this region, the optimal number of bumpers changes from 1 to 2 due to increases in particle threat size.

Figure 3.6-7 shows the sensitivity of optimal protective structures design variables (including optimal number of bumpers) to total bumper/wall separation. No transition region is found from 5 to 30 cm total separation. An increase in total separation from 10 to 15 cm results in a 33% reduction in weight.

Figures 3.6-8 through 3.6-11 show ballistic limit curves for the combined (shatter and 0.8-Wilkinson) multibumper predictor. Seven curves are shown in each figure corresponding to seven different first bumper thicknesses. The baseline Space Station protective structures design is found behind the first bumper. The separation between first and second bumpers is

varied from 2 to 8 inches across the four curves. The transition region from projectile shatter to vaporization is assumed to be in the 7-8 km/sec region and is not well understood. Curves like these are useful in determining protective structures measures of performance for advanced shielding systems.

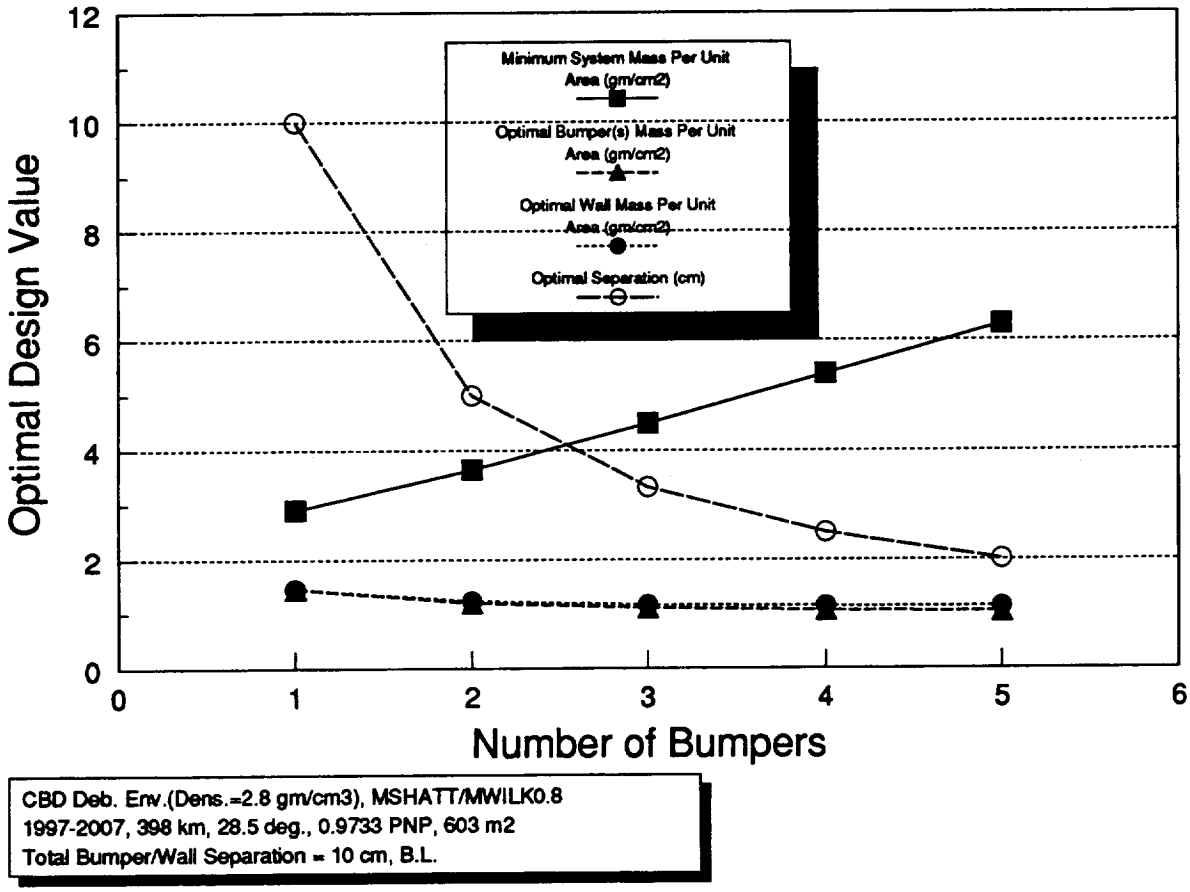

Figure 3.6-1. Determining Optimal Number of Bumpers

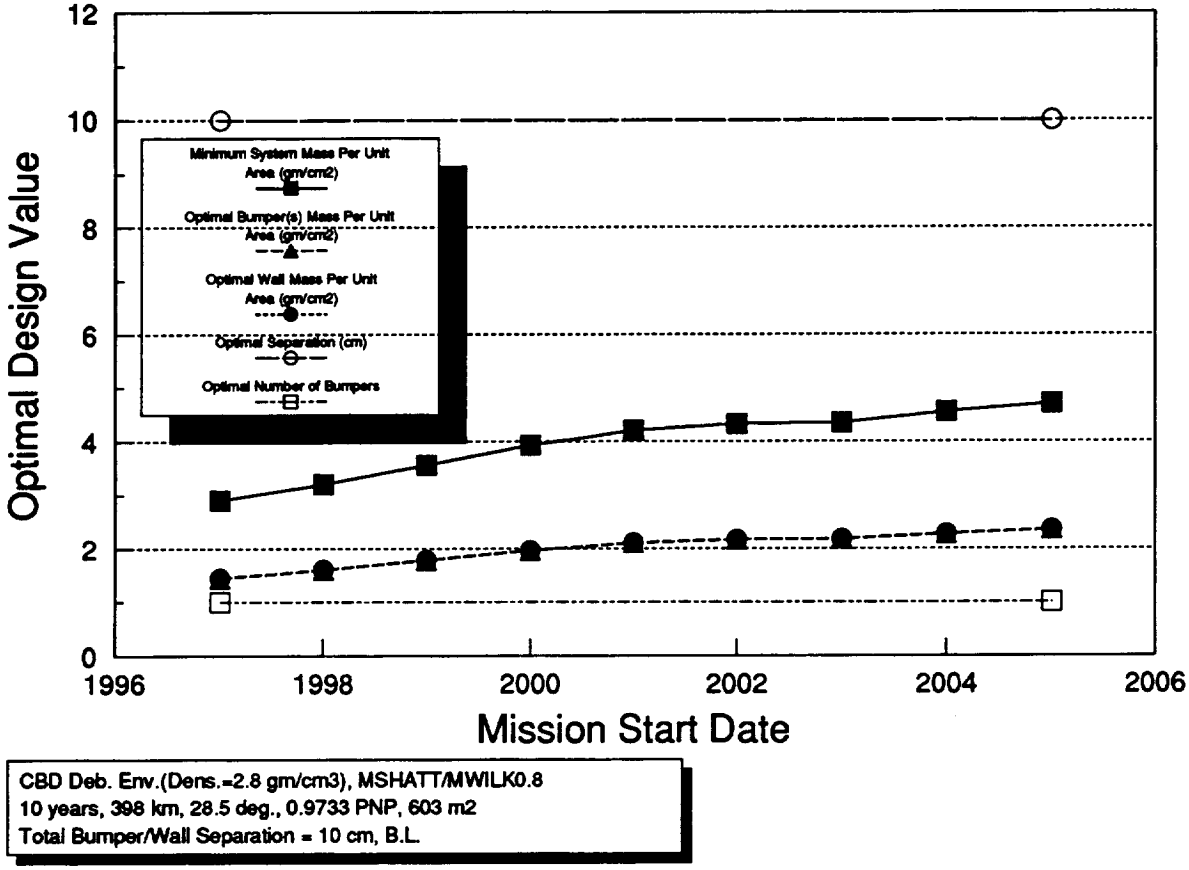

Figure 3.6-2. Optimal Protective Structures Design Values vs. Mission Start Date

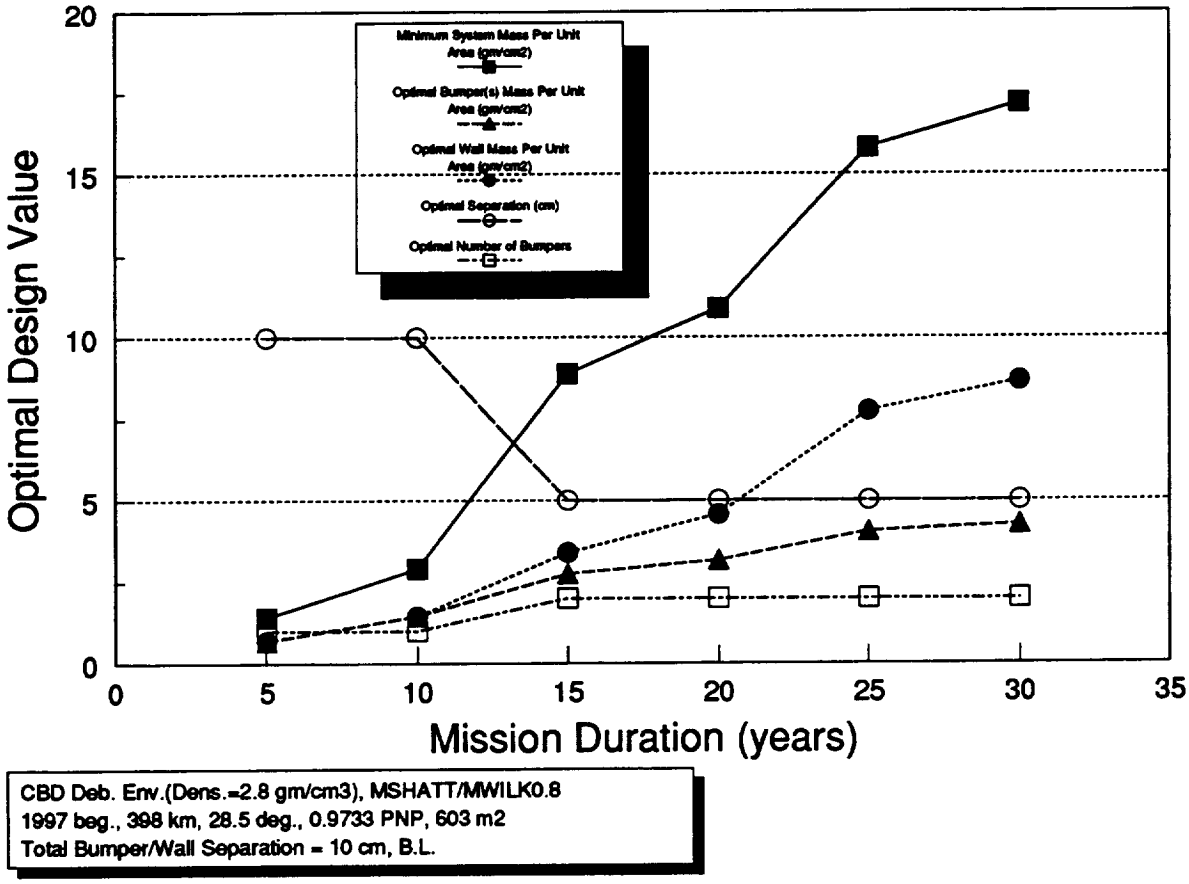

Figure 3.6-3. Optimal Protective Structures Design Values vs. Mission Duration

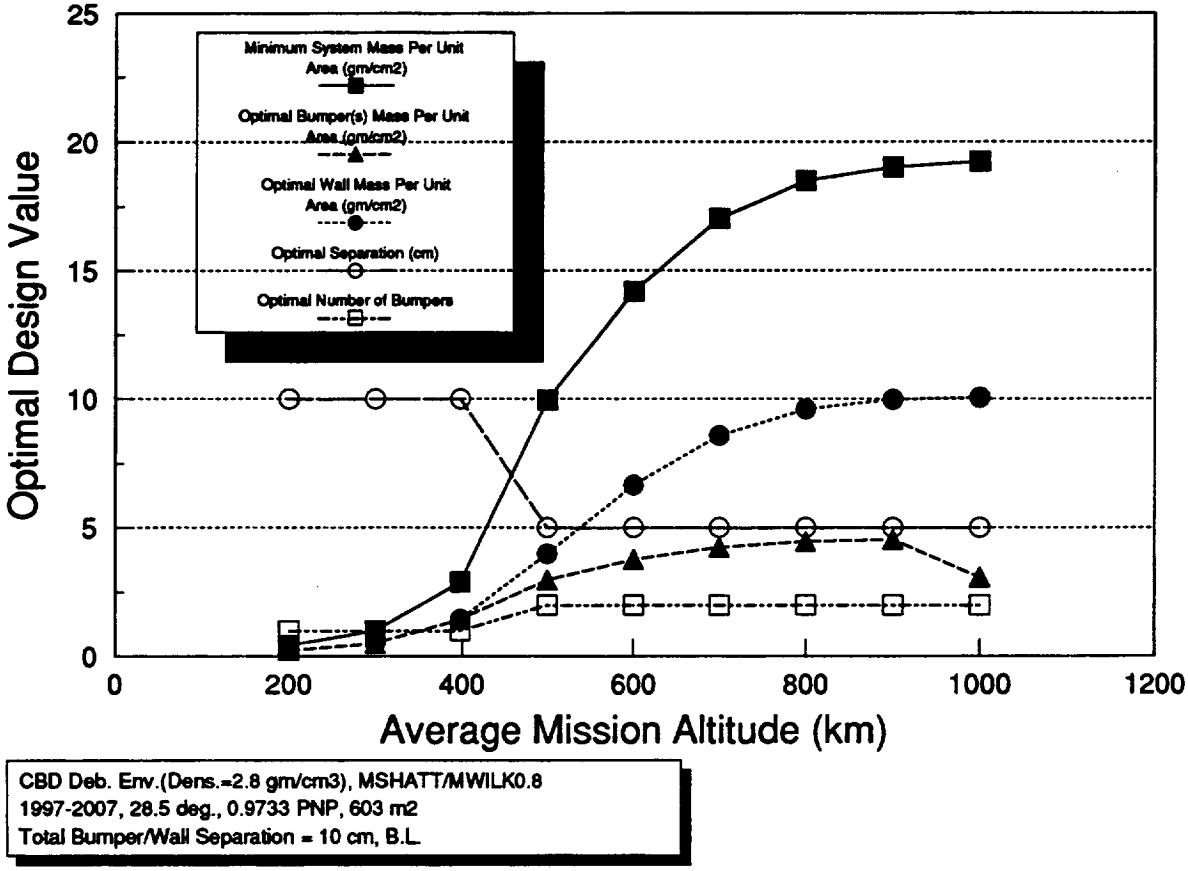

Figure 3.6-4. Optimal Protective Structures Design Values vs. Average Mission Altitude

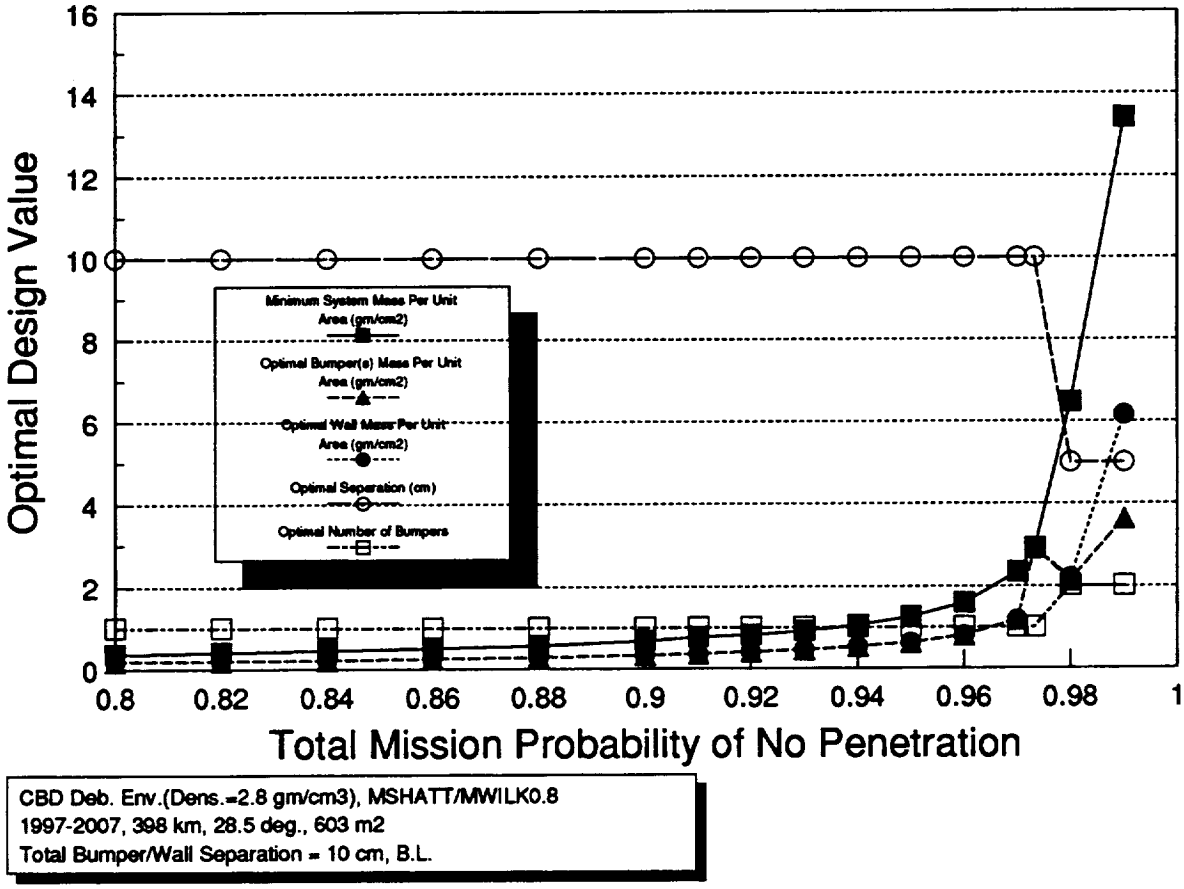

Figure 3.6-5. Optimal Protective Structures Design Values vs. Total Mission PNP

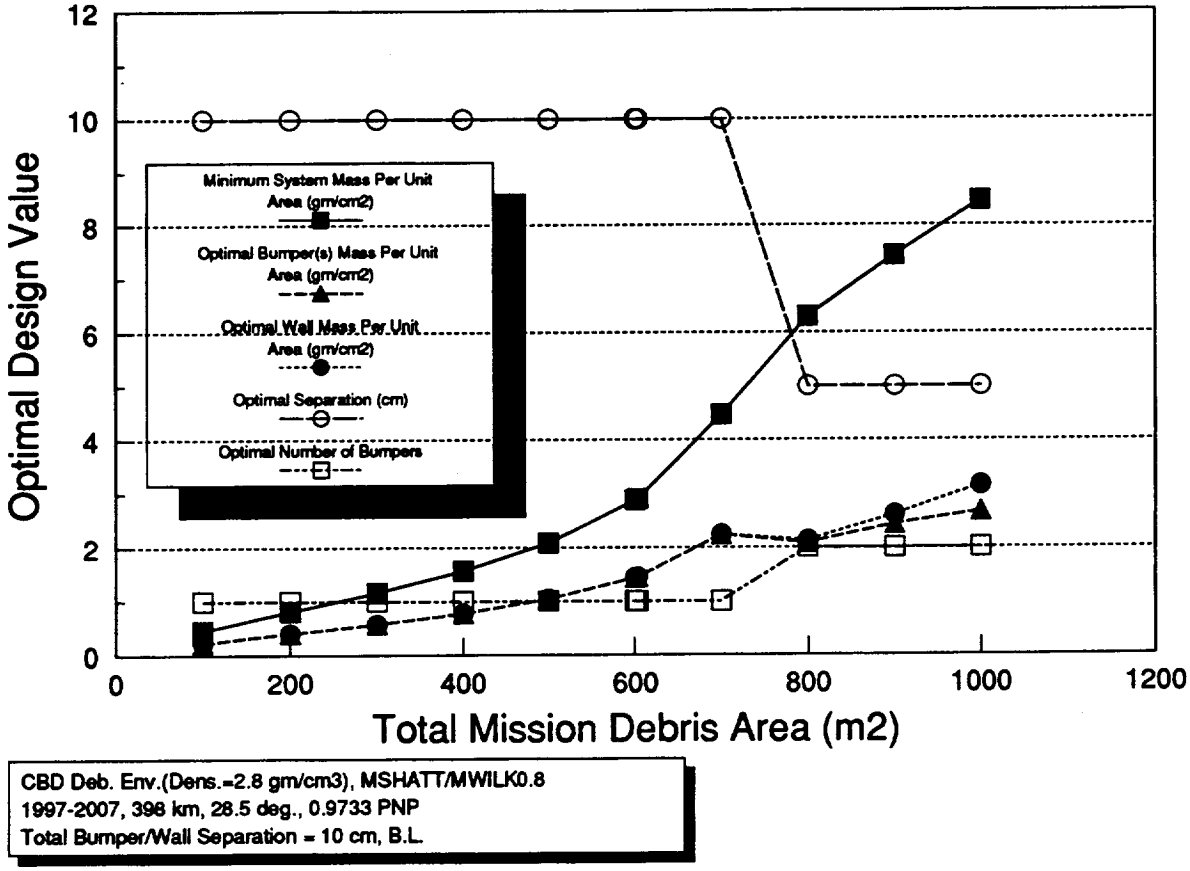

Figure 3.6-6. Optimal Protective Structures Design Values vs. Total Mission Debris Area

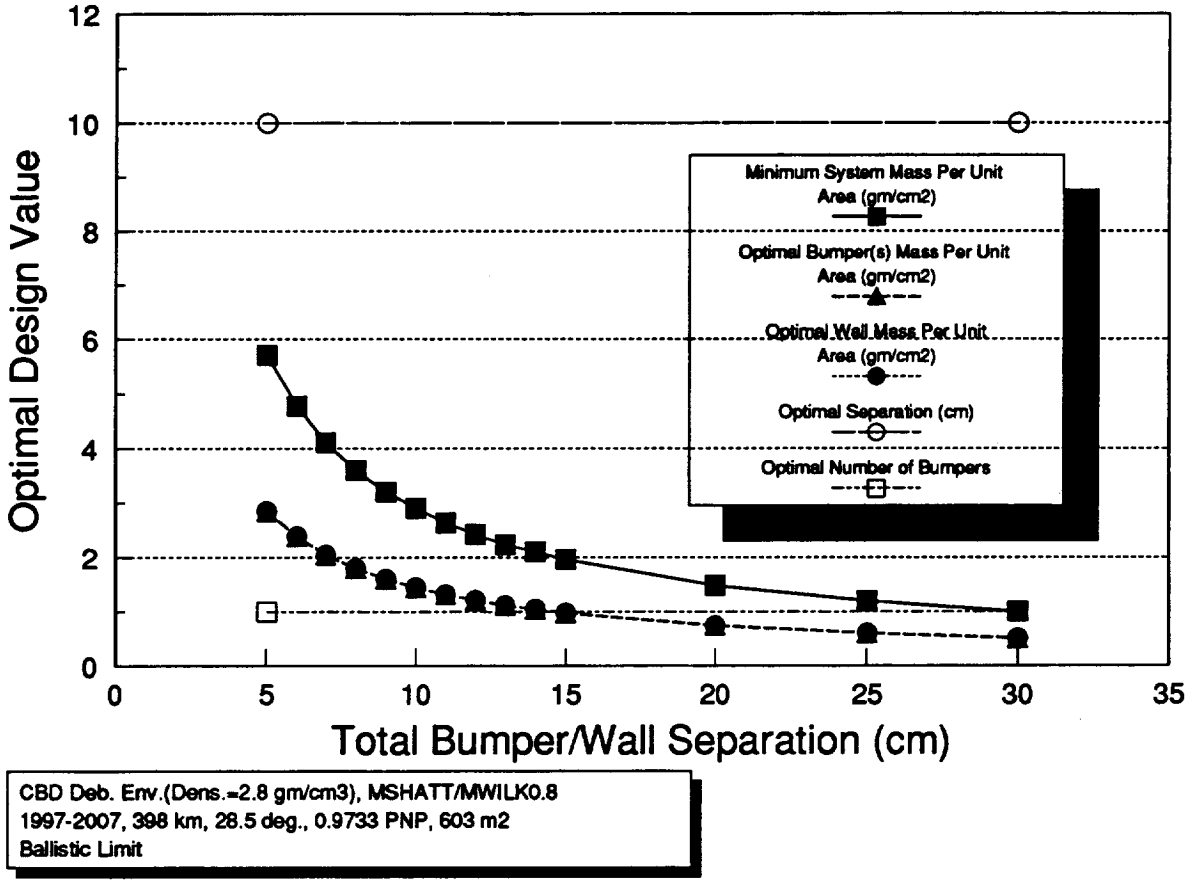

Figure 3.6-7. Optimal Protective Structures Design Values vs. Total Bumper/Wall Separation

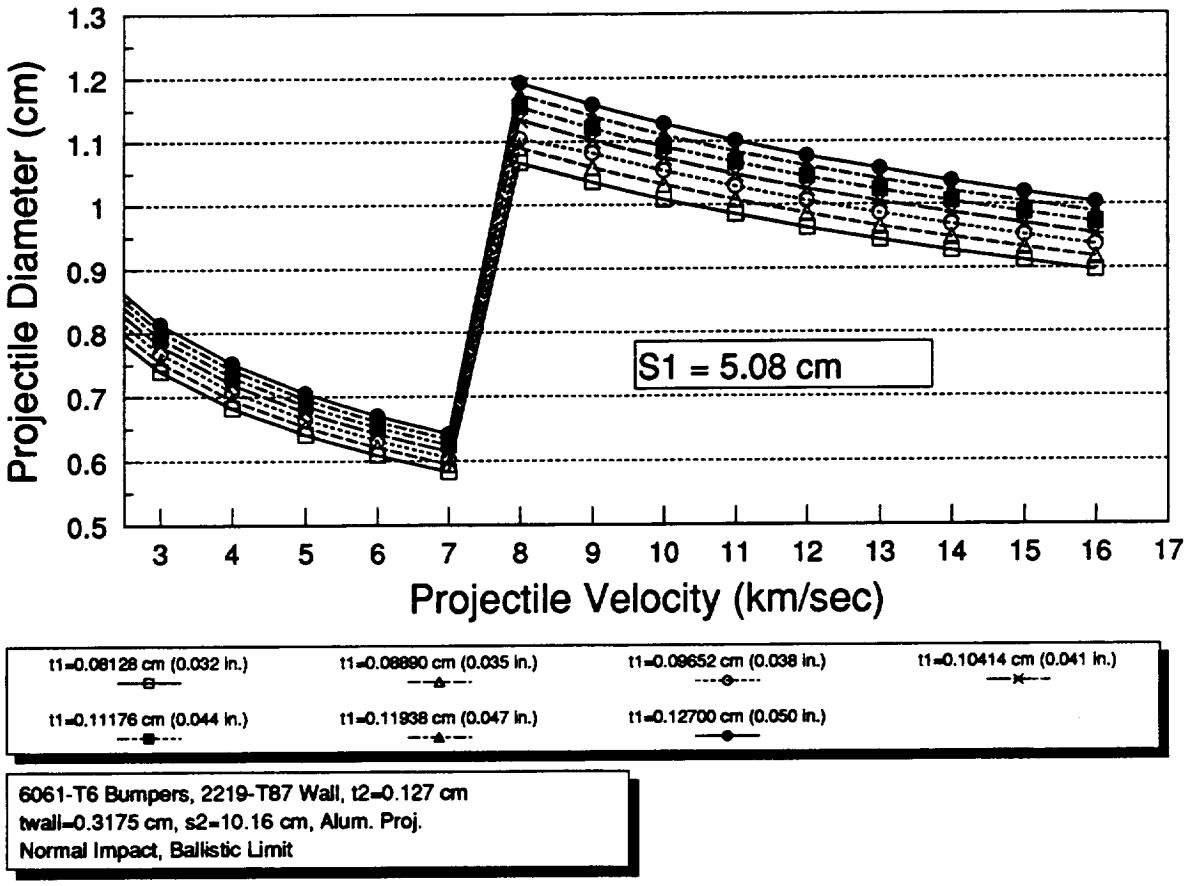

Figure 3.6-8. Ballistic Limit Curve for Front Separation of 5.08 cm

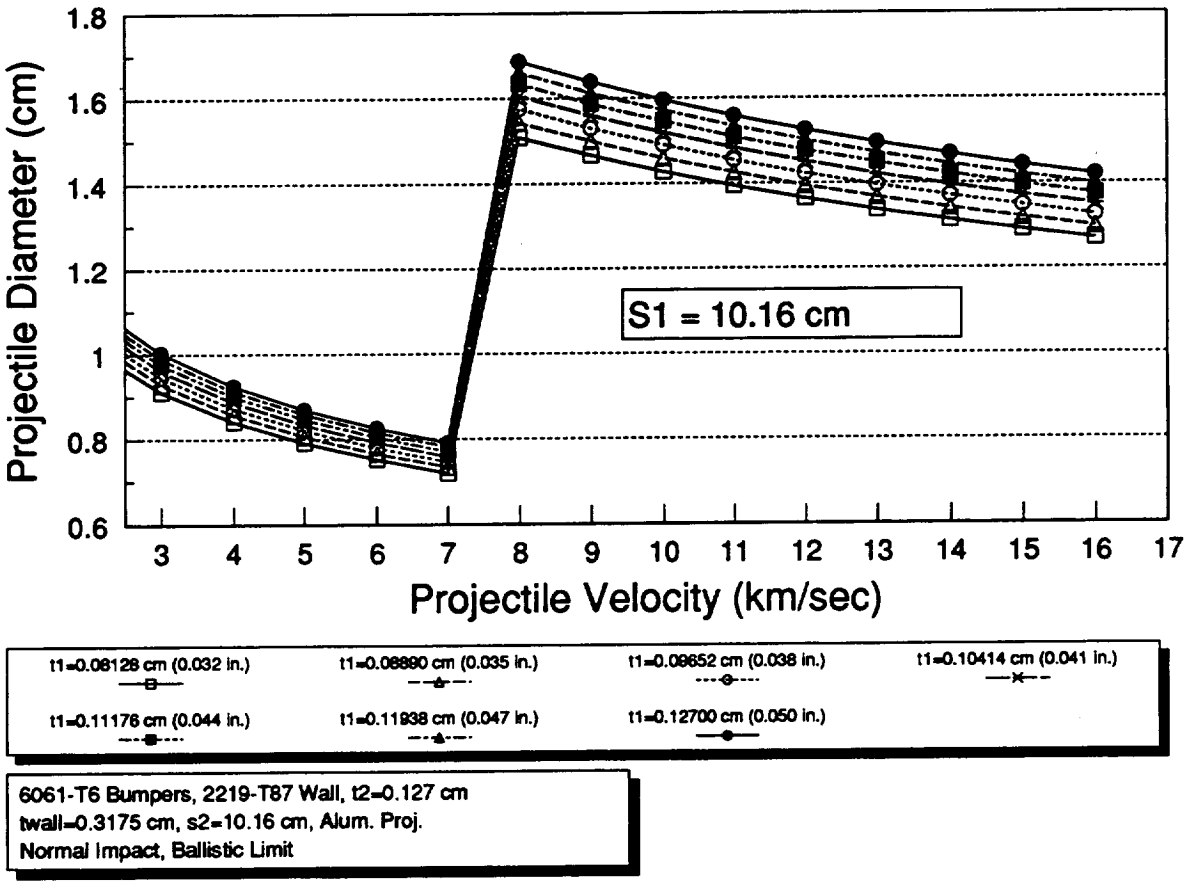

Figure 3.6-9. Ballistic Limit Curve for Front Separation of 10.16 cm

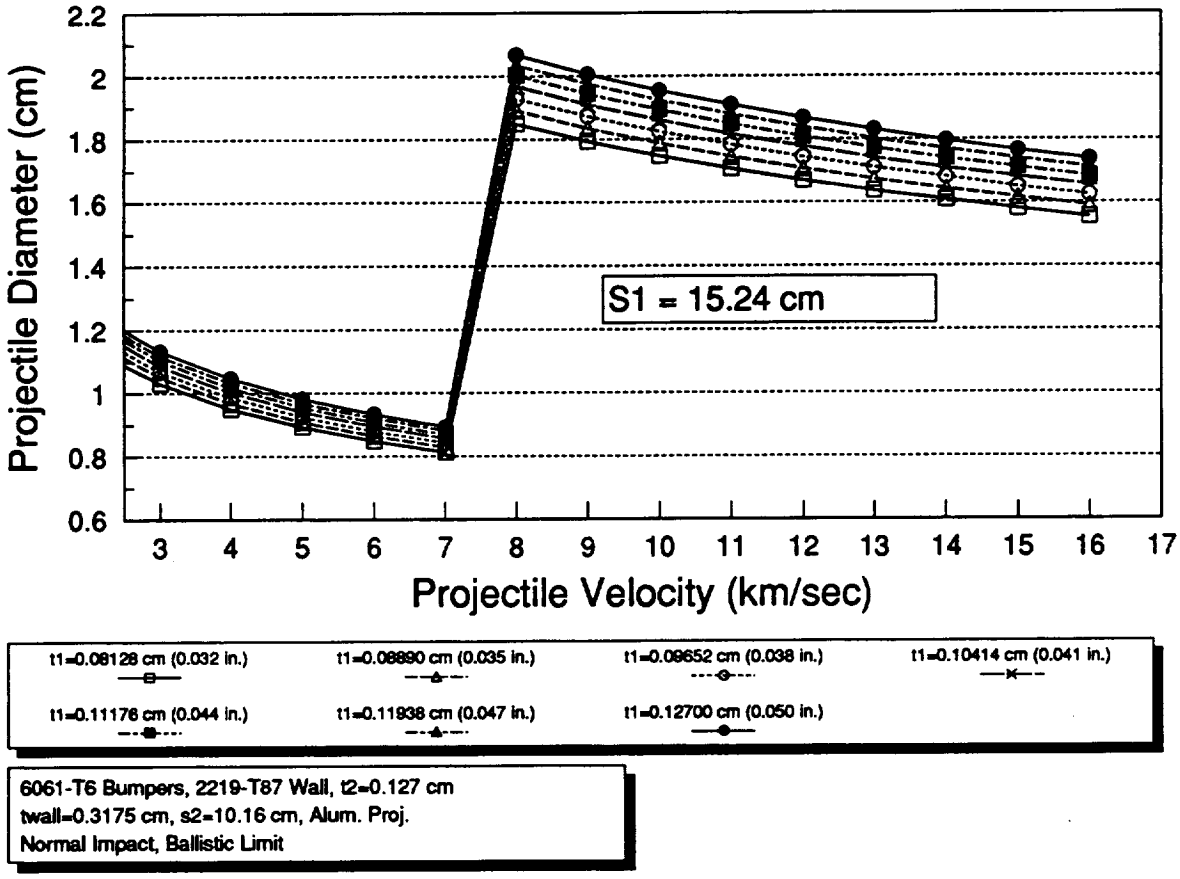

Figure 3.6-10. Ballistic Limit Curve for Front Separation of 15.24 cm

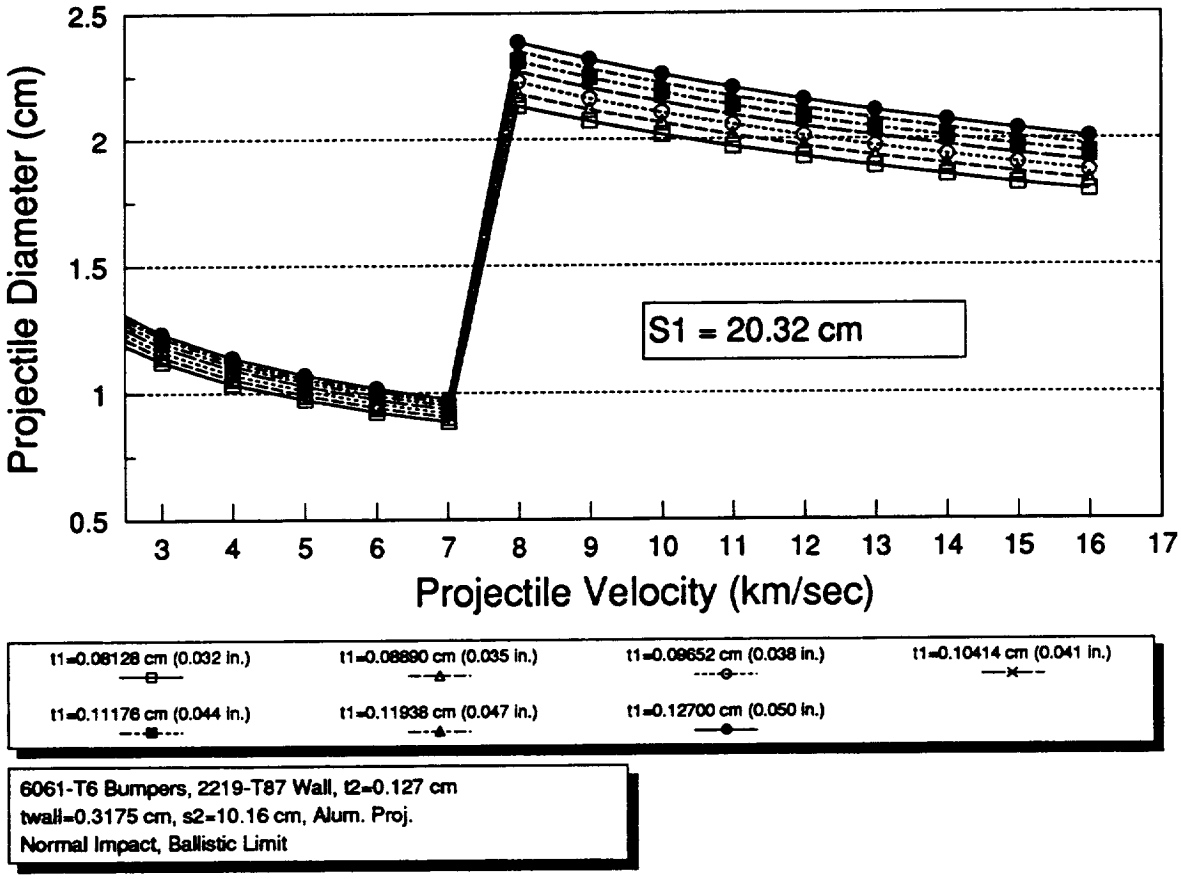

Figure 3.6-11. Ballistic Limit Curve for Front Separation of 20.32 cm

3.7 Intrinsically Nonlinear Regression For Multibumper Projectile Shatter

The intrinsically nonlinear regression form is given by

$$N = \sum_{i=1}^{T} (K_i d^{a_{1_i}} \rho_p^{a_{2_i}} V^{a_{3_i}} \left[\cos\left(\frac{\theta}{(n-1)^{a_{9_i}}} \right) \right]^{a_{4_i}} \left(\prod_{j=1}^{n-1} S_j \right)^{\frac{a_{5_i}}{a_{10_i}}}$$

$$\cdot \left(\prod_{j=1}^{n-1} \rho_j t_j \right)^{\frac{a_{6_i}}{a_{11_i}}} (\rho_n t_n)^{a_{7_i}} (n-1)^{a_{8_i}} \qquad [3.7-1]$$

To date, the addition of posynomial terms has not shown significant advantages or improvements over a single term posynomial for the combined multibumper database. Multiple term posynomial predictors, multiple databases, and separation of variables are approaches currently under investigation (but beyond the scope of this effort).

3.8 Conclusions and Recommendations

Conclusions

1. Intrinsically Linear Posynomial Regression Can Be Performed to Statistically Significant Levels for Multiple Bumpers.
2. Residual Plot vs. Number of Bumpers Draws Suspicion to That Parameter.
3. Other Residual Plots Seem Appropriate.
4. Resulting Geometric Program has 0 Degree of Difficulty.
5. Optimal Areal Densities are Equal for Bumper(s).
6. Optimal Bumper(s) and Wall Areal Densities are Generally Not Equal.
7. Bumper Areal Density Dominates Wall Areal Density for Single Bumper Case.
8. Wall Areal Density Dominates Bumper Areal Densities for Multiple Bumpers.
9. Optimal Individual Separations are Equal.
10. Optimal Number of Bumpers Increases with Increasing Particle Diameter. (Note Transition Region Between d=1 cm and d=1.25 cm. particle sizes.)
11. Penalty for Selecting Wrong Number of Bumpers is Not Symmetric about Optimal Solution.
12. Protective Structures Design Sensitivity to Velocity is Flat with Constant Optimal Number of Bumpers = 1.
13. Transition from Single to Double Bumper System is Found for Total Standoffs Between 15 and 20 cm.
14. Impact Angle Sensitivity is Monotonically Decreasing with Constant Optimal Number of Bumpers = 1.
15. Transition from Single to Double Bumper System is Found for Particle Densities Between 4.5 and 5 gm/cm^3.
16. Minimum System Mass Per Unit Area is Sensitive to Wall Penetration Factor. (Transition From 2 Bumpers to 1 is Found Between 0.5 and 0.6.)
17. Minimum System Mass Per Unit Area is Sensitive to the Number of Bumpers.
18. Three Year Schedule Slippage Results in 33% Increase in Design.
19. Optimal Protective Structures Design is Very Sensitive to Mission Duration.
20. Transition Region From 1 to 2 Bumpers is Between 10 and 15 Year Durations.
21. Optimal Protective Structures Design is Very Sensitive to Average Mission Altitude Above 400 km.
22. Transition Region From 1 to 2 Bumpers is Between 400 and 500 km Altitudes.
23. Optimal Protective Structures Design is Very Sensitive to Mission PNP Above 0.96.
24. Knee of the PNP Curve is Compatible With Baseline Requirement of 0.9733.
25. Transition Region From 1 to 2 Bumpers is Between 0.9733 and 0.98 PNP. (0.9955 and 0.9966/Element).
26. Optimal Protective Structures Design is Very Sensitive to Total Debris Area.
27. Transition Region From 1 to 2 Bumpers is Between 700 and 800 m^2.
28. Optimal Protective Structures Design is Sensitive to Total Bumper/Wall Separation Between 5 and 20 cm.
29. Knee of the Separation Curve Appears to Be Between 10 and 15 cm.
30. Shift to 15 cm Separation Results in About 33% Reduction in Protective Weight.

Recommendations

1. Perform Second Order Sensitivities.
2. Perform PNP Requirements Balancing Among Critical Elements.
3. Investigate Configuration Build-up Timelines/Augmentation.
4. Disjoin Multibumper Database Into Single, Double, and Triple Databases.
5. Disjoin Posynomial Form Into Impact Parameters and Configuration Parameters.

4 PROJECTILE SHAPE EFFECTS TASK

SAIC developed posynomial regression techniques and combined them with posynomial optimization techniques for application to this area. These techniques are available for immediate application to the test data resulting from projectile shape effects testing. Currently, limited test data produces unclear results when attempts are made to correlate data from various projectile shapes. Results are inconclusive. Further investigation of the projectile shape effects includes methodologies found in sources such as "A Preliminary Investigation of Projectile Shape Effects In Hypervelocity Impact of a Double-Sheet Structure," by R. H. Morrison, NASA-TN-6944, August 1972, but will remain inconclusive until further test are performed. A summary of literature in this area follows.

Burch reasoned that for multiplate systems, both projectile geometry and material play a significant role in terms of the characterization of hypervelocity impact damage. More specifically, Piekutowski provides visual confirmation of the effect that cylinder inclination at impact has on debris cloud features and rear wall damage severity. Shockey reports that provided the cylinder length exceeds both its diameter and the target plate thickness, at least part of the projectile will remain solid, independent of velocity. He also states that disk-type projectiles (L/D < 1) tend to be more completely vaporized, and that rod-like projectiles tend to remain in the solid state. Backman adds that pointed penetrators pierce, while blunt-shaped projectiles plug.

Morrison considered cylinders of various L/D ratios fired at near 0 degree inclination, and found that cylinders were generally, and often considerably, better penetrators than spheres. (This is due to the lack of vaporization and shatter of the entire rod, the spike in the debris cloud, and the fact that the debris cloud front for cylinders travels about 14% faster than for spheres.) Specifically, Morrison found that on an equal mass basis, cylinders with L/D of 3/2 were the most damaging to double sheet structures, followed by L/D ratios of 1/2 and 1, respectively. Morrison kept a constant

L/D of 1/2, decreased L and D simultaneously, and found that a cylinder could achieve the same penetrability as a sphere at 1/3 the mass. Next, he kept the cylinder diameter constant, decreased the length systematically, and found that the same penetrability could be achieved with 1/7 the mass of the sphere. Counterintuitively, he discovered that for L/D ratios between 1/7 and 1/2, the lower ratios are more effective penetrators of 2-sheet structures, given equal mass. To quote Morrison, "Thus, the use of only spherical projectiles in testing double-sheet structures can be misleading. In fact, this practice has yielded nonconservative empirical equations now in use in the design of impact-resistant spacecraft structures. Although cylinders are no more typical of meteoroid shapes than spheres, the damage incurred by actual meteoroids is undoubtedly being underestimated by a significant factor." Obviously, this conclusion is even more pertinent for space debris impacts.

5 REFERENCES

[1]Adeli, H., and Kamal, O., Efficient Optimization of Space Trusses, *Computers and Structures*, Vol. 24, No. 3, 1986.

[2]Anderson, C. E., "Ballistic Impact: The Status of Analytical and Numerical Modeling," Int. J. Impact Engng., Vol. 7, No. 1, 1988.

[3]Atrek, E., et Al, *New Directions in Optimal Structural Design*, Wiley-Interscience, 1984.

[4]Avriel, M., *Advances in Geometric Programming*, Plenum Press, New York, 1980.

[5]Avriel, M., *Nonlinear Programming Analysis and Methods*, Prentice-Hall, Inc., Englewood Cliffs, New Jersey, 1976.

[6]Avriel, M., "A Condensation Method for a Class of Algebraic Programs," Stanford Univ., 1975.

[7]Backman, M. E., and Goldsmith, W., "The mechanics of Penetration of Projectiles Into Targets," Int. J. Impact Engng., pp. 1-99.

[8]Bartle, R. G., *The Elements of Real Analysis*, John Wiley and Sons, Inc., 1976.

[9]Bate, R. R., *Fundamentals of Astrodynamics*, Dover Publications, Inc., 1971.

[10]Bazaraa, M. S., and Jarvis, J. J., *Linear Programming and Network Flows*, John Wiley and Sons, Inc., 1977.

[11]Bazaraa, M. S., and Shetty, C. M., *Nonlinear Programming*, John Wiley and Sons, Inc., 1979.

[12]Beale, E. M. L., "Global Optimization as an Extension of Integer Programming," Towards Global Optimisation 2, 1978.

[13]Beckenbach, E., and Bellman, R., *An Introduction to Inequalities*, Yale University, 1961.

[14]Beightler, C., and Phillips, D. T., *Applied Geometric Programming*, John Wiley and Sons, Inc., 1976.

[15]Birkhoff, G., and MacLane, S., *A Survey of Modern Algebra*, Macmillan Publishing Co., Inc., 1977.

[16]Blanchard, B. S., and Fabrycky, W. J., *Systems Engineering and Analysis*, Prentice-Hall, Inc., 1981.

[17]Bless, S. J., "Hypervelocity Penetration of Ceramics," Int. J. Impact Engng., Vol. 5, 1987.

[18]Boddy, J. A., and Moss, W. L., "Weight Optimization Using Geometric Programming," Society of Aeronautical Weight Engineers, May 1970.

[19]Boyce, W. E., and DiPrima, R. C., *Elementary Differential Equations and Boundary Value Problems*, John Wiley & Sons, Inc., 1977.

[20]Brar, G. S., "Geometric Programming for Engineering Design Optimization," Ohio State University, 1981.

[21]Brimm, D. J., "Unistructure - A New Concept for Light Weight Integrally Stiffened Skin Structures," SAE Technical Paper No. 801231, October 1980.

[22]Brostow, W., *Science of Materials*, John Wiley and Sons, 1979.

[23]Brown, A. S., "Smoothing Intermetallics Brittle Edge," Aerospace America, March 1988.

[24]Budynas, R. G., *Advanced Strength and Applied Stress Analysis*, McGraw-Hill, Inc., 1977.

[25]Burch, G. T., "Multiplate-Damage Study," Boeing Technical Report AFATL-TR-67-116, Sept. 1967.

[26]Burns, S. A., Generalized Geometric Programming With Many Equality Constraints, *International Journal for Numerical Methods in Engineering*, Vol. 24, April 1987.

[27]Catherino, H. A., "Sizing FRP Ballistic Armor," American Society for Metals, 1985.

[28]Christiansen, E., "Evaluation of Space Station Meteoroid/Debris Shielding Materials - Final Report," NASA Contract NAS9-15800, September 1987.

[29]Churchill, R. V., et Al, *Complex Variables and Applications*, McGraw-Hill, Inc., 1976.

[30]Cole, F., et Al, A Comparison Between a Primal and a Dual Cutting Plane Algorithm for Posynomial Geometric Programming Problems, *Journal of Optimization Theory and Applications*, Vol. 47, Oct. 1985.

[31]Coronado, A. R., Gibbins, M. N., Wright, M. A., and Stern, P. H., "Space Station Integrated Wall Design and Penetration Damage Control," Boeing Aerospace Company Final Report, Contract NAS8-36426, July 1987.

[32]Cour-Palais, B. G., "Hypervelocity Impact in Metals, Glass, and Composites," Int. J. Impact Engng., Vol. 5, 1987.

[33]Cour-Palais, B., and Avans, S., "Decision Time on Orbital Debris: Shielding Against Debris," Aerospace America, June 1988.

[34]Cour-Palais, B., "Meteoroid Environment Model - 1969 (Near-Earth to Lunar Surface)," NASA SP-8013, March 1969.

[35]Dembo, R. S., Sensitivity Analysis in Geometric Programming, *Journal of Optimization Theory and Applications*, Vol. 37, May 1982.

[36]Dembo, R. S., Current State of the Art of Algorithms and Computer Software for Geometric Programming, *Journal of Optimization Theory and Applications*, Vol. 26, Oct. 1978.

[37]Dembo, R. S., Dual to Primal Conversion in Geometric Programming, *Journal of Optimization Theory and Applications*, Vol. 26, Oct. 1978.

[38]Department of Defense, "Mil-HDBK-5C, Metallic Materials and Elements for Aerospace Vehicle Structures," September 1976.

[39]Diaz, A., "Geometric Programming for Continuous Design Problems," International Symposium on Optimum Structural Design, October, 1981.

[40]Dixon, L. C. W., *Towards Global Optimisation 2*, North Holland Publishing Co., 1978.

[41]Douglas, F., "Viewport Concept for Space Station Modules," NASA TM-86559, George C. Marshall Space Flight Center, August 1986.

[42]Draper, N., and Smith, H., *Applied Regression Analysis*, John Wiley & Sons, Inc., 1981.

[43]Driver, R. D., *Ordinary and Delay Differential Equations*, Springer - Verlag New York, Inc., 1977.

[44]Duffin, R. J., Peterson, E. L., and Zener, *Geometric Programming*, John Wiley and Sons, Inc., 1967.

[45]Duffin, R. J., and Zener, "Optimization of Engineering Design by Geometric Programming," Carnegie-Mellon Univ., Feb. 1968.

[46]Duffin, R. J., and Peterson, E. L., Geometric Programming With Signomials, *Journal of Optimization Theory and Applications*, Vol. 11, Jan. 1973.

[47]Ecker, J. G., et Al, A Modified Reduced Gradient Method for Dual Posynomial Programming, *Journal of Optimization Theory and Applications*, Vol. 26, No. 2, Oct. 1978.

[48]Elliot, W. H., "Primal Geometric Programs Treated by Sequential Linear Programming," Penn. State Univ., 1976.

[49]Fair, H., "Hypervelocity Then and Now," Int. J. Impact Engng., Vol. 5, 1987.

[50]Friedberg, S. H., et Al, *Linear Algebra*, Prentice-Hall, Inc., 1979.

[51]Gantmacher, F. R., *The Theory of Matrices*, Chelsea Publishing Co., 1977.

[52]Gibbons, J. D., *Nonparametric Statistical Inference*, Marcel Dekker, Inc., 1985.

[53]Goldsmith, W., "Normal and Oblique Impact of Cylindro-Conical and Cylindrical Projectiles on Metallic Plates," Int. J. Impact Engng., Vol. 4, 1986.

[54]Gomulka, J., "Deterministic Vs. Probablistic Approaches to Global Optimisation," Towards Global Optimisation 2, 1978.

[55]Gottfried, B. S., and Weisman, J., *Introduction to Optimization Theory*, Prentice-Hall, Inc., Englewood Cliffs, New Jersey, 1973.

[56]Greszuzck, L., "Impact Dynamics of Metals and Composites - UCLA Short Course Notes," July 1988.

[57]Grosh, D. L., *A Primer of Reliability Theory*, John Wiley and Sons, Inc., 1989.

[58]Haberman, R., *Elementary Applied Partial Differential Equations*, Prentice-Hall, Inc., 1983.

[59]Hack, J. E., *Mechanical Behavior of Metal Matrix Composites*, American Institute of Mining, Metallurgical, and Petroleum Engineers, Inc., 1983.

[60]Hajela, P., Geometric Programming Strategies in Large-Scale Structural Synthesis, *AIAA Journal*, Vol. 24, July 1986.

[61]Hall, M. A., and Peterson, E. L., "Traffic Equilibria Analysed Via Geometric Programming," Northwestern Univ., Feb. 1975.

[62]Herrmann, W., "Review of Hypervelocity Penetration Theories," Int. J. Impact Engng., Vol. 5, 1987.

[63]Hilado, C. J., *Boron Reinforced Aluminum Systems-Vol. 6*, TECHNOMIC Publishing Co., Inc., 1974.

[64]Hilado, C. J., *Boron Reinforced Aluminum Systems-Part II*, Vol. 11, TECHNOMIC Publishing Co., Inc., 1982.

[65]Hillier, F. S., and Lieberman, G. J., *Introduction to Operations Research*, Holden-Day, Inc., 1986.

[66]Hines, W. W., and Montgomery, D. C., *Probability and Statistics in Engineering and Management Science*, John Wiley and Sons, Inc., 1980.

[67]Hogg, R. V., *Introduction to Mathematical Statistics*, Macmillan Publishing Co., Inc., 1978.

[68]Holland, A. S. B., *Complex Function Theory*, Elsevier, North Holland, Inc., 1980.

[69]Hough, C. L., "Optimization of the Second Order Logarithmic Machine Economics Problems by Extended Geometric Programming," Texas A&M University, 1978.

[70]Huang, Y. K., *Shock Waves in Hypervelocity Impact of Metals*, University Microfilms, Inc., 1962.

[71]Ignizio, J. P., A Geometric Programming Model for Space Communication Systems, *Modeling and Simulation*, Vol. 6, April 1975.

[72]Iyengar, N. G. R., and Gupta, S. K., "Programming Methods in Structural Design," Indian Institute of Technology, 1980.

[73]Jastrzebski, Z. D., *The Nature and Properties of Engineering Materials*, John Wiley and Sons, Inc., 1979.

[74]Jones, R. M., *Mechanics of Composite Materials*, Scripta Book Co., 1975.

[75]Kaplan, W., *Advance Calculus*, Addison-Wesley Publishing, Inc., 1973.

[76]Kelly, D. W., A Dual Formulation for Generating Information about Constrained Optima in Automated Design - Based on Geometric Programming, *Computer Methods in Applied Mechanics and Engineering*, Vol. 5, May 1975.

[77]Kessler, D., "Orbital Debris Environment for Spacecraft Designed to Operate in Low Earth Orbit," NASA TM-100471, April 1989.

[78]Kessler, D., "Orbital Debris Environment for Space Station," JSC-20001.

[79]Kessler, D., "Meteoroid Environment Model-1970 [Interplanetary and Planetary]," NASA SP-8038.

[80]Keyser, C. A., *Materials Science in Engineering*, Bell and Howell Co., 1974.

[81]Kothawala, K. S., "Shaping Up: Optimization of Structural Designs," Mechanical Engineering, March 1988.

[82]Kreider., K. G., *Metallic Matrix Composites-Vol. 4*, Academic Press, Inc., 1974.

[83]Kuhlmann-Wilsdorf, D., *New Developments and Applications in Composites*, American Institute of Mining, 1979.

[84]Kyparisis, J., "Optimal Value Bounds and Posynomial Geometric Programs," George Washington University, April 1982.

[85]Lapidus, L., and Pinder, G. F., *Numerical Solution of Partial Differential Equations in Science and Engineering*, John Wiley and Sons, Inc., 1982.

[86]Lavi, A., "A User Manual for Geometric Programming," Carnegie-Mellon Univ., Pittsburgh, PA., Dec., 1974.

[87]Lawrence, R. J., "A Simple Model for the Optimization of Stand-Off Hypervelocity Particle Shields," Int. J. Impact Engng., Vol. 5, 1987.

[88]Leitmann, G., *The Calculus of Variations and Optimal Control*, Plenum Press, New York, 1981.

[89]LeMay, I., *Principles of Mechanical Metallurgy*, Elsevier North Holland, Inc., 1981.

[90]Lootsma, F. A., "Performance Evaluation of Nonlinear Optimization Methods via Pairwise Comparison and Fuzzy Number," Technische Hogeschool, 1984.

[91]Madden, R., "Ballistic Limit of Double-Walled Meteoroid Bumper Systems," NASA TN-3916, Langley Research Center, April 1967.

[92]Madden, R., "Equations for the Comparison of the Ballistic Limit of Single and Double Wall Structures," AIAA Paper No. 69-370, April 1969.

[93]Maiden, C. J., "Investigation of Fundamental Mechanism of Damage to Thin Targets by Hypervelocity Projectiles," Final Report, GM Defense Research Lab., September 1963.

[94]Majid, K. I., *Optimum Design of Structures*, Halsted Press, 1974.

[95]Mancini, L. J., and Wilde, D. J., Interval Arithmetic in Unidimensional Signomial Programming, *Journal of Optimization Theory and Applications*, Vol. 26, No. 2, Oct. 1978.

[96]Martin, H. C., *Introduction to Matrix Methods of Structural Analysis*, McGraw-Hill, Inc., 1966.

[97]McCormick, G. P., *Nonlinear Programming Theory, Algorithms, and Applications*, John Wiley and Sons, Inc., 1983.

[98]McMasters, J. H., "The Optimization of Low-Speed Flying Devices by Geometric Programming," Purdue University, 1975.

[99]Metcalfe, A. G., *Interfaces in Metal Matrix Composites*, Academic Press, Inc., 1974.

[100]Miller, I., and Freund, J. E., *Probability and Statistics for Engineers*, Prentice-Hall, Inc., 1977.

[101]Misra, K. B., "On Optimal Reliability Design - A Review," International Federation of Automatic Control, Triennial World Congress, 6th, August 1975.

[102]Mog, R. A., Spacecraft Protective Structures Design Optimization, *AIAA Journal of Spacecraft and Rockets*, Vol. 28, No. 1, Jan.-Feb. 1991.

[103]Mog, R. A., Lovett, J. N., and Avans, S. L., "Global Nonlinear Optimization of Spacecraft Protective Structures Design," NASA TM-100387, January 1990.

[104]Mog, R. A., "Discrete Nonlinear Optimization of Spacecraft Protective Structures Design - White Paper," SAIC, Aug. 1988.

[105]Mog, R. A., "Comparison of Nonlinear Optimization Techniques for Spacecraft Protective Structures Design - White Paper," SAIC, June 1988.

[106]Mog, R. A., and Price, D. M., "Linear Programming Estimation of the Nonlinear Spacecraft Protective Systems Design Optimization Problem - White Paper," SAIC, March 1988.

[107]Mog, R. A., and Price, D. M., "Optimization Techniques Applied to Passive Measures for In-Orbit Spacecraft Survivability - Final Report," SAIC HV410-12, Contract NAS8-37378, Nov. 1987.

[108]Moon, F. C., "Wave Surfaces Due to Impact on Anisotropic Plates," J. Comp. Mat., Vol. 6, January 1972.

[109]Morris, A. J., On Condensed Geometric Programming in Structural Optimization, *Computer Methods in Applied Mechanics and Engineering*, Vol. 15, Aug. 1978.

[110]Morris, A. J., "The Optimisation of Statically Indeterminate Structures By Means of Approximate Geometric Programming," Royal Aircraft Establishment, April 1974.

[111]Morris, A. J., "Approximation and Complementary Geometric Programming," Royal Aircraft Establishment, April 1974.

[112]Morris, A. J., "Structural Optimisation by Geometric Programming," Royal Aircraft Establishment, April 1974.

[113]Morris, A. J., A Transformation for Geometric Programming Applied to the Minimum Weight Design of Statically Determinate Structures, *International Journal of Mechanical Sciences*, Vol. 17, June 1975.

[114]Morris, A. J., A Primal-Dual Method for Minimum Weight Design of Statically Determinate Structures with Several Systems of Load, *International Journal of Mechanical Sciences*, Vol. 16, Nov. 1974.

[115]Morrison, R. H., "A Preliminary Investigation of Projectile Shape Effects in Hypervelocity Impact of a Double-Sheet Structure," NASA TN D-6944, Aug. 1972.

[116]Mueller, L., "ARALL: An Update," Aerospace Engineering, December 1987.

[117]Musgrave, M. J. P., "On the Propagation of Elastic Waves in Aeolotropic Media," Royal Society - Proceedings, A226, 1954.

[118]Nysmith, C. R., "An Experimental Impact Investigation of Aluminum Double-Sheet Structures," AIAA Hypervelocity Impact Conference, Cincinnati, Ohio, April 30-May 2, 1969, AIAA Paper No. 69-375.

[119]Oswald, P. F., and Kochenberger, G. A., "Optimization of Heat Transfer Designs by Geometric Programming," American Society of Mechanical Engineers, Winter Annual Meeting, November, 1972.

[120]Peterson, E. L., "Fenchel's Duality Theorem in Generalized Geometric Programming," Northwestern Univ., Evanston, IL., Oct. 1976.

[121]Peterson, E. L., "Optimality Conditions in Generalized Geometric Programming," Northwestern Univ., Evanston, IL., May, 1976.

[122]Peterson, E. L., "A Handbook of Geometric Programming," Northwestern Univ., Evanston, IL., July, 1974.

[123]Peterson, E. L., "Saddle Points and Duality in Generalized Geometric Programming," Northwestern Univ., Evanston, IL., August, 1976.

[124]Peterson, E. L., "Reduction and Decomposition of Large Generalized Geometric Programming Problems with Applications," Northwestern Univ., Evanston, IL., 1975.

[125]Peterson, E. L., "The Complementary Unboundedness of Dual Feasible Solution Sets in Convex Programming," Northwestern Univ., Evanston, IL., August, 1975.

[126]Piekutowski, A. J., "Debris Clouds Generated by Hypervelocity Impact of Cylindrical Projectiles With Thin Aluminum Plates," Int. J. Impact Engng, Vol. 5, pp. 509-518, 1987.

[127]Plane, D. R., *Discrete Optimization*, Prentice-Hall, Inc., 1988.

[128]Popov, E. P., *Mechanics of Materials*, Prentice-Hall, Inc., 1978.

[129]Rainville, E. D., and Bedient, P. E., *Elementary Differential Equations*, Macmillan Publishing Co., Inc., 1974.

[130]Ramamurthy, S., "Structural Optimization Using Geometric Programming," Cornell University, 1977.

[131]Ratner, M., et Al, "Solving Geometric Programs Using GRG-Results and Comparisons," Stanford Univ., CA., May 1976.

[132]Reklaitis, G. V., "Investigation of the Computational Utility of Geometric Programming Formulation and Algorithms," Purdue Univ., West Lafayette, IN., Jan. 1981.

[133]Richardson, A. J., "Development of Dual Bumper Wall Construction for Advanced Spacecraft," Journal of Spacecraft and Rockets, Vol. 9, No. 6, June 1972.

[134]Richardson, A. J., "Theoretical Penetration Mechanics of Multisheet Structures Based on Discrete Debris Particle Modeling," Journal of Spacecraft and Rockets, Vol. 7, No. 4, April 1970.

[135]Rijckaert, M. J., and Martens, X. M., Comparison of Generalized Geometric Programming Algorithms, *Journal of Optimization Theory and Applications*, Vol. 26, No. 2, Oct. 1978.

[136]Rijckaert, M. J., and Martens, X. M., Bibliographical Note on Geometric Programming, *Journal of Optimization Theory and Applications*, Vol. 26, No. 2, Oct. 1978.

[137]Rikards, R. B., Dual Problem of Optimizing an Orthotropic Cylindrical Shell, *Mekhanika Polimerov*, September 1973.

[138]Ritger, P. D., and Rose, N. J., *Differential Equations with Applications*, McGraw-Hill, Inc., 1968.

[139]Rosenberg, E., "A Globally Convergent Condensation Method for Geometric Programming," Stanford Univ., CA., Oct. 1979.

[140]Rujikietgumjorn, S., "Development of Predictive Models for Drilling Composite Materials," Texas Technological University, 1978.

[141]Sarma, P. V. L. N., et Al, A Comparison of Computational Strategies for Geometric Programs, *Journal of Optimization Theory and Applications*, Vol. 26, No. 2, Oct. 1978.

[142]Schonberg, W. P., Taylor, R. A., Horn, J. R., "An Analysis of Penetration and Ricochet Phenomena in Oblique Hypervelocity Impact," NASA TM-100319, George C. Marshall Space Flight Center, February 1988.

[143]Schoutens, J. E., *Introduction to Metal Matrix Composite Materials*, DOD Metal Matrix Composites Information Analysis Center, 1982.

[144]Segel, L. A., *Mathematics Applied to Continuum Mechanics*, Dover Publications, Inc., 1987.

[145]Shifrin, C. A., "NASA to Evaluate Two Suit Designs for Space Station," Aviation Week and Space Technology, January 11, 1988.

[146]Shockey, D. A., et al., "Disintegration Behavior of Metal Rods Subjected to Hypervelocity Impact," Int. J. Impact Engng, Vol. 5, pp. 585-593, 1987.

[147]Smith, D. G., "Debris Impact on Earth-Orbiting Spacecraft," Contract NASA-NGT-01-002-099, 1984.

[148]Smith, G. D., *Numerical Solutions of Partial Differential Equations: Finite Difference Methods*, Oxford University Press, 1978.

[149]Smith, R. E., and West, G. S., "Space and Planetary Environment Criteria Guidelines for Use in Space Vehicle Development," NASA TM-82478, George C. Marshall Space Flight Center, 1982.

[150]Snell, M. B., and Bartholomew, P., The Application of Geometric Programming to the Structural Design of Aircraft Wings, *Aeronautical Journal*, Vol. 86, August 1982.

[151]Stewart, G. W., *Introduction to Matrix Computations*, Academic Press, Inc., 1973.

[152]Susko, M., "A Review of Micrometeoroid Flux Measurements and Models for Low Orbital Altitudes of the Space Station," NASA TM-86466, George C. Marshall Space Flight Center, September 1984.

[153]Swift, H. F., "Designing Dual-Plate Meteoroid Shields - A New Analysis," JPL Publication 82-39, March 1982.

[154]Swift, H. F., "The Effects of Bumper Material Properties on the Operation of Spaced Hypervelocity Particle Shields," AIAA Paper No. 69-379, April 1969.

[155]Swokowski, E. W., *Calculus with Analytic Geometry*, Prindle, Weber, & Schmidt, Inc., 1975.

[156]Templeman, A. B., "The Use of Geometric Programming Methods for Structural Optimization," Liverpool Univ., Sept. 1973.

[157]Templeman, A. B., and Winterbottem, S. K., "Structural Design Applications of Geometric Programming," Liverpool Univ., Nov. 1973.

[158]Unklesbay, K., et Al, Optimal Design of Journal Bearings, *International Journal of Engineering Science*, Vol. 11, September 1973.

[159]Vanderplaats, G. N., *Numerical Optimization Techniques for Engineering Design with Applications*, McGraw-Hill, Inc., 1984.

[160]Walvekar, A. G., et Al, Optimal Design of Indeterminate Truss Using Geometric Programming, *Aeronautical Society of India Journal*, Vol. 24, May 1972.

[161]Watson, S. R., and Buede, D. E., *Decision Synthesis*, Cambridge University Press, 1987.

[162]Wheeden, R. L., *Measure and Integral*, Marcel Dekker, Inc., 1977.

[163]Whittle, P., *Optimization Under Constraints*, John Wiley and Sons, Ltd., 1971.

[164]Wilde, D. J., *Globally Optimal Design*, John Wiley and Sons, Inc., 1978.

[165]Wilkinson, J. P. D., "A Penetration Criterion for Double-Walled Structures Subject to Meteoroid Impact," AIAA Journal, Vol. 7, No. 10, October 1969.

[166]Woodward, R. L., "The Interrelation of Failure Modes Observed in the Penetration of Metallic Targets," Int. J. Impact Engng., Vol. 2, 1984.

[167]Wu, C. C., "Design and Modeling of Solar Sea Power Plants by Geometric Programming," Carnegie-Mellon University, April 1976.

[168]Wu, C. T., "Reduction and Restriction Methods for Simplifying and Solving Nonlinear Programming Problems," Northwestern University, 1975.

[169]Yew, C. H., "A Study of Damage in Composite Panels Produced by Hypervelocity Impact," Int. J. Impact Engng., Vol. 5, 1987.

[170]Zhu, G., "Estimation of the Plastic Structural Response Under Impact," Int. J. Impact Engng., Vol. 4, 1986.

[171]Zotos, J., *Mathematical Modeling of the Chemical, Mechanical, and Physical Properties of Engineering Alloys*, D. C. Heath and Co., 1977.

[172]Zukas, J. A., *Impact Dynamics*, John Wiley and Sons, Inc., 1982.

6 APPENDICES

```
C
C                S P I E S
C            SPacecraft Impact Environment Simulation
C      ************************************************
C      ****    Robert A. Mog    ****
C      ****    SAIC Huntsville                ****
C      ************************************************
C
C     Program to model space debris and meteoroid environments
C     for the analysis of in-orbit spacecraft survivability.
C
C
C ********** REVISION JAN 14,1992 *******
C K FACTORS AND SURFACE AREA DIFFER FOR THE BOX
C THEREFORE ADDED SAM & SAD (SURFACE AREA METERIOD & SURFACE AREA DEBRIS)
C
C***************************************
      DOUBLE PRECISION T,DELTAT
      REAL INCL,K,D,H,TI,TF,ET,S,SA,SAD,SAM,PVD(150,3),
     1    DIA,DEN,MASS,VEL,ANGLE,MVEL(100,2),MFL(0:1000,5)
      INTEGER N

      COMMON  /ARRAYS/SOLARFLX(0:150),FL(0:1000,0:3)

C     ****************************************************
C     INITIALIZE PARAMETERS AND ENVELOPING GEOMETRY
C


    CALL GET_PARAMETERS(TI,TF,DMIN_D,DMAX_D,D_D,DV,
     1                  DMIN_M,DMAX_M,D_M,H,INCL,
     2                  NSEED,IDISTFLAG,IMFLAG)
      CALL GEOMETRY(SAD,SAM,K)
C     ****************************************************
C
      CALL GETSLRFLX(TI,TF)
      CALL GET_INCL_FACTOR(INCL,PSI)
      CALL DEB_VEL(INCL,PVD,DV,IMAX_PVD)
C
      IMAX = INT((DMAX_D - DMIN_D) / D_D)
C
C     **** OUTPUT BEGIN AND END MISSION FLUX DISTRIBUTIONS ****
C      **** IF IDISTFLAG IS SET                    ****
C
      IF (IDISTFLAG .EQ. 1) THEN
        OPEN(UNIT=9,STATUS='NEW',FILE='VELDIST.OUT')
        T = TI
        CALL FLUX_DIAMETER(SAD,DMIN_D,DMAX_D,D_D,K,H,PSI,T,TI)
         WRITE(9,525) T
         DO 15 I=0,IMAX
15        WRITE(9,530)  (FL(I,II),II=0,3)
         T = TF
         CALL FLUX_DIAMETER(SAD,DMIN_D,DMAX_D,D_D,K,H,PSI,T,TI)
          WRITE(9,525) T
          DO 16 I=0,IMAX
16         WRITE(9,530)  (FL(I,II),II=0,3)
          WRITE(9,527)
          DO 17 I=1,IMAX_PVD
17         WRITE(9,520)  (PVD(I,II),II=1,3)
      ENDIF
C     ****************************************************

C     OPEN(UNIT=8,STATUS='NEW',FILE='SPIES_D.OUT')
      OPEN(UNIT=11,STATUS='NEW',FILE='PEN99.OUT')
C
C
      T = TI
10    CALL FLUX_DIAMETER(SAD,DMIN_D,DMAX_D,D_D,K,H,PSI,T,TI)
C

C     ****************************************************
C     LOOK UP DIAMETER
C
      X = RAN(NSEED)
      CALL LKUP_DIAMETER(X,DIA,IMAX,N)
C     ****************************************************
```

```
C
C     *************************
C     CALCULATE DENSITY AND MASS
C
      DEN = DENSITY(DIA)
      MASS = CALC_MASS(DIA)
C     *************************
C
C
C     ***********************************************
C     LOOK UP VELOCITY AND CALCULATE IMPACT ANGLE
C
      X=RAN(NSEED)
      CALL LKUP_VEL(PVD,IMAX_PVD,X,VEL,ANGLE)
C     ***********************************************
C
C
C     ****************
C      REVISION JAN 14,1992 - JANEIL HILL
C      SURVIVABILITY MODULE
C      BASED ON VELOCITY
C     ***************
      CALL SURVIVE_HIT(VEL,DIA,DEN,ANGLE)

C     ************************
C     CALCULATE CHANGE IN TIME
C
      X=RAN(NSEED)
      B = 1./FL(N,1)
      DELTAT = LOG(X) * (-B)
      T = T + DELTAT
C     ************************
C     WRITE(8,500) T,DELTAT,DIA,DEN,MASS,VEL,ANGLE
C
      IF (T.GE.TF) GOTO 150
C
      GOTO 10

150   CONTINUE
      CLOSE(8)
      CLOSE(11)
C
C     ******************* METEOROID ENVIRONMENT *********************
C
      IF (IMFLAG .NE. 1) GOTO 200
      OPEN(UNIT=10,STATUS='NEW',FILE='SPIES_M.OUT')
      T = TI
      IMAX = INT(((DMAX_M - DMIN_M) / D_M))
C
C     ****************************************************
C     BUILD METEOROID FLUX AND VELOCITY DISTRIBUTION TABLES
C
      CALL METEOROID_FLUX(SAM,H,DMIN_M,DMAX_M,D_M,MFL)
      CALL GET_METEOROID_VELOCITY(MVEL,IVELMAX)
C     ****************************************************
C
      IF (IDISTFLAG .EQ. 1) THEN
         WRITE(9,525) T
         DO 155 I=0,IMAX
155       WRITE(9,535)  MFL(I,1),MFL(I,3),MFL(I,4),MFL(I,5)
          WRITE(9,537)
         DO 156 I=1,IVELMAX
156       WRITE(9,538)  I,MVEL(I,1),MVEL(I,2)
        CLOSE(9)
      ENDIF
C     *********************************************
C     LOOK UP DIAMETER
C
175   X=RAN(NSEED)
      CALL LKUP_MET_DIAMETER(MFL,X,DIA,IMAX,N)
C     *********************************************
C
C     **** DENSITY IS CONSTANT, SET MASS AND DENSITY ****
      MASS = MFL(N,2)
      DEN = 0.5
      IF(MFL(N,2).LE.1E-06)DEN=2.0
      IF(MFL(N,2).LE.0.01.AND.MFL(N,2).GT.1E-06)DEN=1.0
C     ****************************************************
```

```
C
C     ************************************************
C     LOOK UP VELOCITY
C
      X=RAN(NSEED)
      CALL LKUP_MET_VEL(MVEL,IVELMAX,X,VEL)
C     ************************************************
C
C
C     **** ANGLE IS FIXED ****
      ANGLE = 90.0
C     ************************
C
C
C     ************************************
C     CALCULATE CHANGE IN TIME
C
      X=RAN(NSEED)
      B = 1./MFL(N,3)
      DELTAT = LOG(X) * (-B)
      T = T + DELTAT
C     ************************************
      WRITE(10,510) T,DELTAT,DIA,DEN,MASS,VEL,ANGLE
C
      IF (T.GE.TF) THEN
        CLOSE(10)
        CALL SORT_MERGE
        GOTO 200
      ENDIF
C
     GOTO 175
C
200   CONTINUE
      STOP
500   FORMAT(2X,' D ',2F13.8,2(2X,F6.3),2X,F10.7,2(2X,F6.3))
510   FORMAT(2X,' M ',2F13.8,2(2X,F6.3),2X,F10.7,2(2X,F6.3))
520   FORMAT(2X,3(2X,F6.3))
525   FORMAT(//2X,F13.8)
527   FORMAT(//2X,'Debris  Velocity  Distribution')
530   FORMAT(2X,F6.3,2X,F10.3,2(2X,F6.3))
535   FORMAT(2X,F6.3,2X,F10.3,3(2X,F6.3))
537   FORMAT(//2X,'Meteoroid  Velocity  Distribution')
538   FORMAT(2X,I4,2(2X,F6.3))
      END


      REAL FUNCTION CALC_MASS(D)
      CALC_MASS = 3.1416 * DENSITY(D) * D ** 3. / 6.
      RETURN
      END


      REAL FUNCTION DENSITY(D)
C      IF (D.LT.0.62) THEN
C       DENSITY = 4.0
C     ELSE
C       DENSITY = 2.8 / D ** 0.74
C     ENDIF
        DENSITY = 2.8

      RETURN
      END


      REAL FUNCTION FLUX(K,D,H,PSI,T,S)
      REAL PHI,F1,F2,G1,G2,PSI,K
C     *** FIXED GROWTH RATE P ***
      P = 0.05
      Q=0.02
      QP=0.04
C     ***************************
      PHI  =  10.**(H/200.-S/140.-1.5)/(10.**(H/200.-S/140.-1.5)+1.)
      F1 = 1.22E-05 * D ** (-2.5)
      F2 = 8.1E10 * (D + 700.) ** (-6.)
      G1 = (1 + Q) ** (T-1988.)
      IF(T.GE.2011)THEN
      G1 = (1 + Q) ** (23.)
      G1 = G1*(1 + QP) ** (T-2011.)
```

```
      ENDIF
      G2 = (1 + (P *(T-1988.)))
         HD=(10.0**(2.71828**((-1.0*(LOG(D)-0.78)**2.0)/0.405769)))**0.5
      FLUX = K * HD*PHI * PSI * (F1 * G1 + F2 * G2)
      RETURN
      END


      SUBROUTINE LKUP_DIAMETER(X,DIA,IMAX,N)
      COMMON /ARRAYS/SOLARFLX(0:150),FL(0:1000,0:3)
      I = 0
      IF (X.LT.FL(0,3)) GOTO 100
      DO 50 I = 1,IMAX
50      IF ((X.GE.FL(I-1,3)) .AND. (X.LT.FL(I,3))) GOTO 100
100   CONTINUE
      DIA = FL(I,0)
      N = I
      RETURN
      END

      SUBROUTINE FLUX_DIAMETER(SA,DMIN,DMAX,D,K,H,PSI,T,TI)
      COMMON /ARRAYS/SOLARFLX(0:150),FL(0:1000,0:3)
      REAL FLTOT,PROB,SA,DMIN,DMAX,D,K,H,PSI,T,TI
      S = SOLARFLX(INT((T-TI)*12))
      FLTOT = 0.0
      PROB = 0.0
      IMAX = INT((DMAX-DMIN)/D)
      IF (IMAX .GT. 1000) WRITE(*,*) 'DATA IS TOO LARGE FOR ',
     1      'DEBRIS FLUX ARRAY: FL'
      DO 100 I = 0,IMAX
       DIAMETER = DMIN + I*D
       FL(I,0) = DIAMETER
       FL(I,1) = SA * FLUX(K,DIAMETER,H,PSI,T,S)
       FLTOT = FLTOT + FL(I,1)
100   CONTINUE
      DO 110 I = 0,IMAX
       FL(I,2) = FL(I,1) / FLTOT
       PROB = PROB + FL(I,2)
       FL(I,3) = PROB
110   CONTINUE
C     *** INDICES FOR FL ARE AS FOLLOWS:
C     0 - DIAMETER / 1 - IMPACTS/YEAR / 2 - NORMALIZED / 3 - CUMULATIVE
C     ********************************************************************
      RETURN
      END

      SUBROUTINE GET_INCL_FACTOR(INCL,PSI)
      REAL INCL
      OPEN(UNIT=12,FILE='FLUXFAC.DAT',STATUS='OLD',READONLY)
      IX = 0
      DO 10 WHILE (IX .LT. INCL)
10    READ(12,*,END=20) IX,PSI
      GOTO 30
20    WRITE(*,*) 'ERROR READING FLUXFAC.DAT'
30    CLOSE(12)
      RETURN
      END

      SUBROUTINE GETSLRFLX(TI,TF)
      COMMON /ARRAYS/SOLARFLX(0:150),FL(0:1000,0:3)
      OPEN(UNIT=12,FILE='SOLAR1.FLX',STATUS='OLD',READONLY)
      I1 = INT((TI-1988.)*12.)
      DO 10 I=1,I1
10    READ(12,*)
      I1 = INT((TF-TI)*12.)
      DO 20 I=0,I1
       READ(12,*,ERR=25) S
       SOLARFLX(I) = S
20    CONTINUE
      GOTO 30
25    WRITE(*,*) ' ERROR READING SOLAR1.FLX'
30    CLOSE(12)
      RETURN
      END
```

```
      SUBROUTINE GEOMETRY(SAD,SAM,K)
     REAL R,L,W,H,PI,K
      PI  =  3.141593
5     WRITE(*,100)
      READ(*,110) I
      IF(I.LT.1 .OR. I.GT.3) THEN
        WRITE(*,*) ' Invalid Choice. '
       GOTO 5
      ENDIF
      GOTO  (10,20,30),I
10    WRITE(*,210)
      READ(*,215) R
      SAD = 4 * PI * R * R
      SAM = 4 * PI * R * R
      K = 2.7
      GOTO 50
20    WRITE(*,220)
      READ(*,215) R
      WRITE(*,225)
      READ(*,215) L
      SAD = 2* PI * R * (L + R)
      SAM = 2* PI * R * (L + R)
C
C     *** NEED TO CALCULATE K ***
C
      GOTO 50
 30   WRITE(*,230)
      READ(*,215) L
      WRITE(*,232)
      READ(*,215) W
      WRITE(*,235)
      READ(*,215) H
     K1 = 2.6
     K2 = 1.6
      SAD = K1*W*H + 2*K2*L*H
      SAM = 2*L*W + 2*W*H + 2*L*H
     K = 1.
C
C     *** WITH BOX A DOUBLE K FACTOR IS NEEDED ***
C     FOR NOW IT IS HARD WIRED IN K1 = 2.6 (FRONT) K2 = 1.6 (SIDE)
C
50    WRITE(*,300) SAD,SAM
      RETURN

100   FORMAT(2X,'Input type of enveloping geometry:'/10x,'1 - Sphere'/
     1       10X,'2 - Cylinder'/10X,'3 - Box.'/2X,'Choice?',$)
110   FORMAT(I2)
210   FORMAT(4X,'Sphere:'/6X,'Enter Radius (m) :',$)
215   FORMAT(F7.2)
220   FORMAT(4X,'Cylinder:'/6X,'Enter Radius (m) :',$)
225   FORMAT(6X,'Enter Length (m) :',$)
230   FORMAT(4X,'Box:'/6X,'Enter Length (m) :',$)
232   FORMAT(6X,'Enter Width (m) :',$)
235   FORMAT(6X,'Enter Height (m) :',$)
300   FORMAT(4X,'Surface Area is ',F19.2,' m2',F19.2,' m2')
      END

      SUBROUTINE DEB_VEL(XINCL,XPV,DV,IMAX)
      REAL  XPV(150,3)
     YG=250.0
     YF=0.0
      YC=0.0125
       YE=0.55+0.005*(XINCL-30.0)
        YH=1.0-0.0000757*(XINCL-60.0)**2.0
     YA=2.5
     YB=0.3
       YD=1.3-0.01*(XINCL-30.0)
      YV0=7.7
     IF(XINCL .LE. 60.0)THEN
       YB=0.5
       YG=18.7
         YV0=7.25+0.015*(XINCL-30.0)
     ENDIF
     IF(XINCL .LE. 80.0 .AND. XINCL .GT. 60.0)THEN
        YB=0.5-0.01*(XINCL-60.0)
        YG=18.7+0.0289*(XINCL-60.0)**3.0
```

```
      ENDIF
      IF(XINCL .GT. 100.0)THEN
         YC=0.0125+0.00125*(XINCL-100.0)
      ENDIF
      IF(XINCL .LE. 50.0)THEN
         YF=0.3+0.0008*(XINCL-50.0)**2.0
      ENDIF
      IF(XINCL .GT. 50.0 .AND. XINCL .LE. 80.0)THEN
         YF=0.3-0.01*(XINCL-50.0)
      ENDIF
      XSUMIV=0.0
      IVMAX=1
      IV=1
      XV=1.
100     XPV(IV,1)=XV
      XPV(IV,2)=YG*2.7183**(-1.0*((XV-YA*YV0)/(YB*YV0))**2.0)
       XPV(IV,2)=XPV(IV,2)+YF*2.7183**(-1.0*((XV-YD*YV0)/
      1               (YE*YV0))**2.0)
       XPV(IV,2)=XPV(IV,2)*(2.0*XV*YV0-XV**2.0)
      XPV(IV,2)=XPV(IV,2)+YH*YC*(4.0*XV*YV0-XV**2.0)
      IF(XPV(IV,2) .LE. 0.000)THEN
        XPV(IV,2)=0.000
       IVMAX=IV
       GO TO 150
      ENDIF
      XSUMIV=XSUMIV+XPV(IV,2)
      IV=IV+1
      XV=XV+DV
      GO TO 100
150    PROB = 0.
      DO 200 I=1,IVMAX
         XPV(I,2)=XPV(I,2)/XSUMIV
        PROB = PROB + XPV(I,2)
        XPV(I,3) = PROB
200    CONTINUE
C     ************** INDICES ARE: ****************
C     1 - VELOCITY  2 - NORMALIZED  3 - CUMULATIVE
C     ************************************************
      IMAX = IVMAX
C
     RETURN
     END

      SUBROUTINE LKUP_VEL(XPV,IMAX,R,XV,A)
      REAL  XPV(150,3)
      XV = XPV(1,1)
      DO 10 I = 1,IMAX-1
        IF ((R.GE.XPV(I,3)) .AND. (R.LT.XPV(I+1,3))) THEN
          XV = XPV(I+1,1)
          GOTO 20
        ENDIF
10    CONTINUE
20    CONTINUE
      A = ACOSD(XV/15.4)
      RETURN
      END

     SUBROUTINE GET_PARAMETERS(TI,TF,DMIN_D,DMAX_D,D_D,DV,DMIN_M,
       1       DMAX_M,D_M,H,INCL,NSEED,IDISTFLAG,IMFLAG)
      REAL TI,TF,DMIN,DMAX,D,DV,H,INCL
      INTEGER NSEED
      OPEN(UNIT=12,FILE='SPIES99.IN',STATUS='OLD',READONLY)
      READ(12,*) TI
      READ(12,*) TF
      READ(12,*) DMIN_D
      READ(12,*) DMAX_D
      READ(12,*) D_D
      READ(12,*) DV
      READ(12,*) DMIN_M
      READ(12,*) DMAX_M
      READ(12,*) D_M
      READ(12,*) H
      READ(12,*) INCL
      READ(12,*) NSEED
      READ(12,*) IDISTFLAG
      READ(12,*) IMFLAG
```

```
      CLOSE(12)
      RETURN
      END

      SUBROUTINE METEOROID_FLUX(SA,H,DMIN,DMAX,D,MFL)
      REAL DMIN,DMAX,D,DIAMETER,LOGM,MASS,H,G,NETA,MFLTOT,
     1     MFL(0:1000,5)
C     *** CALCULATION FOR G USES 6378 KM RADIUS FOR EARTH ***
      G = 1.0+6478./(6378.+H)
      NETA = (1 + COS(ASIN(6478. / (6378. + H)))) / 2.
      IMAX = INT((DMAX-DMIN)/D)
      IF (IMAX .GT. 1000) WRITE(*,*) 'MUST RE-DIMENSION METEOROID ',
     1     'FLUX ARRAY.  DATA IS TOO LARGE.'
      MFLTOT = 0.
      PROB = 0.
      DO 10 I=0,IMAX
C       *** MASS CALCULATION USES AVERAGE DENSITY OF .5 G/CM3 ***
        DIAMETER = DMIN + I*D
        DEN = 0.5
        IF(MFL(N,2).LE.1E-06)DEN=2.0
        IF(MFL(N,2).LE.0.01.AND.MFL(N,2).GT.1E-06)DEN=1.0
        MASS = 3.141593 * DEN * DIAMETER ** 3.0 / 6.0
        MFL(I,1) = DIAMETER
        MFL(I,2) = MASS
CCC     LOGM = LOG10(MASS)
CCC     IF (MASS .LE. .000001) THEN
CCC        MFL(I,3) = 10**(-14.339 - 1.584*LOGM - 0.063 * LOGM ** 2)
CCC     ELSE
CCC        MFL(I,3) = 10**(-14.37 - 1.213 * LOGM)
CCC     ENDIF
        C0=3.156E07
        C1=2.2E03
        C2=15.
        C3=1.3E-09
        C4=1.0E11
        C5=1.0E27
        C6=1.3E-16
        C7=1.0E06
        MFL(I,3)=C6/(MASS+C7*MASS**2.0)**0.85
        MFL(I,3)=MFL(I,3)+C3/(MASS+C4*MASS**2.0+C5*MASS**4.0)**0.36
        MFL(I,3)=MFL(I,3)+1.0/(C1*MASS**0.306+C2)**4.38
        MFL(I,3)=C0*MFL(I,3)
C       *** MULTIPLY BY G,NETA, AND NO. OF SEC/YEAR ***
        MFL(I,3) = SA * MFL(I,3) * G * NETA * 31536000.
        MFLTOT = MFLTOT + MFL(I,3)
10    CONTINUE
      DO 20 I=0,IMAX
        MFL(I,4) = MFL(I,3) / MFLTOT
        PROB = PROB + MFL(I,4)
        MFL(I,5) = PROB
20    CONTINUE
C     *** INDICES ARE : **********************
C     1 - DIAMETER    2 - MASS    3 - IMPACTS/YEAR
C     4 - NORMALIZED        5 - CUMULATIVE
      RETURN
      END

      SUBROUTINE GET_METEOROID_VELOCITY(MVEL,IMAX)
      REAL MVEL(100,2),PVEL,PVTOT,PVCUM
      OPEN(UNIT=8,FILE='METVEL.IN',STATUS='OLD',READONLY)
      PVCUM = 0.
      PVTOT = 0.
10    READ(8,*,END=100)I,PVEL
CCC   MVEL(I,1) = PVEL
      IF(I.LT.11)MVEL(I,1)=0.0
      IF(I.GE.11.AND.I.LE.16)MVEL(I,1)=0.112
      IF(I.GT.16.AND.I.LT.55)MVEL(I,1)=3.328E05/(FLOAT(I)**5.34)
      IF(I.GE.55.AND.I.LE.72)MVEL(I,1)=1.695E-04
      PVTOT = PVTOT + MVEL(I,1)
      GOTO 10
100   IMAX = I
      DO 110 I=1,IMAX
        MVEL(I,1) = MVEL(I,1) / PVTOT
        PVCUM = PVCUM + MVEL(I,1)
        MVEL(I,2) = PVCUM
110   CONTINUE
```

```
      CLOSE(8)
      RETURN
      END

      SUBROUTINE LKUP_MET_VEL(MVEL,IMAX,R,VEL)
      REAL VEL,MVEL(100,2)
      VEL = 1.0
      DO 10 I = 1,IMAX-1
        IF ((R.GE.MVEL(I,2)) .AND. (R.LT.MVEL(I+1,2))) THEN
          VEL = FLOAT(I)
          GOTO 20
        ENDIF
10    CONTINUE
20    CONTINUE
      RETURN
      END

      SUBROUTINE LKUP_MET_DIAMETER(MFL,X,DIA,IMAX,N)
      REAL MFL(0:1000,5)
      I = 0
      IF (X.LT.MFL(0,5)) GOTO 100
      DO 50 I = 1,IMAX
50      IF ((X.GE.MFL(I-1,5)) .AND. (X.LT.MFL(I,5))) GOTO 100
100   CONTINUE
      DIA = MFL(I,1)
      N = I
      RETURN
      END

      SUBROUTINE SORT_MERGE
      CHARACTER*58 DDATA2,MDATA2,DDATA1*3,MDATA1*3
      REAL TD,TM
      OPEN(UNIT=8,STATUS='OLD',FILE='SPIES_D.OUT',READONLY)
      OPEN(UNIT=9,STATUS='OLD',FILE='SPIES_M.OUT',READONLY)
      OPEN(UNIT=10,STATUS='NEW',FILE='SPIES_BOTH.OUT')
      READ(8,500,END=100) DDATA1,TD,DDATA2
      READ(9,500,END=200) MDATA1,TM,MDATA2
50    DO 60 WHILE (TD .LE. TM)
        WRITE(10,500) DDATA1,TD,DDATA2
        READ(8,500,END=100) DDATA1,TD,DDATA2
60    CONTINUE
      DO 70 WHILE (TD .GT. TM)
        WRITE(10,500) MDATA1,TM,MDATA2
        READ(9,500,END=200) MDATA1,TM,MDATA2
70    CONTINUE
      GOTO 50
100   READ(9,500,END=300) MDATA1,TM,MDATA2
      WRITE(10,500) MDATA1,TM,MDATA2
      GOTO 100
200   READ(8,500,END=300) DDATA1,TD,DDATA2
      WRITE(10,500) DDATA1,TD,DDATA2
      GOTO 200
300   CLOSE(8)
      CLOSE(9)
      CLOSE(10)
      RETURN
500   FORMAT(2X,A3,F13.8,A58)
      END


      SUBROUTINE SURVIVE_HIT(VEL,DIA,DEN,THETA)
      REAL VEL
C*********************
C     SURVIVABILITY MODULE JAN 14,1992
C     JANEIL HILL
C     VEL   VELOCITY OF PARTICLE
C     BIGN   PERFERATION LEVEL
C     DIA   DIAMETER OF PARTICLE
C     DEN   PARTICLE DENSITY
C     THETA       ANGLE OF IMPACT
C     SI     ARRAY OF SEPERATION OF BUMPER
C     RHOI ARRAY OF DENSITY OF BUMPER
C     THI    BUMPER THICKNESS
C     N      NUMBER OF BUMPERS
C**********************
C FOR NOW ALL THE VARIABLES THAT WILL BE READ IN ARE HARDWIRED HERE
```

```
      REAL SI(10),RHOI(10),THI(10),LN

      LN = .401
      N = 2
      THI(1) = .127
      THI(2) = .3175
      SI(1) = 10.16
      RHOI(1) = 2.71
      RHOI(2) = 2.81


      IF (VEL .LE. 7.5) THEN
        TEMP1 = 1.0
        TEMP2 = 1.0
        DO I=1,(N-1)
            TEMP1 = TEMP1 * SI(I)
            TEMP2 = TEMP2 *(RHOI(I) * THI(I))
        END DO
        BIGN =(  ( 3.801*DIA**1.0301 * DEN**.3892 * VEL**.2879 *
     &       (COSD(THETA/(N-1))**.3288)) /
     &       (TEMP1**(.4826 / (N-1)**.65) * TEMP2**(.3464/(N-1)**.65) *
     &       (RHOI(N)*THI(N))**.2929 * (N-1)**.6137)  ) - 1.
        WRITE(11,*) BIGN
      ELSE
C **** IF VELOCITY > 7.5)
        TEMP1 = 1.0
        TEMP2 = 1.0
        DO I=1,(N-1)
            TEMP1 = TEMP1 * SI(I)**2.
            TEMP2 = TEMP2 *(RHOI(I) * THI(I))
        END DO
        RMPUA = (1.25*DIA * DEN) / TEMP2
        IF (RMPUA .GT. 1.0000) THEN
          TN = (.364 * (1.25*DIA)**4. *DEN**2. * VEL * COSD(THETA)) /
     &          (LN * TEMP1 * TEMP2 * RHOI(N))
        ELSE
C **** RMPUA <= 1
          TN = (.364 *(1.25*DIA)**3.* DEN* VEL * COSD(THETA) ) /
     &         (LN * TEMP1 * RHOI(N) )
        END IF
        IF (TN .GE. THI(N)) THEN
          WRITE(11,*) ' 1.500'
        ELSE
          WRITE (11,*) ' 0.000'
        ENDIF

      ENDIF

      RETURN
      END
```